DOKUZ EYLÜL UNIVERSITY
GRADUATE SCHOOL OF NATURAL AND APPLIED SCIENCES

SOLAR PHOTOCATALYTIC TREATMENT OF SOME RECALCITRANT POLLUTANTS

by
Deniz AKTEN

October, 2007
İZMİR

SOLAR PHOTOCATALYTIC TREATMENT OF SOME RECALCITRANT POLLUTANTS

A Thesis Submitted to the
Graduate School of Natural and Applied Sciences of Dokuz Eylül University
In Partial Fulfillment of the Requirements for the Degree of Master of Science
in Environmental Engineering, Environmental Science Program

by
Deniz AKTEN

October, 2007
İZMİR

M.Sc THESIS EXAMINATION RESULT FORM

We have read the thesis entitled **"SOLAR PHOTOCATALYTIC TREATMENT OF SOME RECALCITRANT POLLUTANTS"** completed by **DENİZ AKTEN** under supervision of **PROF. DR. AYŞE FİLİBELİ** and we certify that in our opinion it is fully adequate, in scope and in quality, as a thesis for the degree of Master of Science.

Prof. Dr. Ayşe FİLİBELİ

Supervisor

(Jury Member)

(Jury Member)

Prof.Dr. Cahit HELVACI
Director
Graduate School of Natural and Applied Sciences

ACKNOWLEDGMENTS

The author greatly acknowledges the efforts of Prof. Dr. Ayşe FİLİBELİ, the advisor of the thesis, for her invaluable advices, continuous supervision and considerable concern in carrying out the study. It has been a great honour and privilege for the author to work with her.

The author also greatly acknowledges Dr. Neval BAYCAN for supervising this study, for her valuable suggestion, encouragement and support in this thesis. It has been a great honour and privilege for the author to work with her also.

The author is thankful to Dr. Zihni YILMAZ, Assoc. Prof. Dr. İlgi K. KAPDAN for their advices, comments and evaluations throughout the conduct of the study.

The author is thankful to laboratory technicians Yaşariye OKUMUŞ, Yılmaz SAĞER and Orhan ÇOLAK for their helps in her experimental studies.

The author is thankful to MSc. Ebru Ç. ÇATALKAYA for her valuable helps in various steps of the thesis, endless support, motivation and friendship.

This work was generously supported by TÜBİTAK (The Scientific and Technological Research Council of Turkey). The author also thanks TÜBİTAK for supporting the 104Y354 numbered project financially.

The author is also thankful to her friends Özgül ÇAKIN, H. H. Miraç GÜL and Özgün ANDİÇ for their support, morale motivation, unforgettable friendship, generosity and understanding.

The author would like to extend her sincere thanks to Prof. Dr. Füsun SENGÜL for sharing this subject of the thesis.

The author finally would like to thank to her family for their love, moral support and encouragement.

Deniz AKTEN
Environmental Eng.

SOLAR PHOTOCATALYTIC TREATMENT OF SOME RECALCITRANT POLLUTANTS

ABSTRACT

The major objectives of this thesis were to investigate solar treatment as a treatment alternative of certain industrial wastewaters and to optimise reaction conditions according to Box-Wilson Experimental Design Method. Another objective was to investigate the effectiveness of Fe(III)/H_2O_2/Solar-UV and Fe(III)/TiO_2/Solar-UV processes for the treatment of synthetic wastewater and selected industrial wastewaters which are containing high chemical oxygen demand (COD), biochemical oxygen demand (BOD), total organic carbon (TOC) and color.

One of the Advanced Oxidation Process (AOP) techniques is the Fe(III)/H_2O_2/Solar-UV process. Fe(III)/H_2O_2/Solar-UV process employed strong oxidants of hydrogen peroxide (H_2O_2) to degrade organic carbon, especially under the promotion of solar irradiation and catalyst addition (Fe(III)). Titanium dioxide (TiO_2) was used in palce of H_2O_2 as an oxidant in the Fe(III)/TiO_2/Solar-UV process to compare efficiencies of two processes.

A batch solar reactor was designed to carry out experimental studies. The solar reactor consists of sun light collectors, water preparation tank, circulation pump and a control panel.

In the first part of the experimental studies, synthetic wastewater treatment was studied with the azo dye Remazol Brilliant Blue R-A at a concentration of 50mg/L. Before starting experimentation with solar reactor some preliminary works were done in the laboratory to determine ranges of chemical dosages. So, H_2O_2 concentrations were studied from 803.1 to 2677mg/L, TiO_2 concentrations were studied from 50 to 250mg/L, Fe(III) concentrations were studied from 0 to 1.0mM and the flowrate of wastewater varied from 10 to 50L/h in all Fe(III)/H_2O_2/Solar-UV and Fe(III)/H_2O_2/Solar-UV processes. Experimental points and conditions were

determined according to the Box-Wilson Experimental Design Method. In the second part of the experimental studies, textile and paper industry wastewater treatment was studied with the solar reactor according to the Box-Wilson Experimental Design Method at the same experimantal points and conditions and TOC and color removal efficiencies were compared.

Samples were taken at the beginning of the experiments with solar reactor and after every hour during eight hours batch treatment and analysed for COD, BOD, TOC and color. Adsorbable organic halogens (AOX) also analysed during the paper industry wastewater experiments. Wavelenght scan was conducted for each of synthetic wastewater, textile industry watewater and paper industry wastewater to find out the wavelenght that color measurements would be done.

After eight hours batch treatment of synthetic wastewater with Fe(III)/H_2O_2/Solar-UV process maximum color removal efficiency was 100% and maximum TOC removal efficiency was 85%. Maximum color and TOC removal efficiencies were 98% and 59%, respectively, with Fe(III)/TiO_2/Solar-UV process. Maximum color and TOC removal efficiencies were 64% and 72%, respectively, with Fe(III)/H_2O_2/Solar-UV process and 97% and 100% with Fe(III)/TiO_2/Solar-UV process after eight hours batch treatment of textile industry wastewater. Maximum color and TOC removal efficiencies were 89% and 89%, respectively, with Fe(III)/H_2O_2/Solar-UV process and 83% and 64% with Fe(III)/TiO_2/Solar-UV process after eight hours batch treatment of paper industry wastewater.

In summary, the desinged solar reactor is an effective tool for the treatment of industrial wastewaters. Another finding is Fe(III)/H_2O_2/Solar-UV and Fe(III)/TiO_2/Solar-UV processes are effective alternative treatment processes for industrial wastewaters.

Keywords: Solar treatment, Box-Wilson experimental design method, Advanced oxidation techniques.

BAZI KALICI KİRLETİCİLERİN SOLAR FOTOKATALİTİK ARITIMI

ÖZ

Bu tezin en önemli amaçları, bazı endüstriyel atıksuların arıtılmasında solar arıtımın alternatif bir yöntem olarak incelenmesi ve Box-Wilson Deneysel Tasarım Yöntemine göre reaksiyon koşullarının optimizasyonunun sağlanmasıdır. Bir diğer amaç ise, Fe(III)/H_2O_2/Solar-UV ve Fe(III)/TiO_2/Solar-UV proseslerinin sentetik atıksu ve yüksek kimyasal oksijen ihtiyacı (KOİ), biyokimyasal oksijen ihtiyacı (BOİ), toplam organik karbon (TOK) ve renk içeren seçilmiş endüstriyel atıksuların arıtımındaki verimlerinin araştırılmasıdır.

İleri arıtma tekniklerinden bir tanesi Fe(III)/H_2O_2/Solar-UV yöntemidir. Fe(III)/H_2O_2/Solar-UV yöntemi, genellikle solar radyasyon ve katalizör eklenmesi ile geliştirilerek, hidrojen peroksidin (H_2O_2) organik karbonu güçlü bir şekilde indirgemesini sağlar. Fe(III)/TiO_2/Solar-UV yönteminde hidrojen peroksit yerine titanyum dioksit kullanılarak iki yöntemin verimleri karşılaştırılmıştır.

Deneysel çalışmaların yürütülmesi için bir kesikli solar reaktör tasarlanmıştır. Bu solar reaktör güneş ışığı kolektörleri, su hazırlama tankı, sirkülasyon pompası ve bir kontrol panelinden oluşmaktadır.

Deneysel çalışmaların ilk kısmında, 50 mg/L konsantrasyonunda Remazol Brilliant Blue R-A azo boyası ile hazırlanan sentetik atıksu arıtımı çalışılmıştır. Deneysel çalışmalara başlamadan önce kimyasal dozlarının belirlenmesi için laboratuarda bazı ön çalışmalar yapılmıştır. Fe(III)/H_2O_2/Solar-UV ve Fe(III)/$TİO_2$/Solar-UV yöntemleri ile yapılan tüm deneylerde H_2O_2 803.1 ve 2677mg/L konsantrasyonları arasında çalışılmıştır, TiO_2 50 ve 250mg/L konsantrasyonları arasında çalışılmıştır, Fe(III) 0 ve 1.0mM konsantrasyonları arasında çalışılmıştır ve atıksu debisi 10 ve 50L/h arasında değişmiştir. Deneysel noktalar ve koşullar Box-Wilson Deneysel Tasarım Yöntemi'ne göre belirlenmiştir.

Deneysel çalışmaların ikinci kısmında, solar reaktör ile Box-Wilson Deneysel Tasarım Yöntemi'ne göre belirlenen aynı deneysel noktalar ve koşullarda tekstil ve kâğıt endüstrisi atıksularının arıtılması çalışmaları yapılmıştır. TOC ve renk giderim verimleri karşılaştırılmıştır.

Solar reaktör ile yapılan deneylerden önce ve sekiz saat kesikli arıtım boyunca saat başı örnek alınarak KOİ, BOİ, TOK ve renk analizleri yapılmıştır. Kâğıt endüstrisi atıksuyu ile yapılan çalışmalarda adsorplanabilir organik halojenür (AOX) analizleri de yapılmıştır. Sentetik atıksu, tekstil endüstrisi atıksuyu ve kâğıt endüstrisi atıksuyunun her birinde renk okumalarının yapılacağı dalga boyunun saptanması için dalga boyu taraması yapılmıştır.

Sentetik atıksuyun Fe(III)/H_2O_2/Solar-UV yöntemi ile sekiz saat kesikli arıtımı sonucunda %100 renk ve maksimum %84 TOK giderimi sağlanmıştır. Fe(III)/TiO_2/Solar-UV yönteminde ise bu değerler sırası ile %98 ve %59'dur. Tekstil endüstrisi atıksuyun sekiz saat kesikli arıtımı sonucunda Fe(III)/H_2O_2/Solar-UV ve Fe(III)/TiO_2/Solar-UV yöntemleri ile elde edilen maksimum renk ve TOK giderimleri sırası ile %64 ve %72 ile %97 ve %100'dür. Kâğıt endüstrisi atıksuyun sekiz saat kesikli arıtımı sonucunda Fe(III)/H_2O_2/Solar-UV ve Fe(III)/TiO_2/Solar-UV yöntemleri ile elde edilen maksimum renk ve TOK giderimleri sırası ile %89 ve %89 ile %83 ve %64'dir.

Özetle, tasarlanan solar reaktör endüstriyel atıksuların arıtımı için uygun bir sistemdir. Bir başka sonuç ise, Fe(III)/H_2O_2/Solar-UV ve Fe(III)/TiO_2/Solar-UV yöntemleri endüstriyel atıksuların arıtımı için etkili alternatif yöntemlerdir.

Anahtar Sözcükler: Solar arıtma, Box-Wilson deneysel tasarım yöntemi, İleri oksidasyon teknikleri.

CONTENTS

Page

THESIS EXAMINATION RESULT FORM……...……ii
ACKNOWLEDGEMENTS…….....iii
ABSTRACT…….....v
ÖZ....…….....vii

CHAPTER ONE – INTRODUCTION……..1

1.1 Introduction……..…….....1

1.2 Objectives and Scope…….....3

CHAPTER TWO – LITERATURE REVIEW……5

2.1 General Information on Advanced Oxidation Processes……...5

2.2 Theoretical Background…….9
2.2.1 Photo-Fenton-like Process (UV /H_2O_2/Fe(III))……..9
2.2.2 Solar TiO_2 Catalysis (UV/TiO_2/Fe(III))……9
2.2.3 AOX Problem in Wastewaters…….10
2.2.4 Photocatalytic Reactor Types……...11
2.2.4.1 General Information…….11
2.2.4.2 Parabolic Trough Reactor (PTR)……..12
2.2.4.3 Thin Film Fixed Bed Reactor (TFFBR)……...13
2.2.4.4 Compound Parabolic Collecting Reactor (CPCR)…….....14
2.2.4.5 Double Skin Sheet Reactor (DSSR)…….16

CHAPTER THREE – MATERIALS AND METHODS……...17

3.1 Materials……...17

3.2 Methods……18
3.2.1 Analytical Methods……..18
3.2.1.1 Chemical Oxygen Demand (COD) Analysis……...18
3.2.1.2 Biochemical Oxygen Demand (BOD_5) Analysis…….19
3.2.1.3 Total Organic Carbon (TOC) Analysis……19
3.2.1.4 Color Analysis……..……19
3.2.1.5 Adsorbable Organic Halogen Compounds (AOX) Analysis……...19
3.2.2 Photodegradation Experiments…….19
3.2.2.1 Solar Reactor……19
3.2.2.2 Box–Wilson Central Composit Design……22
3.2.2.3 Photocatalytic Experimental Procedure with Synthetic Wastewater…….....26
3.2.2.4 Photocatalytic Experimental Procedure with Industrial Wastewaters……..27

CHAPTER FOUR – RESULTS AND DISCUSSION……28

4.1 Application of Box–Wilson Experimental Design Method for the Solar Degradation of Synthetic Wastewater by Advanced Oxidation Processes….28
4.1.1. Photo-Fenton-like Process (Fe(III)/H_2O_2/Solar-UV)…….28
4.1.1.1 Introduction…….28
4.1.1.2 Experimental Procedure……..29
4.1.1.3 Regression Model……30
4.1.1.3.1 Decolorization…….36
4.1.1.3.1 TOC removal……...39
4.1.2 Solar TiO_2 Catalysis (Fe(III)/ TiO_2/Solar-UV)……...42
4.1.2.1 Introduction……42
4.1.2.2 Experimental Procedure……..42

4.1.2.3 Regression Model……44
4.1.2.3.1 Decolorization……50
4.1.2.3.2 TOC removal……...……...53

4.2 Application of Box–Wilson Experimental Design Method for the Solar Degradation of Textile Industry Wastewater by Advanced Oxidation Processes……57
4.2.1 Introduction……..57
4.2.2 Wastewater characterization……57
4.2.3 Photo-Fenton-like Process (Fe(III)/H_2O_2/Solar-UV)……...58
4.2.3.1 Experimental Procedure……...58
4.2.3.2 Regression Model……58
4.2.3.2.1 Decolorization……64
4.2.3.2.2 TOC removal……...67
4.2.4 Solar TiO_2 Catalysis (Fe(III)/ TiO_2/Solar-UV)……70
4.2.4.1 Experimental Procedure……70
4.2.4.2 Regression Model ……..70
4.2.4.2.1 Decolorization……76
4.2.4.2.2 TOC removal……...79

4.3 Application of Box–Wilson Experimental Design Method for the Solar Degradation of Paper Industry Wastewater by Advanced Oxidation Processes……84
4.3.1 Introduction……..……84
4.3.2 Wastewater characterization……85
4.3.3 Photo-Fenton-like Process (Fe(III)/H_2O_2/Solar-UV)……...85
4.3.3.1 Experimental Procedure……...85
4.3.3.2 Regression Model……86
4.3.3.2.1 Decolorization……..91
4.3.3.2.2 TOC removal……94
4.3.4 Solar TiO_2 Catalysis (Fe(III)/TiO_2/Solar-UV)…….……97
4.3.4.1 Experimental Procedure……...97

4.3.4.2 Regression Model…….97
4.3.4.2.1 Decolorization……103
4.3.4.2.2 TOC removal……..106

CHAPTER FIVE – CONCLUSIONS AND RECOMMENDATIONS……111

5.1 Conclusions……111

5.2 Recommendations……..……115

REFERENCES……116

APPENDICES

CHAPTER ONE
INTRODUCTION

1.1 Introduction

Large amounts of dyes are annually produced and applied in many different industries, including the textile, paper, leather, cosmetic, pharmaceutical and food industries. The decolorization of wastewaters is still a major environmental concern because the synthetic dyes used are difficult to remove by the conventional wastewater treatment systems based on adsorption and aerobic biodegradation. In spite of the low toxic effect on receiving bodies, the dyes constitute an aesthetic problem, a few hydroxyl- and carboxyl- substituted amines and some of these aromatic amines can be toxic and carcinogenic.

Synthetic dyes and pigments released into the environment mainly in the form of wastewater effluents by textile, leather and printing industries cause severe ecological problems. These compounds have a great variety of colors and chemical structures and are recalcitrant to microbial attack. Most of the dyes are non-toxic, except for azo-dyes which comprise a large percentage of synthetic dyes and are degraded into potentially carcinogenic amines. Moreover, their color causes an aesthetic problem in the receiving waters (Bali & Karagözoğlu, 2007).

However, the degradation of such compounds by either mixed cultures or isolated enzymes is usually very slow. Conventional treatments of textile effluents such as coagulation, flocculation, sorption, electrochemical and oxidative degradation are limited by their high costs. Furthermore, since most of these processes achieve the removal by separation, they merely transfer the pollutants from one phase to another, leaving a problem of disposal of transferred material. Consequently, dyes have to be removed from wastewater before discharge. In the past, effluents containing azo dyes have been treated by adsorption onto activated carbon or by chemical coagulation. However, these traditional methods mainly transfer the contaminants from wastewater to solid wastes. Therefore, advanced oxidation is a potential alternative to

decolorize and to reduce recalcitrant wastewater loads from textile dyeing and finishing effluents (Bali, 2004).

The presence of toxic and/or refractory compounds in the discharge of wastewaters and in some cases in water supplies is, today, a topic of global concern. One other important group of such chemicals is the halogenated organic compounds. Halogenated organic compounds, particularly chlorinated organic compounds are generated from a number of industrial manufacturing processes, mainly including pulp and paper, dyestuffs, pesticides, metal-organic compounds, process wastewater with high adsorbable organic halogens (AOX) content, wastewater from the explosive production industry. The fate of halogenated organic compounds in the environment is of great importance as these compounds are found to be toxic, recalcitrant and bioaccumulating in organisms and hence their discharge into the environment must be regulated (Baycan, 2005).

Biological treatment is generally used for the removal of organic pollutants from wastewater and its great popularity for serving this vital function results largely from its low cost and its effectiveness for removing many soluble and colloidal organics. Nevertheless, industrial effluents are known to contain above mentioned toxic and/or non-biodegradable organic substances and considerable variation exists in the literature on the efficiency of conventional aerobic as well as anaerobic biological treatment processes for the removal of chlorinated hydrocarbons. The microorganisms used in biological treatment can easily be destroyed by shock loading or rapid increases in the amount of toxic material fed to the process. A considerable period of time may be required to reestablish an adequate population of microorganisms to treat the waste. Unfortunately, there is no single, simple approach that can guarantee success. In fact, the prediction of the removal of individual toxic organic chemicals remains a very difficult task, with disparities in performance between lab-scale and full-scale systems.

In many cases, conventional treatment technologies, such as air stripping, carbon adsorption, biological treatment, and chemical precipitation have limitations. Therefore, various treatment technologies have been developed over the last 10 to 15 years in order to cost-effectively meet these requirements. One such group of technologies is commonly referred to as advanced oxidation processes (AOPs). AOPs have been proposed as potentially powerful methods which are capable of transforming such kind of pollutants into harmless substances (Baycan, 2005). Various methods have been employed for the generation of hydroxyl radicals such as Fe(III)/H_2O_2/UV or Fe(III)/ TiO_2/UV. These can quickly and non-selectively oxidize a broad range of organic pollutants (Bali & Karagözoğlu, 2007).

Among many AOPs, solar treatment processes (combination of H_2O_2, Fe(II)/Fe(III) and solar irradiation, specially) has been approved to be rather effective in degradation and mineralization of single organic toxicants and the mixtures of various organic wastes, including high TOC (Xu, Wang & Hao, 2007).

1.2 Objectives and Scope

This thesis is designed to investigate solar treatment as a treatment alternative of a synthetic dye (Remazol Brilliant Blue R-A) and certain industrial wastewaters (textile and paper). Investigate of effluent characteristics, examining the possible wastewater treatment methods that would result the best reduction in pollution content were the main aims of the thesis.

The major objectives of this thesis can be summarized as follows;

- To investigate feasibility of solar oxidation first time in Turkey by using a solar reactor.

- To investigate effectiveness of various advanced oxidation technologies for the treatment of synthetic dye Remazol Brilliant Blue R-A and textile and paper industry wastewaters by using a solar reactor.

- To determine most effective advanced oxidation process for the treatment of synthetic dye Remazol Brilliant Blue R-A and textile and paper industry wastewaters.

- To investigate the removal performances of solar oxidation methods such as hydrogen peroxide (H_2O_2) or titanium dioxide (TiO_2) oxidation based on the removal of COD, BOD, TOC and color.

- To evaluate the effects of reaction conditions such as oxidant concentration, catalyst concentration, flowrate and the combinations of the parameters and other conditions on wastewater treatment performance by employing a Box–Wilson experimental design.

- To decide the most appropriate oxidant concentration, catalyst concentration and flowrate for COD, BOD, TOC and color removal.

- To evaluate the effects of operation conditions for the selected oxidation methods.

- To determine the optimum chemical dosages for each advanced oxidation method to reach better efficiency.

- To determine oxidant concentration, catalyst concentration, flowrate for the advanced oxidation process.

In the scope of this study, some advanced oxidation technologies which are Fe(III)/H_2O_2/Solar-UV or Fe(III)/TiO_2/Solar-UV were applied by using Box-Wilson Central Composit Design Method for determination of optimum conditions for treatment of the synthetic dye Remazol Brilliant Blue R-A and textile and paper industry wastewaters. COD, BOD, TOC and color parameters were used in order to evaluate and compare the treatment performance of these different oxidation methods.

CHAPTER TWO
LITERATURE REVIEW

2.1 General Information on Advanced Oxidation Processes

The wastewater treatment is based upon various mechanical, biological, physical and chemical processes. In fact, this is a combination of many operations like filtration, flocculation or chemical oxidation of organic pollutants. After filtration and elimination of particles in suspension, the biological treatment is the ideal process (natural decontamination). Unfortunately, all organic pollutants are not biodegradable and there is a class of products noted as bio-recalcitrant organic compounds. The last progresses in the decontamination of water concern the treatment of these compounds. These methods rely on the formation of highly reactive chemical species, which degraded the more recalcitrant molecules into biodegradable compounds. These are called the advanced oxidation processes (AOPs).

Advanced Oxidation Processes (AOPs) are of considerable interest for the treatment of wastewaters containing toxic and/or refractory organic pollutants, contaminated surface and ground waters and for the production of ultrapure water. AOPs are light-induced oxidation processes (Legrini, Oliveros & Braun, 1993).

The successful application of AOPs depends primarily on the nature of the pollutants. All AOPs are based on the generation of hydroxyl radicals (initiator) from an oxidant to be added. It is generally accepted that the oxidant species of these AOPs is the hydroxyl radical (•OH) which can be generated in water through different combination of oxidants, like ozone and hydrogen peroxide or of a single oxidant and UV radiation. Once the hydroxyl radicals are produced, they oxidize organic and inorganic substrates (M, R-H …) according to the general reactions (2.1) to (2.3), ultimately resulting in the mineralization of the organic compound (Braun & Oliveros, 1997).

* hydrogen abstraction

$$\bullet OH + R\text{-}H \rightarrow H_2O + \bullet R \qquad \text{(Eq. 2.1)}$$

* electrophilic addition

$$\bullet OH + R_2C{=}CR_2 \rightarrow \bullet CR_2\text{-}C(OH)R_2 \qquad \text{(Eq. 2.2)}$$

* electron transfer

$$\bullet OH + M^n \rightarrow M^{n+1} + (HO^-)_{aq} \qquad \text{(Eq. 2.3)}$$

The hydroxyl radical which is used as a basic oxidation radical in too many advanced oxidation processes has high thermodynamic oxidation potential. Oxidation potentials of some oxidants present in water are listed in Table 2.1. The hydroxyl radical reacts with organic pollutants $1x10^6$~$1x10^9$ times faster in comparison to ozone (O_3). Rate constants of some organic compounds which react with O_3 and •OH are listed in Table 2.2 (EPA, 1998).

Table 2.1 Oxidation potential of several oxidants in water.

Oksidant	**Oxidation potential (eV)**
(•OH)	2,80
$O(^1D)$	2,42
O_3	2,07
H_2O_2	1,77
ClO_2	1,50
Cl_2	1,36
O_2	1,23

Table 2.2. Rate constants for O_3 and •OH reactions with organic compounds in water

	Rate constants (1/Ms)	
Compound Type	**O_3**	**•OH**
Acetylene	50	10^8 - 10^9
Alcohol	10^{-2} - 1	10^8 - 10^9
Aldehyde	10	10^9
Alkane	10^{-2}	10^6 – 10^9
Carboxylic Acid	10^{-3} - 10^{-2}	10^7 – 10^9
Ketone	1	10^9 – 10^{10}
Olefin	1 – 450x10^3	10^9 – 10^{11}
Phenol	10^3	10^9 – 10^{10}

The factors affecting the performance of an individual AOP for an individual pollutant can be summarized as; (1) concentration and type of the organic pollutant, (2) concentration of the oxidant, (3) concentration of the catalyst, (4) power of the UV lamp or light intensity, (5) pH of the solution, (6) temperature of the medium and (7) the other constituents present in water (hydroxyl radical scavengers).

The concentration of the oxidant added is important because concentrations exceeding a certain stoichiometric ratio, such as in the case of H_2O_2, may not improve the respective maximum degradation. This may be due to autodecomposition of H_2O_2 to oxygen and water and the recomposition of •OH radicals as follows:

$$2\ H_2O_2 \rightarrow 2H_2O + O_2 \qquad \text{(Eq. 2.4)}$$

$$\bullet OH + H_2O \rightarrow H_2O + HO_2\bullet \qquad \text{(Eq. 2.5)}$$

Since the •OH radicals react with H_2O_2, the H_2O_2 itself contributes to the •OH scavenging capacity, thus, decreases of amount of •OH radicals reacting with organics. Therfore, H_2O_2 should be added at the optimal concentration to achieve the best degradation (Bali, 2002).

The amount of added catalyst (Fe(III)), especially in Photo-Fenton-like process, is another important factor because addition of Fe(III) above a certain concentration also does not effect the degradation. Higher concentration than the optimum one even may result in a brown turbidity that hinders the absorption of the UV light required for photolysis and causes the recombination of •OH radicals.

It is desirable that the ratio of H_2O_2 and Fe(III) should as small as possible, so that the recombination can be avoided and the sludge production from the iron complex is also reduced (Neyens & Baeyens, 2003).

Many organic and inorganic chemicals in the environment absorb sunlight and undergo transformation to new molecular species. As implied by the term AOPs, light energy is one of the essential components of an AOP technology. Depending on the type of AOP technology employed UV radiation of wavelengths from 100 to 400 nm or visible radiation (400 to 700 nm) is used to produce •OH. The UV spectrum is arbitrarily into three bands (Augugliaro at al., 1996).

- UV-A (315 to 400 nm)
- UV-B (280 to 315 nm)
- UV-C (100 to 280 nm)

UV-A and UV-C are generally used for the environmental applications. UV-A radiation is also referred to as long-wave radiation, near-UV radiation, or black light. Most UV-A lamps have their peak emission at 365 nm, and some have their peak emission at 350 nm. UV-C radiation, which is also referred to as short-wave radiation, is used for disinfection of water and wastewater.

2.2 Theoretical Background

2.2.1 Photo-Fenton-like Process (Fe(III)/H_2O_2/UV)

The Photo-Fenton-like reaction is a widely used catalytic oxidation method based on electron transfer between H_2O_2 and metal ions (Fe(III)) serving as homogeneous catalyst enhanced by irradiation with UV-visible light. This effectiveness has been proven by the total mineralization of many organic compounds in aqueous solution (Neyens & Baeyens, 2003).

The reasons for the positive effect of irradiation on the degradation rate include the photoreduction of Fe(III) to Fe^{2+} ions, which produce new •OH radicals with H_2O_2 according to the following mechanisms:

$$Fe^{3+} + H_2O_2 \xrightarrow{h\nu} Fe^{2+} + \bullet OH + H^+ \quad \text{(Eq. 2.6)}$$

$$H_2O_2 \xrightarrow{h\nu} 2\bullet OH \quad (\lambda<400nm) \quad \text{(Eq. 2.7)}$$

The main compounds absorbing light in the Fenton system are Fe(III)complexes, e.g. $[Fe^{3+}(OH)^-]^{2+}$ and $[Fe^{3+}(RCO_2)^-]^{2+}$ which produce additional Fe^{2+} by following photo-induced, ligand-to-metal charge-transfer reactions:

$$[Fe^{3+}(OH)^-]^{2+} \xrightarrow{h\nu} Fe^{2+} + \bullet OH \quad (\lambda<\text{ca. } 450nm) \quad \text{(Eq. 2.8)}$$

$$[Fe^{3+}(RCO_2)^-]^{2+} \xrightarrow{h\nu} Fe^{2+} + CO_2 + \bullet R \quad (\lambda< \text{ ca. } 500nm) \quad \text{(Eq. 2.9)}$$

Additionally, Eq. 2.8 yields •OH radicals, while Eq. 2.9 results in a reduction of the TOC content of the system due to the decarboxylation of organic-acid intermediates.

2.2.2 Solar TiO_2 Catalysis (Fe(III))/TiO_2/UV)

The solar heterogeneous photocatalytic detoxification process consists in utilizing the near-UV part of the solar spectrum (wavelength 315 to 400 nm), to photoexcite a semiconductor catalyst in the presence of oxygen. Either bound hydroxyl radical or free holes, which attack oxidizable contaminants, are generated producing a progressive breaking of molecules yielding to CO_2, H_2O and dilute inorganic acids. The most commonly used catalyst is the semiconductor TiO_2 (cheap, non-toxic and abundant product) (Mahmoodi, Arami & Limaee, 2006).

Titanium dioxide (TiO_2) was used as the photocatalyst in the experiments. The mass of TiO_2 was scaled and then added to the solution in the reactor to obtain a uniform concentration at the desired amount (see chapter 4.1.2.2).

2.2.3 AOX Problem in Wastewaters

The AOX is a measure for halogenated organic compounds and is an important parameter for the characterization of industrial wastewaters. A large number of AOX causing substances show a significant eco-toxicity. Those wastewaters often cause technical and financial problems for specific industrial branches. In addition to direct entry of organohalogen bonding compounds into water, the indirect AOX entry still exists, with which one AOX-causal substances only form themselves in the water/wastewater. It is well known that, chlorination of the drinking water or swimming pool water caused the unwanted formation of chloroform and other halogenated follow-ions for example the chloramines. Another source of the AOX in wastewater is the application of chlorous budget cleaners (chloramine T, chloramine BARS, sodium hypochlorite, chloric lime). Concerning hypochlorite is the following chemical balance substantial (Baycan, 2005);

$$Cl_2 + 3H_2O \rightleftharpoons OCl^- + Cl^- + 2H_3O^+ \qquad \text{(Eq. 2.10)}$$

The chloride addition can be formulated in a simplified manner as follows:

$$Cl_2 + RH\,C = C\,HR \rightarrow RH\,CCl - C^+\,HR + Cl^- \quad \text{(Eq. 2.11)}$$

$$Cl^- + RH\,CCl - C^+\,HR \rightarrow RH\,CCl - CCl\,HR \quad \text{(Eq. 2.12)}$$

Many industrial wastewaters have extraordinary high chloride ion concentrations due to the extensive use of sodium chloride. High Cl^- concentrations may cause serious corrosive problems with reactor components consisting of stainless steel. Dissolved chloride ions react rapidly with •OH radicals as described by the following equation;

$$\bullet OH + Cl^- \rightarrow \bullet ClOH^- \quad \text{(Eq. 2.13)}$$

$$\bullet ClOH^- + H^+ \rightarrow \bullet Cl + H_2O \quad \text{(Eq. 2.14)}$$

$\bullet ClOH^-$ can decompose to yield chlorine radical (Eq. 2.14). Chlorine radicals can add to C=C double bonds of compounds present during AOP treatment, thus generating chlorinated hydrocarbons (Eq. 2.15). Hence, this process may lead to an undesirable increase of the global parameter AOX;

$$\bullet Cl + R_2C{=}CR_2 \rightarrow \bullet R_2ClC - CR_2 \rightarrow\rightarrow\rightarrow \text{chlorohydrocarbons, formation of AOX.} \quad \text{(Eq. 2.15)}$$

2.2.4 Photocatalytic Reactor Types

2.2.4.1 General Information

The artificial generation of photons required for the detoxification of polluted water is the most important source of costs during the operating of photocatalytic wastewater treatment plants. This suggests to use the sun as an economically and ecologically sensible light source. With at typical UV-flux near the surface of the earth of 20–30 W/m^2 the sun puts 0.2–0.3 mol photons/m^2/h in the 300–400 nm range at the process disposal. Principally these photons are suitable for destroying water pollutants in photocatalytic reactors (Ajona & Vidal, 2000).

Contrary to solar thermal processes, which are based on the collection of large quantities of photons of all wavelengths to reach a specific temperature range, solar photochemical processes are based on the collection of only high-energy short-wavelength photons to promote photochemical reactions. Most of the solar photochemical processes use UV or near-UV sunlight (300–400 nm), but in some photochemical synthesis processes, up to 500 nm sunlight can be absorbed and photo-Fenton heterogeneous photocatalysis uses sunlight up to 580 nm. Sunlight at wavelengths over 600 nm is normally not useful in any photochemical process (Augugliaro at al., 1996).

Over the last 15 years several reactors for the solar photocatalytic water treatment have been developed and tested. In the following, the four most frequently used reactor concepts will be presented.

2.2.4.2 Parabolic Trough Reactor (PTR)

A parabolic trough reactor (PTR) concentrates the parallel (direct) rays of the photocatalytically active ultra-violet part of the solar spectrum by a factor of 30–50 and can be characterized as a typical plug flow reactor. This reactor type had been chosen for the first solar detoxification loops constructed in the USA in Albuquerque (by Sandia National Laboratories), in California (by Lawrence Livermoore Laboratories) and in Spain in Almeria (by the Plataforma Solar de Almeria, PSA). Parallel to investigations under direction of NREL and Sandia National Laboratories in New Mexico (USA) and in California several research groups from different European countries, funded by the European Community, have tested the parabolic trough reactor installed at the PSA (Spain) for solar wastewater treatment in the early 1990s.

Figure 2.1 shows a schematic flow chart of the installation at the PSA. The reactor located at the Plataforma Solar de Almeria in Spain contained a total volume of 419 L and consisted of six parabolic trough modules connected in series (type ‘‘Helioman’’ from Mannesmann, initially designed for the conversion of solar

radiation into heat) which were controlled by a two-axial (azimuth and elevation) tracking system. The solar rays were concentrated by parabolic trough mirrors (total aperture area: 192m^2) with an aluminized UV-reflective surface and focused on borosilicate glass tubes (total length: 108 m, illuminated volume: 242 L), which were filled with the contaminated aqueous TiO_2 suspensions moving at flow rates between 250 and 3500 L/h. Due to losses caused by reflectivity, translucence and system errors the yield of the UV-light photons reaching the contaminated suspensions is about 58% of the original light intensity entering the aperture plane (Bahnemann, 2004).

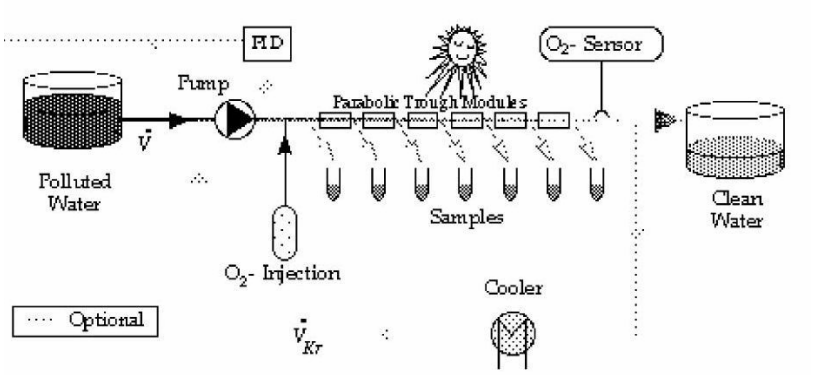

Figure 2.1 Flow Chart of the PTR installation located at the Plataforma Solar de Almeria in Spain.

2.2.4.3 Thin Film Fixed Bed Reactor (TFFBR)

One of the first solar reactors not applying a lightconcentrating system and thus being able to utilize the diffuse as well as the direct portion of the solar UV-A irradiation for the photocatalytic process is the thin-film-fixed-bed reactor (TFFBR) depicted in Figure 2.2. It should be noted that under AM (air mass) 1.5 conditions the diffuse (E_{dif} (300–400nm) = 24.3W/m^2) and direct (E_{dir} (300–400nm) = 25.0W/m^2) portion of the solar radiation reaching the surface of the earth are almost equal. This means that a light concentrating system, e.g. a parabolic trough reactor can in principal only employ half of the solar radiation available in this particular spectral region. The most important part of the thin-film-fixed-bed reactor is a sloping plate

(width 0.6m x height 1.2m) coated with the photocatalyst (e.g., titanium dioxide) and rinsed with the polluted water in a very thin film (~100µm). The flow rate is controlled by a cassette peristaltic pump and can be varied between 1 and 6.5 L/h (Bahnemann, 2004).

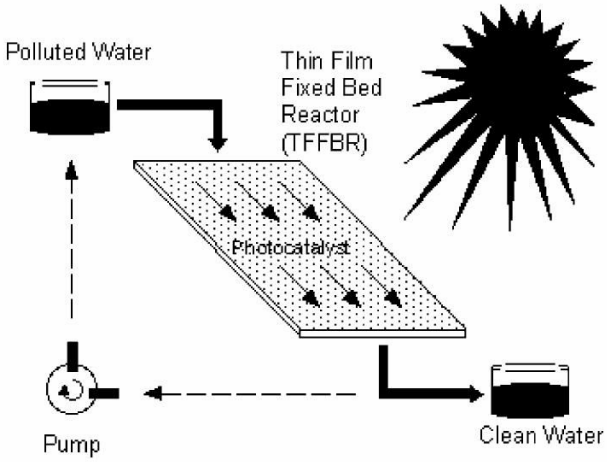

Figure 2.2 Flow chart of a TFFBR reactor

2.2.4.4 Compound Parabolic Collecting Reactor (CPCR)

A compound parabolic collecting reactor (CPCR) is a trough reactor without light concentrating properties. It differs from a conventional parabolic trough reactor by the shape of its reflecting mirrors. A reflector of a parabolic trough reactor has a parabolic profile with the reaction pipe in its focal line. Consequently only paralel light entering the parabolic trough can be focused into the reaction pipe and a sun-tracking system is required. The shape of a CPCR's reflector usually consists of two half circular profiles side by side, and a parabolic continuation at both outer sides of the circles. The focal line is located closely above the connection of the two circles. This geometry enables light entering from almost any direction to be reflected into the focal line of the CPCR, i.e., most of the diffuse light entering the module can also be employed for the photocatalytic reaction. Due to this geometry a CPCR exhibits only a small concentration factor (<1.2). The CPCRs at the Plataforma Solar de Almeria in Spain (PSA) manufactured by Industrial Solar Technology Corporation, Denver, Colorado (USA), have a concentration factor of 1.15, i.e., this type of reactor has practically no light concentrating properties.

Moreover, a CPCR must not necessarily track the sun due to its geometry. The azimuth should be adjusted to the complementary angle a of the geographical altitude and the pipes should be aligned south and from top to bottom. A schematic view of one CPCR-module at the PSA is given in Figure 2.3. The angle of incidence a is adjusted to 37^{o} for all CPCR modules at the PSA.

One CPCR-module of the PSA consists of eight paralel reflectors made from polished aluminum. This material has very good reflection properties especially in the UV-region of the solar spectrum. In the spectral range of 295–387nm its reflection efficiency is 83.2%. A single CPCR reflector has a length of 1.22m and a width of 0.152m, i.e., the effective reflecting area of one module, consisting of eight reflectors adds up to $1.48m^2$. The overall reflecting area of all six modules is $8.9m^2$. A reaction pipe made of a transparent fluoropolymer (teflon) is fixed in the focal line of each CPCR reflector, through which the suspension containing the photocatalyst and the pollutant circulates. The transmissivity of teflon in the spectral range under consideration is 76.8%, thus limiting the achievable reactor efficiency to 63.9%. The absorber pipe is as long as the module (1.22m), has an inner diameter of 48mm and consequently an illuminated volume of 2.21L per pipe. The connectors between the absorber pipes consist of polypropylene; the overall illuminated volume of all 6 modules adds up to 106L. The achievable flow rates in the CPCR-module field at the PSA are between 2250 and 8000L/h and the minimum required volume is 248L (Bahnemann, 2004).

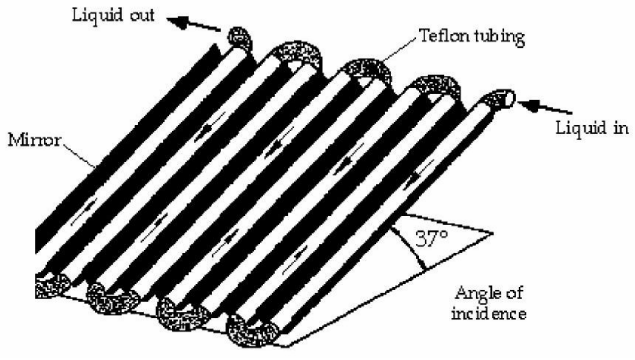

Figure 2.3 Schematic view of one CPCR-module installed at the Plataforma Solar de Almeria in Spain.

2.2.4.5 Double Skin Sheet Reactor (DSSR)

A new kind of non-concentrating reactor is the double skin sheet reactor (DSSR). It consists of a flat and transparent structured box made of plexiglas. The inner structure of the reactor is schematically drawn in Figure 2.4. The suspension containing the model pollutant and the photocatalyst is pumped through these channels. The comparison of the spectral irradiance of the sun (AM 1.5) with the transmission spectrum of the plexiglas used to manufacture the double skin sheets evinces that the UV-A portion of the solar spectrum below 400nm nicely matches with the onset of the plexiglas transmission. This type of reactor can utilize both the direct and the diffuse portion of the solar radiation in analogy to the CPCR. After the degradation process the photocatalyst has to be removed from the suspension either by filtering or by sedimentation for both reactors.

The DSSR consists of a modified double-skin sheet (SDP 16/32) manufactured by the Röhm GmbH in Darmstadt (Germany). One module has a length of 1400mm, a width of 980mm and contains 30 channels each of which being 28.5mm by 12mm, and their total inner volume adds up to 14.4L in a single sheet.

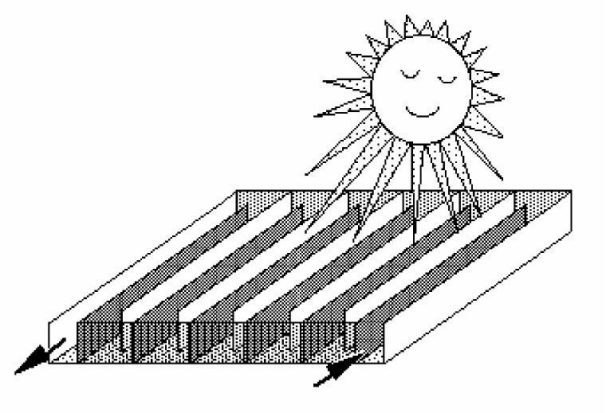

Figure 2.4 Schematic view of a DSSR reactor showing the inner structure of the transparent structured box made of plexiglas

CHAPTER THREE
MATERIALS AND METHODS

3.1 Materials

In the experimental studies, different chemical and photochemical oxidation processes were applied to the synthetic wastewaters and pre-treated industry effluents taken from the existing full-scale treatment plant outlets for investigation of treatment performance.

The azo dye Remazol Brilliant Blue R-A, which is used in textile dyestuffs in the Turkish textile industry, was used to prepare synthetic wastewater without further purification. An amount of 1g/L Remazol Brilliant Blue R-A stock solutions were prepared for further dilution to obtain solutions of desired concentrations. Aqueous solution of azo dye was prepared with distilled water and concentration of the dyestuff in the solution was adjusted to 50mg/L in all experiments. Characteristics of the azo dye used in the study are listed in Table 3.1.

The materials used as oxidants in oxidation experiments were; hydrogen peroxide (H_2O_2) and titanium dioxide (TiO_2). H_2O_2 solution (35% (w/w)), in stable form, was provided from Merck. The powder form of TiO_2 (Degussa p25) was used in titanium dioxide photocatalysis. Iron sulphate ($Fe_2(SO_4)_3 \cdot 7H_2O$) used as source of Fe(III), was analytical grade and obtained from Merck. An amount of 10g/L Fe(III) stock solution were prepared for further dilution to obtain solutions of desired concentrations. Fe(III) stock solution was stored at dark place to prevent reduction of Fe(III). In order to prevent further oxidation of organics, excess H_2O_2 should be removed. For this aim, MnO_2 was added to collected aqueous samples. Distilled water was used in cleaning and experimentation.

Table 3.1 Main characteristics of Remazol Brilliant Blue R-A

Usage	Textile dyestuffs
Composition	C.I. Reactive Blue 19
Form	Powder
Color	Dark blue
Odor	Odourless
Solubility	>100g/L
pH	4.5 – 6.5 (20 °C, 30g/L)
Thermic decomposition	>200°C
Chemical oxygen demand (COD)	1250mg/L
Biochemical oxygen demand (BOD)	425mg/L
Total organic carbon (TOC)	475.40mg/L

3.2 Methods

3.2.1 Analytical Methods

The measured parameters of wastewater during the experiments were chemical oxygen demand (COD, mg/L), biochemical oxygen demand (BOD_5, mg/L), total organic carbon (TOC, mg/L), adsorbable organic halogen compounds (AOX, µg/L) and color (pt-co).

3.2.1.1 Chemical Oxygen Demand (COD) Analysis

COD measurements were carried out according to procedures given in Standard Methods for the Examination of Water and Wastewater (21st Ed. 2005), open reflux method 5220 B.

3.2.1.2 Biochemical Oxygen Demand (BOD_5) Analysis

BOD_5 measurements were carried out according to procedures given in Standard Methods for the Examination of Water and Wastewater (21st Ed. 2005), 5 day BOD test, 5210 B.

3.2.1.3 Total Organic Carbon (TOC) Analysis

Total organic carbon (TOC) analyses were carried out by using a DOHRMANN DC-190 High Temperature TOC Analyser. The instrument was calibrated by standard solutions of potassium hydrogen pthalate (KHP, 3.125-50, 50-1000mg/L) and calibration curves were established by linear regression.

3.2.1.4 Color Analysis

A HACH-LANGE DR 5000 model spectrophotometer was used for the color measurements.

3.2.1.5 Adsorbable Organic Halogen Compounds (AOX) Analysis

A AOX-MT 20 Analyser was used for adsorbable organic halogen compounds measurements in µg/L unit.

3.2.2 Photodegradation Experiments

3.2.2.1 Solar Reactor

All experiments are performed in a batch solar reactor with a total volume of 40L. The solar reactor consists of sun light collectors, water preparation tank, circulation pump and a control panel. The sun light collectors are made of borosilicate glass cylindrical tubes and do not contain any metal parts. Eigth borosilicate glass tubes are in serial connected in conjunction with plastic cylindrical particals. One tube has

a length of 100cm and a diameter of 3cm. The sun light collectors are mounted on a fixed platform tilted 37^{o} (local latitude) and connected in series so that the water flows directly from one to another and finally to the water preparation tank. A circulating pump then returns the water to the collectors.

Aluminum UV-reflective screens are also situated on the plate which are focused on borosilicate glass tubes. This geometry enables light entering from almost any direction to be reflected into the focal line of the tubes and the light entering the tubes can also be employed for the photocatalytic reaction.

Water preparation tank is made of stainless steel. The water preparation tank has double layers; inner layer is used for experimental water and and the outer layer is used for cooling water and they have diameters of 40 and 46cm, respectively. The water preparation tank has a lid for filling and dosing of experimental reagents. In addition, there is a thermocouple in the water preparation tank to measure the reaction temperature and a mechanical mixer. Circulating pump is used to provide circulation of experimental water between preparation tank and sun light collectors. The maximum capasity of the circulating pump is 500L/h and also there is a flowmeter integrated with the circulation pump. Whole system is controled by the control panel. Front and back viewes of the pilot scale solar reactor are shown in Figure 3.1.

(a)

(b)

Figure 3.1 (a) Front view of the pilot scale solar reactor (b) Back view of the pilot scale solar reactor

3.2.2.2. Box–Wilson Central Composit Design

A fitting and analyzing response surface is greatly facilitated by the proper choice of an experimental design. When selecting a response surfaces design, some of the features of a desirable design are as follows;

1. Provides a reasonable distrubution of data points (and hence information) throughout the region of interest.

2. Allows model adequacy, including lack of fit, to be investigated.

3. Allows experiments to be performed in blocks.

4. Allows designs of higher-order to be built up sequentially.

5. Provides an interval estimate of errors.

6. Does not require a large number of runs.

7. Does not require too many levels of the independent variables.

8. Ensure simplicity of calculation of the model parameters.

The Box–Wilson experimental design, commonly called ‘a central composite design’, is a response surface methodology used for evaluation of a dependent variable as functions of independent variables (Bali, 2004). The Box–Wilson design is an empirical modeling technique devoted to the evaluation of the relationship of a set of controlled experimental factors and observed results.

Chemical and biological reaction mechanisms, characterization and designment of engineering systems and optimization of process are mainly application areas of Box-Wilson statistical design method. Box-Wilson statistical design method erduces

development time and overall costs, denotes effects of independent parameters on dependent parameters, determines which independent parameter is the most effective one and produces combinations of independent parameters that provides optimum design conditions.

Basically this optimization process involves three major steps; performing the statistically designed experiments, estimating the coefficients in a mathematical model, and predicting the response and checking the adequacy of the model.

(a) Recognition of and Statement of the Problem. It is often not simple to realize that a problem requiring experimentation exists, nor is it simple to develop a clear and generally accepted statement of this problem. It is necessary to develop all ideas about the objectives of the experiment. A clear statement of the problem often contributes substantially to be a beter understanding of the phenomena and the final solution of the problem. The Box–Wilson statistical experimental design was employed to determine the effects of operating variables on removal efficiencies and to find the combination of variables resulting in maximum removal efficiency of each parameter in this study.

(b) Selection of Design Parameters and Ranges. The experimenter chooses the factors to be varied in the experiment, the ranges over which these factors will be varied, and the specific levels at which runs will be made. Independent variables (X_1, X_2, …) and their studyind ranges and dependent variables (Y_1, Y_2, …) are determined in this study.

(c) Determination of Experimental Points. Maximum, minimum, intermediate and center points of choosen independent variables are calculated by using following equations (Eq. 3.1-3.2). Coded forms of the calculated values of variables are given in Table 3.2.

$$center = \frac{(\max + \min)}{2} \quad \text{(Eq. 3.1)}$$

$$intermediate = \text{center} \pm \left[\frac{\max - \min}{2N} \right] \quad \text{(Eq. 3.2)}$$

where;

$N=P^{½}$;

P = number of independent variable

Table 3.2 Coded forms of the calculated values of variables

value	**coded form**
maximum	+k
minimum	-k
İntermediate	±1
center	0

(d) Permorming the Experiments. The experiments consist of six axial (A), eight factorial (F) and centre points. The centre point is repeated three times at least. Axial points are where an independent variable is at the extreme (max or min) point and the other independent variables are at the center points. Factorial points are made of combinations of intermediate points of independent variables. Finally, center points are where all the independent variables are at their center points. In this study, the center point was repeated four times and there were 18 runs totally. Structure of a Box-Wilson Experimental Design for three factors are given in Table 3.3.

Table 3.3 Structure of a Box-Wilson Experimental Design for three factors.

	Replicate	No	X1	X2	X3
Axial points	1	A1	+k	0	0
	1	A2	-k	0	0
	1	A3	0	+k	0
	1	A4	0	-k	0
	1	A5	0	0	+k
	1	A6	0	0	-k
Factorial points	1	F1	1	1	1
	1	F2	1	1	-1
	1	F3	1	-1	1
	1	F4	1	-1	-1
	1	F5	-1	1	1
	1	F6	-1	1	-1
	1	F7	-1	-1	1
	1	F8	-1	-1	-1
Centre points	4	C	0	0	0
Total runs =18					

(e) Data Analysis. If the experiment has been designed correctly and if it has been performed according to the desing, then the statistical methods required are not elaborated. Graphical mehtods play an important role in data interpretation. Computation was carried out using multiple regression analysis using the least squares method in this study. The following response function (Eq. 3.3) was used in correlating the removal efficiencies of each parameter. A STATISTICA computer program was employed for the determination of the coefficients of equation by regression analysis of the experimental data for each .

$$Y = b_0 + b_1X_1 + b_2X_2 + b_3X_3 + b_{12}X_1X_2 + b_{13}X_1X_3 + b_{23}X_2X_3 + b_{11}X_1^2 + b_{22}X_2^2 + b_{33}X_3^2 \quad \text{(Eq. 3.3)}$$

where;

Y = predicted yield

b_0 = constant

b_1, b_2, b_3 = linear coefficients

b_{12}, b_{13}, b_{23} = cross product coefficients

b_{11}, b_{22}, b_{33} = quadratic coefficients.

3.2.2.3 Photocatalytic Experimental Procedure With Synthetic Wastewater

For a standard reaction run, 40L of aqueous solution was used with the azo dye Remazol Brilliant Blue R-A. Concentration of the dyestuff in the solution was adjusted to 50mg/L. The sun light collectors were covered with a covering before the beginning of each run. Then, Fe(III) and H_2O_2 or TiO_2 at different amounts were injected into the reactor. The circulating pump was got to work and the sun light collectors were filled with the solution. The time at which the covering is unclosed was considered time zero or the beginning of the experiment which was taking place simultaneously with the addition of H_2O_2 or TiO_2. Sampling took place at the beginning of the experiment and hourly. Reaction time was 8h. Samples were analyzed immediately to avoid further reaction.

Wavelength scan was done to find out peak wavelength that gives maximum absorbance. Peak wavelength and maximum absorbance were found 629nm and 2.893, respectively, for a Remazol Brilliant Blue R-A solution at a concentration of 1g/L. Then, a calibration curve was established by linear regression with standard solutions of Remazol Brilliant Blue R-A (10-1000mg/L) to find out relationship between absorbance and concentration at 629nm. Results of wavelength scan and calibration curve are given in Appendix–A.

3.2.2.4 Photocatalytic Experimental Procedure with Industrial Wastewaters

For each reaction run, 15L of industrial wastewater was used without dilution. Photocatalytic experiments with industrial wastewaters carried on in the same manner like synthetic wastewaters.

The significant point that must be noticed was variation of characteristics of industrial wastewaters from time to time. So, it always needed to know initial COD, BOD, TOC, AOX and color measurements. In especial, textile industry wastewaters had different colors at times depending on production processes. Therefore, wavelength scan was done for every set of new wastewater samples taken from the wastewater treatment plants of industries.

CHAPTER FOUR
RESULTS AND DISCUSSION

4.1 Application of Box–Wilson Experimental Design Method for the Solar Degradation of Synthetic Wastewater by Advanced Oxidation Processes

4.1.1. Photo-Fenton-like Process (Fe(III)/H_2O_2/Solar-UV)

4.1.1.1 Introduction

Before starting experimentation with solar reactor some preliminary works were done in the laboratory to determine ranges of chemical dosages. 500mL aqueous solution of the azodye Remazol Brilliant Blue R-A was prepared at a concentration of 50mg/L in a beaker. Then Fe(III) and H_2O_2 at different amounts were injected into the beaker and they were mixed with a Jar test apparatus for 105min at 200rpm. Color and TOC concentrations were analized at predetermined time intervals. Addition of H_2O_2 was started from a stoichiometric factor of [H_2O_2]/[COD] molar ratio as 1.0. Observed color and TOC efficiencies were very high in a short time. Then stoichiometric factor decreased to 0.7, 0.5 and 0.3 respectively. Observed color and TOC efficiencies increased when stoichiometric factor decreased from 1.0 to 0.5. As stoichiometric factor decreased from 0.5 to 0.3, observed color and TOC efficiencies decreased. So, H_2O_2 concentrations were studied from 803.1mg/L (0.3xsto) to 2677mg/L (1.0xsto) in all Fe(III)/H_2O_2/Solar-UV processes. Fe(III) concentrations ranged from 0 to 1.0mM. All laboratory experimentation results are depicted at Appendix-B (Figure B1–B.5).

This chapter includes the application of Box-Wilson Experimantal Design Method for the solar degradation of synthetic wastewater by advanced oxidation.

4.1.1.2 Experimental Procedure

Experimental procedure with synthetic wastewater which prepared with the azodye Remazol Brilliant Blue R-A was explained in chapter 3.2.2.3.

H_2O_2 and Fe(III) concentration and flowrate were chosen as the independent variables and designated as X_1, X_2 and X_3 respectively. The H_2O_2 concentration (X_1) was calculated according to the COD with a range of convenient stoichiometric factors from 0.3 to 1.0. The Fe(III) concentration (X_2) was between 0 and 1.0mM according to preliminary laboratory works and flowrate (X_3) was between 10 and 50L/h. Color and TOC removal efficiencies were chosen as the dependent variables and designed as Y_1 and Y_2, respectively. Experimental points of design are presented in Table 4.1 and experimental conditions are presented in Table 4.2.

Table 4.1 Experimental points determined by the Box–Wilson statistical design (synthetic wastewater, Fe(III)/H_2O_2/Solar-UV process)

Points	**H_2O_2 (mg/L)**	**Fe(III) (mM)**	**Q (L/h)**
	X_1	**X_2**	**X_3**
+k	2677 (1.0xsto)	1.00	50.0
+1	2281 (0.85xsto)	0.79	41.5
0	1740 (0.65xsto)	0.50	30.0
−1	1199 (0.45xsto)	0.21	18.5
−k	803.1 (0.3xsto)	0.00	10.0

Table 4.2 Experimental conditions determined by the Box–Wilson statistical design (synthetic wastewater, Fe(III)/H_2O_2/Solar-UV process)

Axial points				**Factorial points**			
No.	H_2O_2 (mg/L)	Fe(III) (mM)	Q (L/h)	No.	H_2O_2 (mg/L)	Fe(III) (mM)	Q (L/h)
A1	2677	0.50	30	F1	2281	0.79	41.5
A2	803.1	0.50	30	F2	2281	0.79	18.5
A3	1740	1.00	30	F3	2281	0.2	41.5
A4	1740	0.00	30	F4	1199	0.79	41.5
A5	1740	0.50	50	F5	2281	0.21	18.5
A6	1740	0.50	10	F6	1199	0.21	41.5
Center points				F7	1199	0.79	18.5
C	1740	0.50	30	F8	1199	0.21	18.5

4.1.1.3 Regression Model

Totally, 18 experiments were done. Figure 4.1-4.6 depict variation of decolorization and TOC removal efficiency with irradiation time. Computation was carried out using multiple regression analysis that uses the least squares method. The following response functions (Eq. 4.1 and 4.2) were utilized in the correlating of the color removal efficiency (Y_C) and TOC removal efficiency (Y_{TOC}) with other independent parameters ($X1$–$X3$). The Statistica computer program was employed for the determination of the coefficients of response functions by regression analysis of the experimental data. Response functions with calculated coefficients were given in Eq. 4.1 and 4.2, and were used in calculation of predicted values of color and TOC removal efficiencies. Observed and predicted color and TOC removal efficiencies with COD and BOD removal efficiencies were given in Table 4.3.

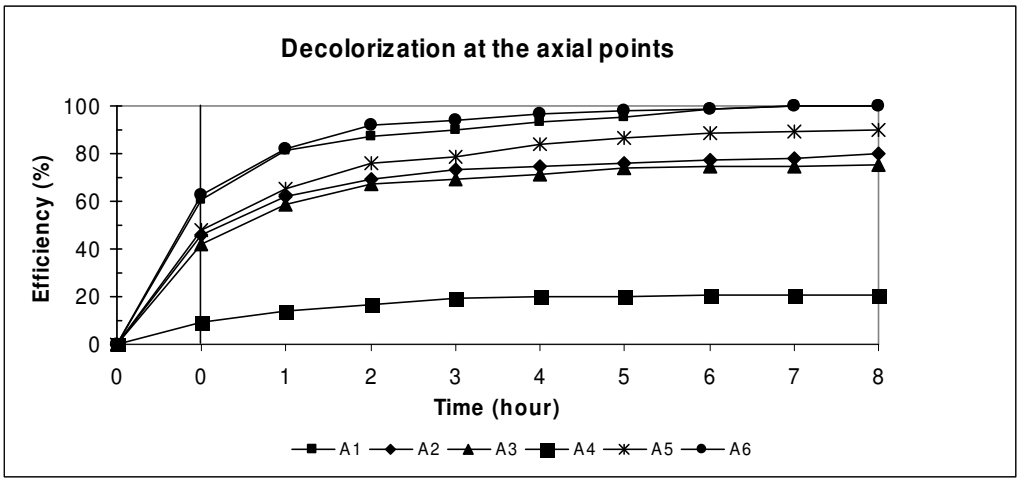

Figure 4.1 Variation of decolorization efficiency with irradiation time at axial points with Fe(III)/H_2O_2/Solar-UV process

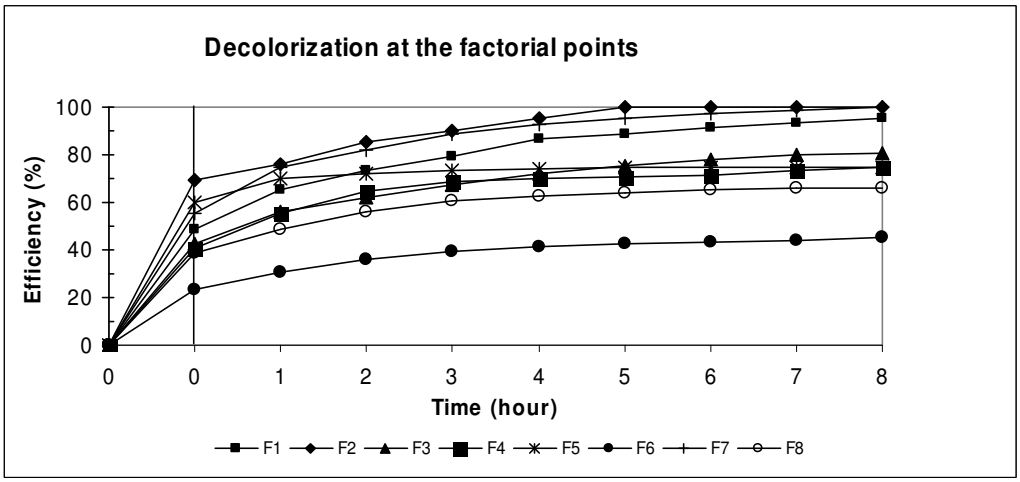

Figure 4.2 Variation of decolorization efficiency with irradiation time at factorial points with Fe(III)/H_2O_2/Solar-UV process.

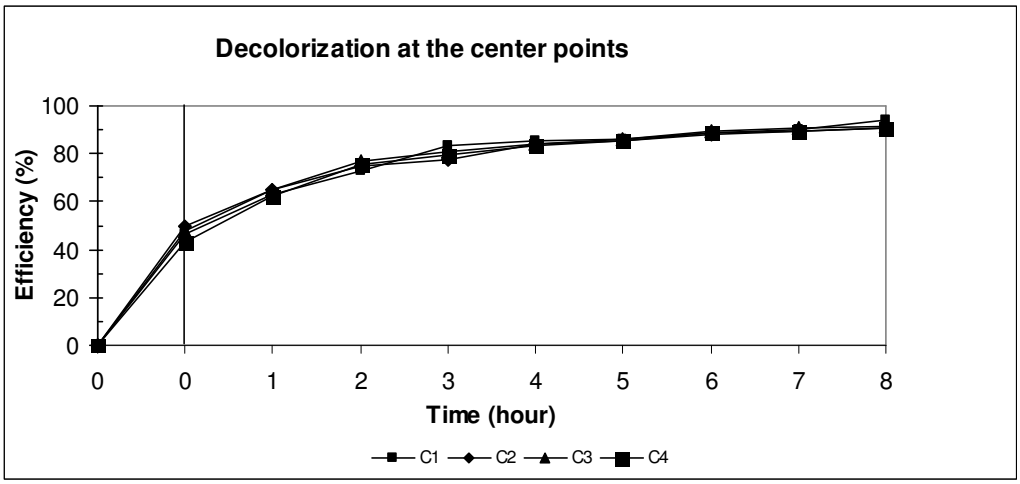

Figure 4.3 Variation of decolorization efficiency with irradiation time at center points with Fe(III)/H_2O_2/Solar-UV process.

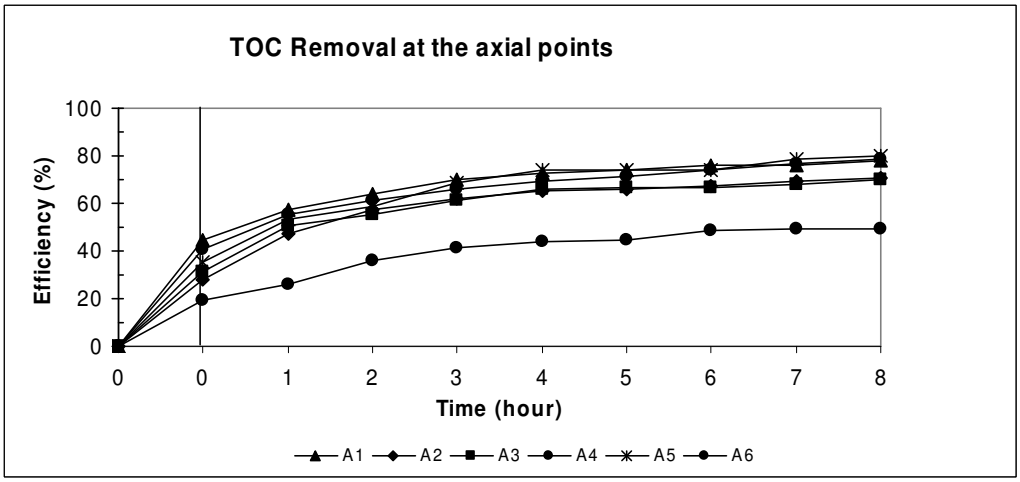

Figure 4.4 Variation of TOC removal efficiency with irradiation time at axial points with Fe(III)/H_2O_2/Solar-UV process.

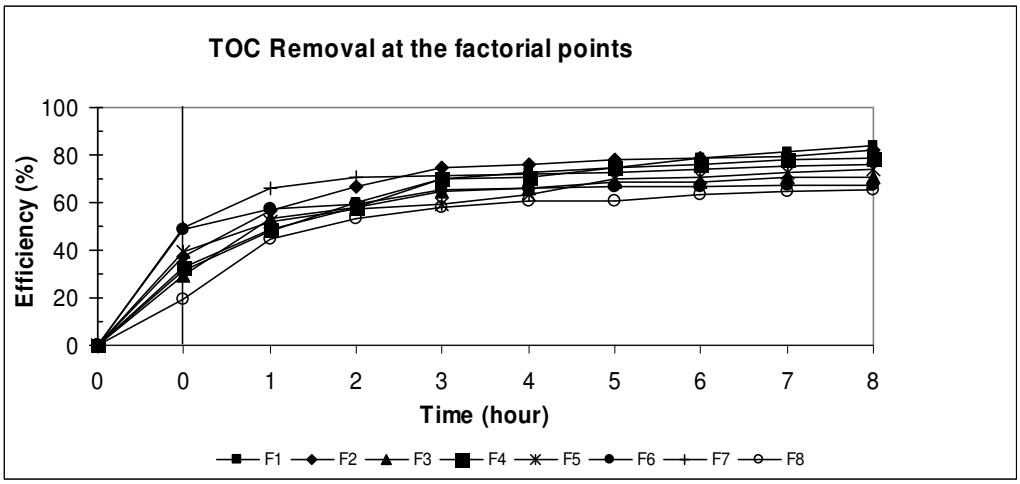

Figure 4.5 Variation of TOC removal efficiency with irradiation time at factorial points with Fe(III)/H_2O_2/Solar-UV process.

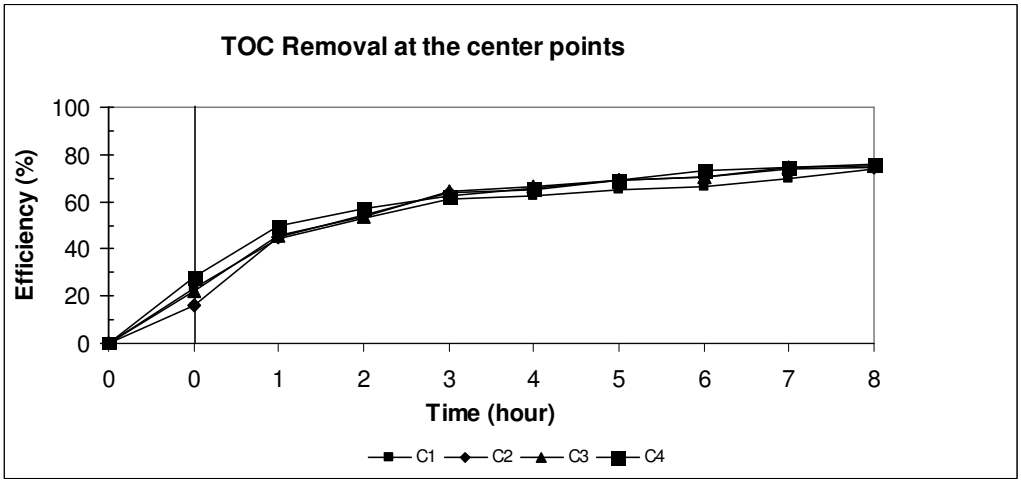

Figure 4.6 Variation of TOC removal efficiency with irradiation time at center points with Fe(III)/H_2O_2/Solar-UV process.

Response function (Y_{COL}) for color removal;

$$Y_{COL} = 52.94061 - 0.00711\ X_1 + 260.23400\ X_2 - 2.51497\ X_3 - 0.01804\ X_1X_2 + 0.00095\ X_1X_3 - 0.56884\ X_2X_3 + 2.01508*10^{-7}\ X_1^2 - 164.67191\ X_2^2 - 0.01261 X_3^2 \quad (R^2 = 0.9843) \qquad \text{(Eq. 4.1)}$$

Response function (Y_{TOC}) for TOC removal;

$$Y_{TOC} = 61.17977 + 0.00093\ X_1 + 65.50105\ X_2 - 0.88533\ X_3 - 0.00139\ X_1X_2 - 0.00011\ X_1X_3 + 0.21449\ X_2X_3 + 2.24901*10^{-6}\ X_1^2 - 50.37281\ X_2^2 - 0.01698\ X_3^2 \quad (R^2 = 0.9430) \qquad \text{(Eq. 4.2)}$$

The correlation coefficients (R^2) were 0.9843 and 0.9430 for Y_{COL} and Y_{TOC}, respectively, indicating a good agreement between the observed and predicted values of color and TOC removal efficiencies.

Table 4.3 Observed and predicted color and TOC removal efficiencies determined by the Box–Wilson statistical design with COD and BOD removal efficiencies (synthetic wastewater, Fe(III)/H_2O_2/Solar-UV process).

No.	% Color removal		% TOC removal		% BOD removal	% COD removal
	observed	predicted	observed	predicted	observed	Observed
A1	100	100	78	81	55	68
A2	80	79	71	72	55	68
A3	75	74	70	72	45	68
A4	22	27	50	53	32	36
A5	90	89	80	82	55	30
A6	100	100	78	81	55	36
F1	95	96	84	82	55	49
F2	100	97	82	81	55	36
F3	81	78	71	69	32	46
F4	75	76	79	78	32	68
F5	75	71	74	71	45	49
F6	45	46	67	65	55	36
F7	100	100	76	75	45	68
F8	66	63	65	64	45	52
C1	94	91	74	75	77	68
C2	90	91	74	75	77	68
C3	91	91	75	75	77	68
C4	90	91	76	75	77	68

Maximum color and TOC removal efficiencies were 100% and 84% and were achieved at A1 (2677mg/L H_2O_2, 0.5mM Fe(III) and 30L/h flowrate) and F1 (2281mg/L H_2O_2, 0.79mM Fe(III) and 41.5L/h flowrate) experimental conditions, respectively. More experimental results were needed to better comment on the regression model. Color and TOC removal efficiencies were predicted by using Eq. 4.1 and 4.2 when flowrate kept constant at minimum (10L/h), average (30L/h) and maximum (50L/h) value in order. Results are given in Figure 4.7-4.12.

4.1.1.3.1 Decolorization

(a) At minimum flowrate (Q=10L/h);

Color removal efficiencies with Fe(III)/H_2O_2/Solar-UV process of synthetic wastewater at minimum flowrate are presented in Figure 4.7.

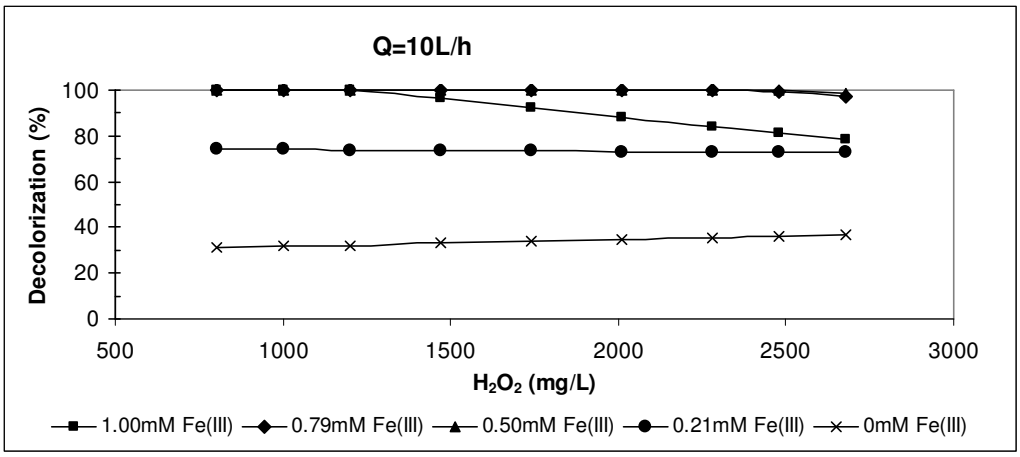

Figure 4.7 Variation of decolorization efficiency of synthetic wastewater at minimum flowrate with Fe(III)/H_2O_2/Solar-UV process.

Color removal efficiencies varied between 31% and 100% at minimum flowrate. The efficiency increased with increasing Fe(III) concentration. However, increasing the initial Fe(III) concentration enhanced the oxidation up to a certain point at which Fe(III) started to inhibit the color removal efficiency, and thus, after reaching the maximum efficiency that can be achieved at a certain Fe(III) concentration, the decreasing trend of predicted efficiency increased with the increasing of Fe(III) concentration. At Fe(III) concentrations higher than 0.79 mM, treatment efficiency decreased as shown in Figure 4.7.

In addition, the efficiency increased with increasing H_2O_2 concentration. But when Fe(III) concentration was lower than 0.50mM, increasing H_2O_2 concentration did not change the efficiency. Therewith, color removal efficiency decreased with increasing H_2O_2 concentration when Fe(III) concentration was

higher than 0.79mM. The decrease in removal efficiency at high oxidant concentrations is thought to be due to the side reactions taking place between the •OH radicals and the excess H_2O_2. When the flowrate was at minimun value, optimum concentrations of H_2O_2 and Fe(III) were 2281mg/L and 0.79mM, respectively to achieve maximum color removal efficiency.

However, this does not mean that these concentrations are also valid for different concentrations of the dyestuffs because it has already been reported that although the [H_2O_2]/[COD] molar ratio was kept constant, the removal efficiency can decline with increasing concentrations of pollutant due to, (a) the scavanging effect of high concentrations of H_2O_2 on •OH radicals, (b) the scavanging effect of intermediate products produced during the decomposition of pollutant; and (c) the decrease in the fraction of light absorbed by hydrogen peroxide due to the intermediate products.

(b) At average flowrate (Q=30L/h);

Color removal efficiencies with Fe(III)/H_2O_2/Solar-UV process of synthetic wastewater at average flowrate are presented in Figure 4.8.

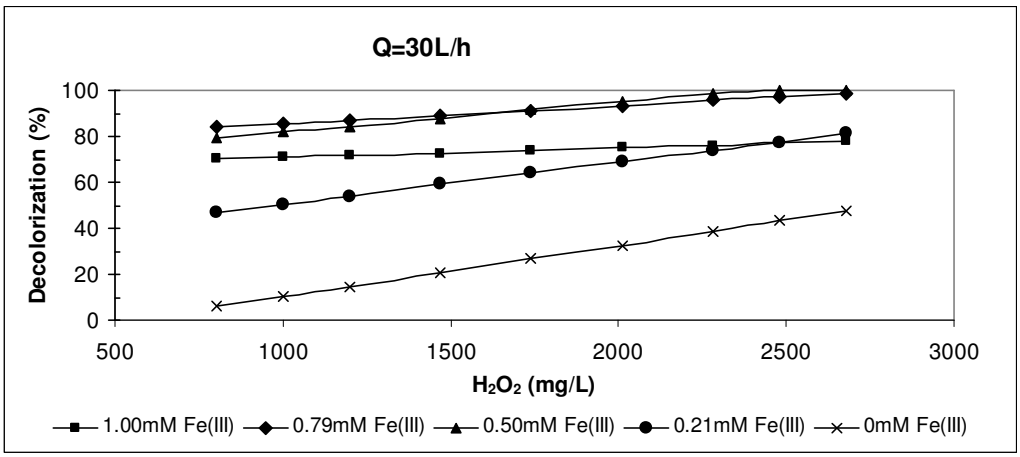

Figure 4.8 Variation of decolorization efficiency of synthetic wastewater at average flowrate with Fe(III)/H_2O_2/Solar-UV process.

Color removal efficiencies varied between 6% and 100% at average flowrate. The efficiency increased with increasing H_2O_2 concentration. In addition, efficiency increased with the increasing Fe(III) concentration from 0 to 0.50mM. The efficiency decreased with the increasing Fe(III) concentration from 0.50 to 1.00mM. Moreover, increasing trend of efficiency decreased when Fe(III) concentration was higher than 0.5mM. When Fe(III) concentration was 1.00mM increase in efficiency was about 0%. It was due to the fact that recolorization of water took place by higher Fe(III) concentration. When the flowrate was at an average value, optimum concentrations of H_2O_2 and Fe(III) were 2677mg/L and 0.50mM, respectively, to achieve maximum color removal efficiency.

(c) At maximum flowrate (Q=50L/h);

Color removal efficiencies with Fe(III)/H_2O_2/Solar-UV process of synthetic wastewater at maximum flowrate are presented in Figure 4.9.

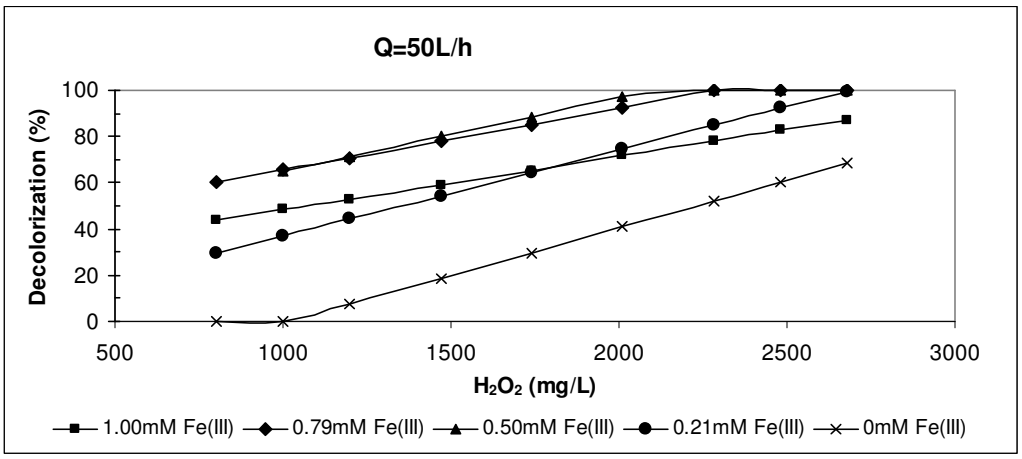

Figure 4.9 Variation of decolorization efficiency of synthetic wastewater at maximum flowrate with Fe(III)/H_2O_2/Solar-UV process.

Color removal efficiencies varied between 0% and 100% at maximum flowrate. Efficiency was nearly 0% when H_2O_2 concentration was lower than 1199mg/L as and Fe(III) concentration was 0.0mM. Efficiency increased with increasing H_2O_2 concentration but efficiency decreased when Fe(III) concentration was higher than 0.5mM. When the flowrate was at a maximum value, optimum concentrations of

H_2O_2 and Fe(III) were 2281mg/L and 0.50mM, respectively, to achieve maximum color removal efficiency.

As a consequence, 100% color removal efficiency was achieved when H_2O_2 and Fe(III) concentrations were between 2281 and 2677mg/L and 0.50 and 0.79mM, respectively, as flowrate was between 10 and 50L/h. Efficiency decreased with increase of flowrate. Efficiency was highest when the flowrate was minimum.

4.1.1.3.1 TOC removal

(a) At minimum flowrate (Q=10L/h);

TOC removal efficiencies with Fe(III)/H_2O_2/Solar-UV process of synthetic wastewater at minimum flowrate are presented in Figure 4.10.

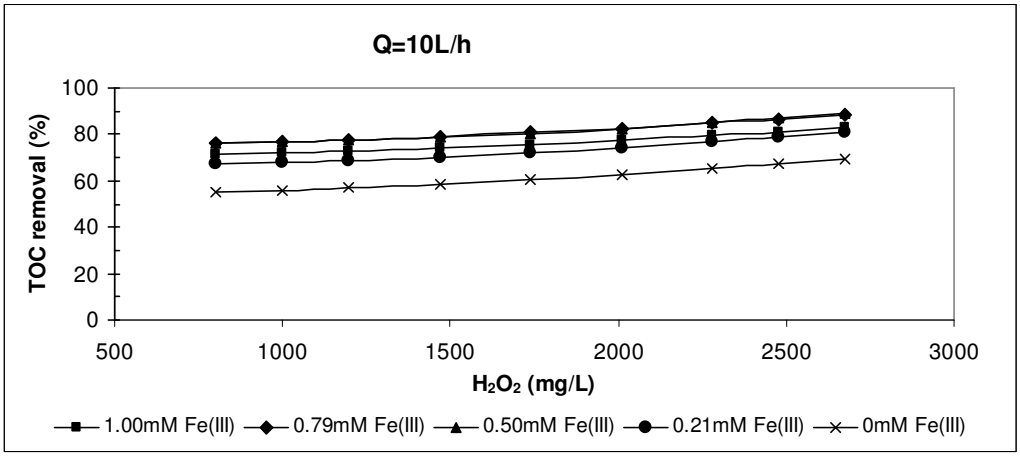

Figure 4.10 Variation of TOC removal efficiency of synthetic wastewater at minimum flowrate with Fe(III)/H_2O_2/Solar-UV process.

TOC removal efficiencies ranged from 55% to 89% at minimum flowrate. The efficiency increased with increase in Fe(III) concentration. However, increasing the initial Fe(III) ion concentration enhanced the oxidation, then Fe(III)started to inhibit the TOC removal efficiency. Thus, after reaching the maximum efficiency that can be achieved at a certain Fe(III) concentration, efficiency decreased with

the increase of Fe(III) concentration. At Fe(III) concentrations higher than 0.79 mM, efficiency was decreased as shown in Figure 4.10.

In addition, the efficiency increased with increasing H_2O_2 concentration. But there were no significant differences when Fe(III) concentration was ranged from 0.50 to 0.79mM. When the flowrate was at a minumun value, optimum concentrations of H_2O_2 and Fe(III) were 2677mg/L and 0.79mM, respectively, to achieve maximum TOC removal efficiency.

(b) At average flowrate (Q=30L/h);

TOC removal efficiencies with Fe(III)/H_2O_2/Solar-UV process of synthetic wastewater at average flowrate are presented in Figure 4.11.

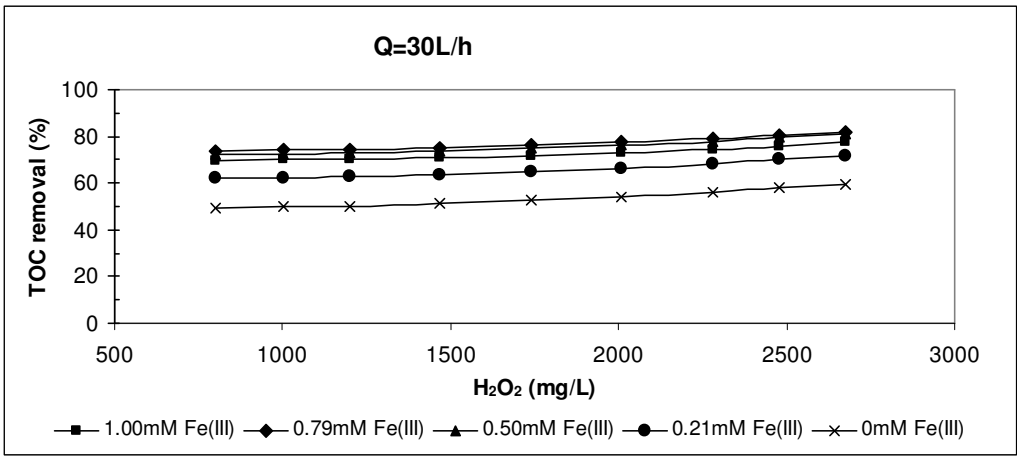

Figure 4.11 Variation of TOC removal efficiency of synthetic wastewater at average flowrate with Fe(III)/H_2O_2/Solar-UV process.

TOC removal efficiencies ranged from 49% to 82% at average flowrate. Increasing of flowrate from 10L/h to 30L/h decreased efficiency from 89.04 to 82.07 at the same H_2O_2 and Fe(III) concentrations which were 2677mg/L and 0.79mM, respectively, at which maximum efficiency was achieved. In the same manner, at a higher Fe(III) concentration than 0.79mM, TOC removal efficiency decreased as shown in Figure 4.11. Maximum efficiency achieved at a 2677mg/L

H_2O_2 concentration when the Fe(III) concentration was 0.79mM at average flowrate.

(c) At maximum flowrate (Q=50L/h);

TOC removal efficiencies with Fe(III)/H_2O_2/Solar-UV process of synthetic wastewater at maximum flowrate are presented in Figure 4.12.

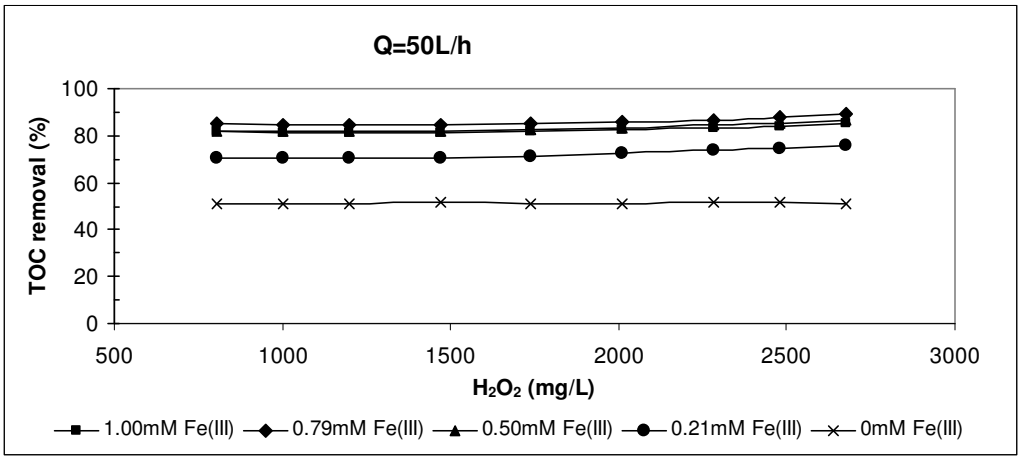

Figure 4.12 Variation of TOC removal efficiency of synthetic wastewater at maximum flowrate with Fe(III)/H_2O_2/Solar-UV process.

TOC removal efficiencies ranged from 51% to 89% at maximum flowrate. Increasing of flowrate from 30L/h to 50L/h increased efficiency from 83% to 89% but increasing of flowrate from 10 to 50L/h did not change efficiency almost. Increasing H_2O_2 concentration did not increase efficiency significantly. But in the same manner, at a higher Fe(III) concentration than 0.79mM, TOC removal efficiency decreased as shown in Figure 4.12. Maximum efficiency achieved at a 2677mg/L H_2O_2 concentration when the Fe(III) concentration was 0.79mM at maximum flowrate.

Throughout the Fe(III)/H_2O_2/Solar-UV process, optimum flowrate was determined as 10L/h. In addition, decrease of flowrate increased color and TOC removal efficiency. Although high TOC removal efficiency was determined at

high H_2O_2 concentration, high H_2O_2 concentration started to inhibit color removal efficiency. Maximum color removal efficiency was achieved at a condition of 2281mg/L H_2O_2, 0.79mM Fe(III) and 10L/h. TOC removal efficiency was calculated at this experimental condition by using response function (Eq. 4.2). Predicted TOC removal efficiency was 85%, which was acceptable. As a conclusion, experimental condition which maximum color removal efficiency was achieved (10L/h flowrate, 0.79mM Fe(III) and 2281mg/L H_2O_2) was accepted optimum experimental condition for color (100%) and TOC removal (85%). Consequently, 10L/h flowrate, 0.79mM Fe(III) and 2281mg/L H_2O_2 were determined for optimum treatment condition of synthetic wastewater of Remazol Brilliant Blue R-A textile dyestuff at a concentration of 50mg/L for Fe(III)/H_2O_2/Solar-UV process.

4.1.2 Solar TiO_2 Catalysis (Fe(III)/TiO_2/Solar-UV)

4.1.2.1 Introduction

As in Fe(III)/H_2O_2/Solar-UV process, some preparatory works has done in the laboratory to determine ranges of chemical dosages for Fe(III)/ TiO_2/Solar-UV process. Fe(III) concentrations were chosen as those for Fe(III)/H_2O_2/Solar-UV process and varied from 0 to 1.0mM. TiO_2 concentration was started to study at a concentration of 250mg/L. Then TiO_2 concentration decreased from 250 to 50mg/L (250, 200, 100 and 50) to investigate variation of color and TOC removal efficiency. All laboratory experimentation results are depicted at Appendix-B (Figure B.6-B.10).

4.1.2.2 Experimental Procedure

Experimental procedure with synthetic wastewater which prepared with the azodye Remazol Brilliant Blue R-A was explained in chapter 3.2.2.3.

The time at which addition of TiO_2 was considered time zero. Samples were taken at hourly and filtered from a blue band paper to remove solid particals from water. Filtrate was taken to measure absorbance and TOC. In addition to this, samples were centrifuged for 10 minutes at 6000rpm and filtered from base filter paper for the same aim. Color and TOC removal efficiencies achieved with blue band filtration were higher than the efficiencies achieved with base band filtration. As a consequence, results of analysis which were achieved with blue band filtration are presented in this study. In addition COD and BOD parameters were measured at influent and effluent samples to investigate treatibility.

TiO_2 and Fe(III) concentrations and flowrate were chosen as the independent variables and designated as X_1, X_2 and X_3 respectively. The TiO_2 concentration was between 50 and 250mg/L, while Fe(III) concentration (X_2) was between 0 and 1.0mM, and flowrate (X_3) was between 10 and 50L/h. Color and TOC removal efficiencies were chosen as the dependent variables and designed as Y_1 and Y_2, respectively. Experimental points of design are presented in Table 4.4 and experimental conditions were presented in Table 4.5.

Table 4.4 Experimental points determined by the Box–Wilson statistical design (synthetic wastewater, Fe(III)/TiO_2/Solar-UV process)

Points	**TiO_2 (mg/L)**	**Fe(III) (mM)**	**Q (L/h)**
	X_1	**X_2**	**X_3**
+k	250.00	1.00	50.0
+1	207.74	0.79	41.5
0	150.00	0.50	30.0
−1	92.26	0.21	18.5
−k	50.00	0.00	10.0

Table 4.5 Experimental conditions determined by the Box–Wilson statistical design (synthetic wastewater, Fe(III)/TiO_2/Solar-UV process)

Axial points				**Factorial points**			
No.	TiO_2 (mg/L)	Fe(III) (mM)	Q (L/h)	No.	TiO_2 (mg/L)	Fe(III) (mM)	Q (L/h)
A1	250	0.50	30	F1	207.74	0.79	41.5
A2	50	0.50	30	F2	207.74	0.79	18.5
A3	150	1.00	30	F3	207.74	0.2	41.5
A4	150	0.00	30	F4	92.26	0.79	41.5
A5	150	0.50	50	F5	207.74	0.21	18.5
A6	150	0.50	10	F6	92.26	0.21	41.5
Center points				F7	92.26	0.79	18.5
C	150	0.50	30	F8	92.26	0.21	18.5

4.1.2.3 Regression Model

Figure 4.13-4.18 depict variation of decolorization and TOC removal efficiency with irradiation time. Computation was carried out using multiple regression analysis that uses the least squares method. The following response functions (Eq. 4.3 and 4.4) were utilized in the correlating of the color removal efficiency (Y_C) and TOC removal efficiency (Y_{TOC}) with other independent parameters ($X1$–$X3$). The Statistica computer program was employed for the determination of the coefficients of response functions by regression analysis of the experimental data. Response functions with calculated coefficients were given in Eq. 4.3 and 4.4 and were used in calculation of predicted values of color and TOC removal efficiencies. Observed and predicted color and TOC removal efficiencies with COD and BOD removal efficiencies were given in Table 4.6.

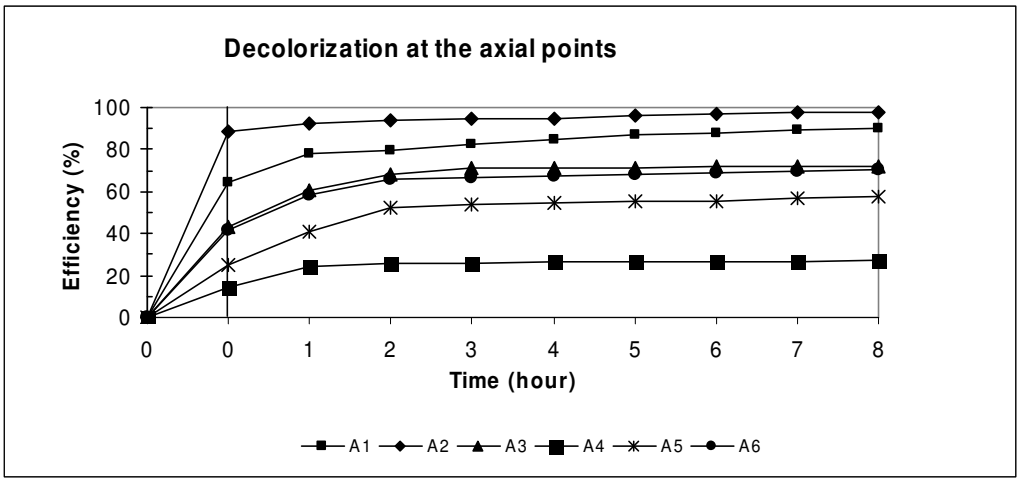

Figure 4.13 Variation of decolorization efficiency with irradiation time at axial points with Fe(III)/TiO_2/Solar-UV process

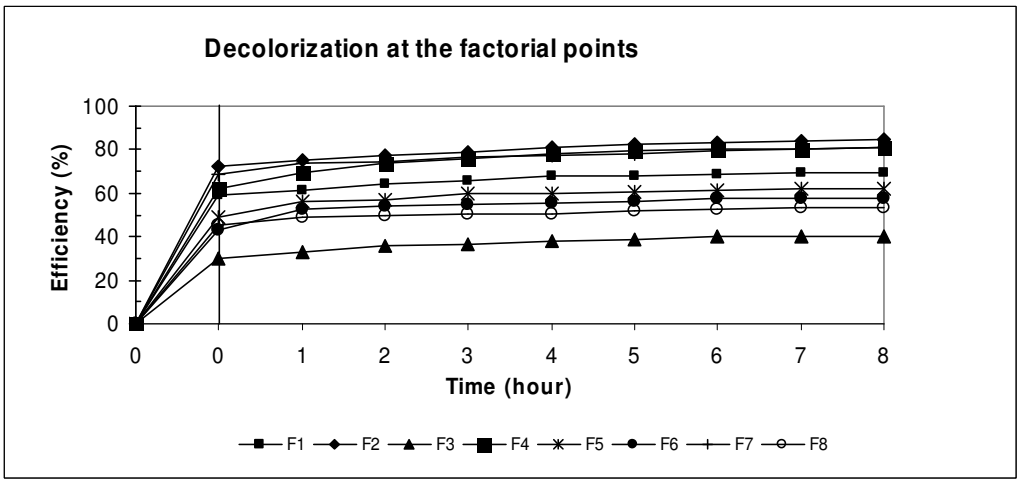

Figure 4.14 Variation of decolorization efficiency with irradiation time at factorial points with Fe(III)/TiO_2/Solar-UV process

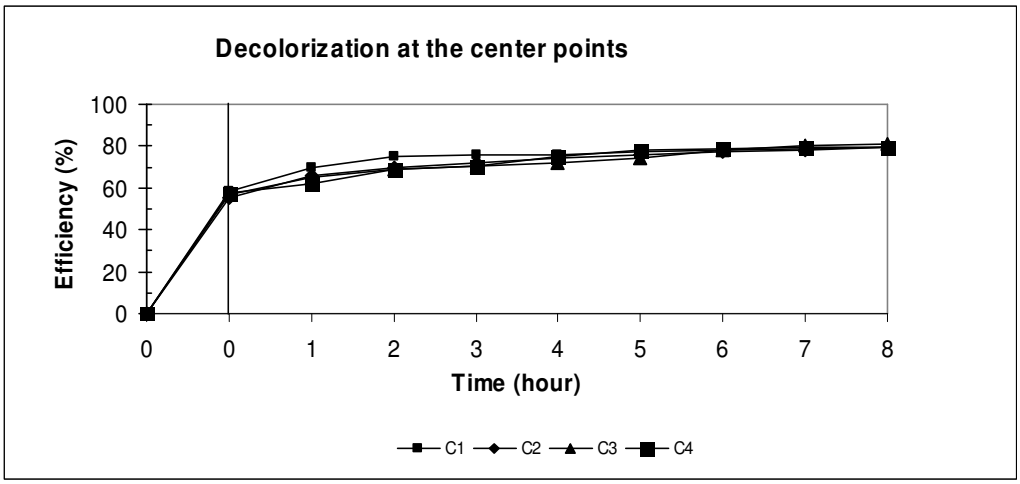

Figure 4.15 Variation of decolorization efficiency with irradiation time at center points with Fe(III)/TiO_2/Solar-UV process

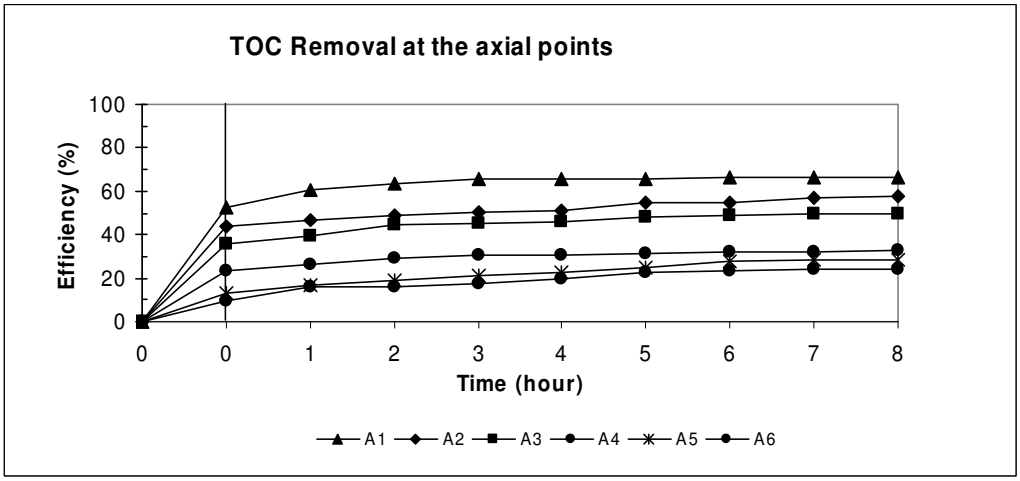

Figure 4.16 Variation of TOC removal efficiency with irradiation time at axial points with Fe(III)/TiO_2/Solar-UV process.

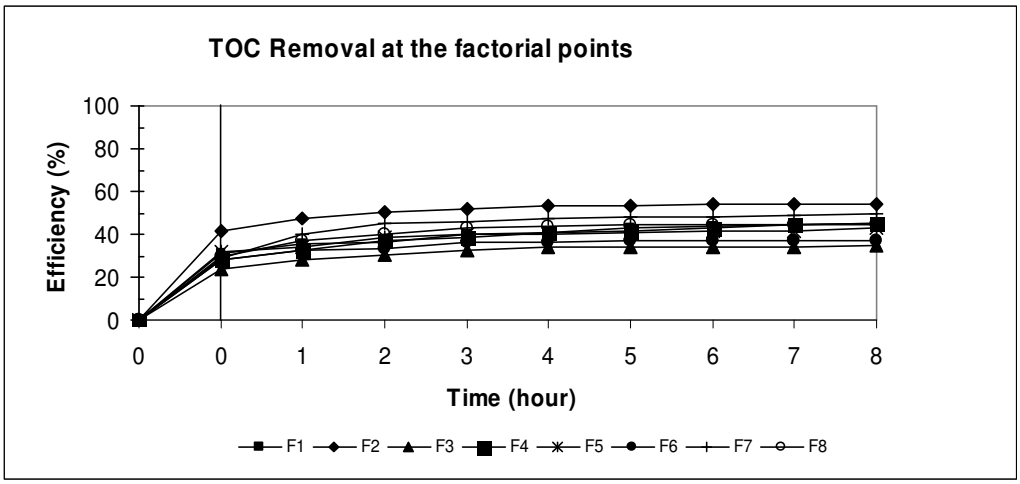

Figure 4.17 Variation of TOC removal efficiency with irradiation time at factorial points with Fe(III)/TiO_2/Solar-UV process.

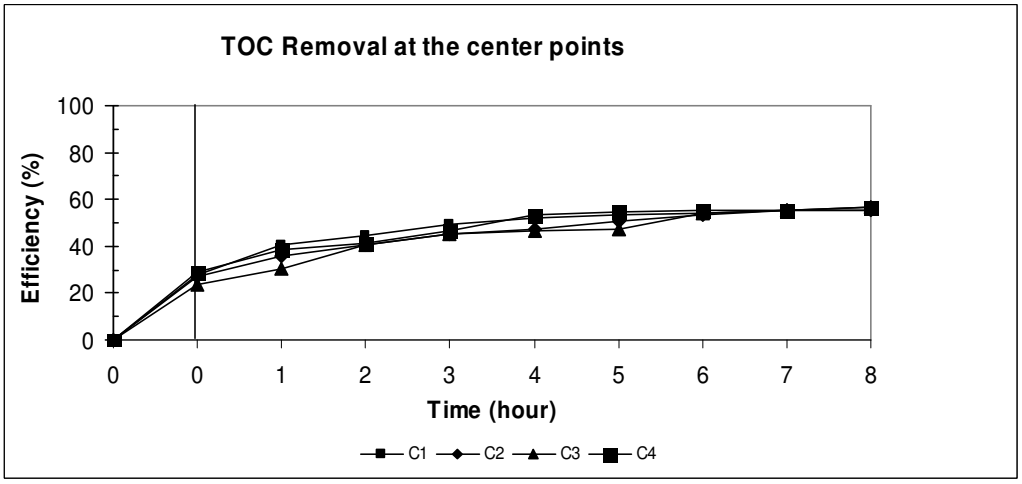

Figure 4.18 Variation of TOC removal efficiency with irradiation time at center points with Fe(III)/TiO_2/Solar-UV process.

Response function (Y_{COL}) for color removal;

$$Y_{COL} = -0.15857 - 0.19713\ X_1 + 166.23839\ X_2 + 3.34221\ X_3 + 0.00274\ X_1X_2 - 0.00767\ X_1X_3 + 0.11522\ X_2X_3 + 0.00130\ X_1^2 - 126.51361\ X_2^2 - 0.04312\ X_3^2 \quad (R^2 = 0.9930) \qquad \text{(Eq. 4.3)}$$

Response function (Y_{TOC}) for TOC removal;

$$Y_{TOC} = -13.84953 - 0.15106\ X_1 + 86.61411\ X_2 + 3.74798\ X_3 + 0.04041\ X_1X_2 - 0.00151\ X_1X_3 + 0.03841\ X_2X_3 + 0.00066\ X_1^2 - 74.26810\ X_2^2 - 0.06248\ X_3^2 \quad (R^2 = 0.9717) \qquad \text{(Eq. 4.4)}$$

The correlation coefficients (R^2) were 0.9930 and 0.9717 for Y_{COL} and Y_{TOC}, respectively indicating a good agreement between the observed and predicted values of color and TOC removal efficiencies.

Table 4.6 Observed and predicted color and TOC removal efficiencies determined by the Box–Wilson statistical design with COD and BOD removal efficiencies (synthetic wastewater, Fe(III)/TiO_2/Solar-UV process).

No.	% Color removal		% TOC removal		% BOD removal	% COD removal
	observed	predicted	observed	predicted	observed	observed
A1	90	89	66	65	55	52
A2	98	96	58	61	64	63
A3	72	70	50	47	55	55
A4	27	26	24	28	36	42
A5	58	56	29	27	64	68
A6	70	69	33	35	64	60
F1	70	70	45	48	55	52
F2	84	87	54	54	45	44
F3	40	43	34	35	64	68
F4	81	84	45	46	64	68
F5	62	61	43	42	50	52
F6	58	57	37	35	64	62
F7	81	81	50	49	64	60
F8	53	55	42	38	45	49
C1	79	80	56	56	77	68
C2	79	80	55	56	77	68
C3	81	80	57	56	77	68
C4	80	80	57	56	77	68

Maximum color and TOC removal efficiencies were 98% and 66% and were achieved at A2 (50mg/L TiO_2, 0.5mM Fe(III) and 30L/h flowrate) and A2 (250mg/L TiO_2, 0.5mM Fe(III) and 30L/h flowrate) experimental conditions, respectively. More experimental results were needed to comment the regression model better. Color and TOC removal efficiencies were predicted by using Eq. 4.3 and 4.4 when flowrate kept constant at minimum (10L/h), average (30L/h) and maximum (50L/h) value in order. Results are given in Figure 4.19-4.24.

4.1.2.3.1 Decolorization

(a) At minimum flowrate (Q=10L/h);

Color removal efficiencies with Fe(III)/TiO_2/Solar-UV process of synthetic wastewater at minimum flowrate are presented in Figure 4.19.

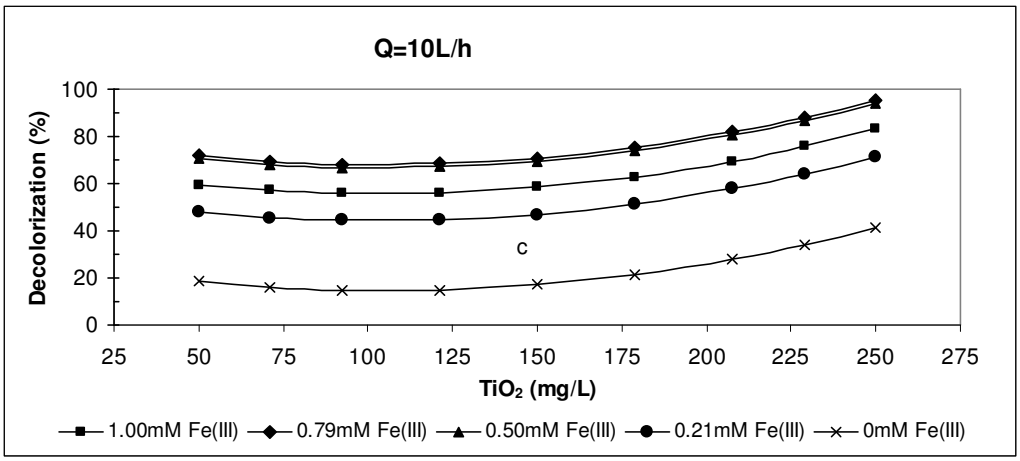

Figure 4.19 Variation of decolorization efficiency of synthetic wastewater at minimum flowrate with Fe(III)/TiO_2/Solar-UV process.

Color removal efficiencies varied between 15% and 95% at minimum flowrate. The efficiency increased with increasing Fe(III) concentration from 0 to 0.79mM but decreased with increasing Fe(III) concentration from 0.79 to 1.0mM. There was no significant difference between decolorization efficiencies when Fe(III) concentration was 0.5 and 0.79mM. Nevertheless, maximum efficiency was achieved at a Fe(III) concentration of 0.79mM. The addition of Fe(III) more than 0.79mM did not enhance the process performance. Increasing the initial TiO_2 concentration from 50 to 125 mg/L resulted in a decrease in color removal efficiency. But, increasing the initial TiO_2 concentration from 125 to 250 mg/L enhanced the oxidation up. Herewith, 0.79mM Fe(III) and 250mg/L TiO_2 concentrations were found to be the optimum treatment conditions when the flowrate was at 10L/h.

(b) At average flowrate (Q=30L/h);

Color removal efficiencies with Fe(III)/TiO_2/Solar-UV process of synthetic wastewater at average flowrate are presented in Figure 4.20.

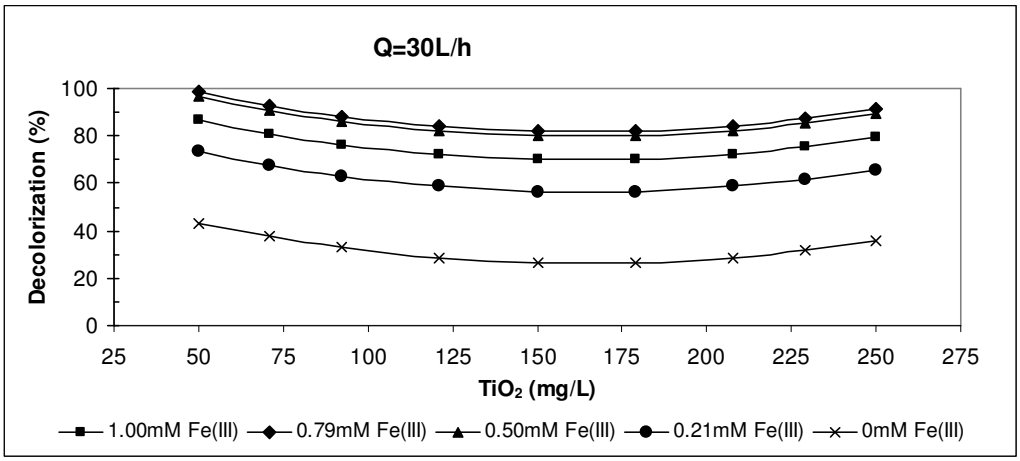

Figure 4.20 Variation of decolorization efficiency of synthetic wastewater at average flowrate with Fe(III)/TiO_2/Solar-UV process.

Color removal efficiencies varied between 26% and 98% at average flowrate. As seen from the results, when the flowrate increased from 10 to 30L/h, maximum color removal efficiency increased from 95% to 98%. In addition, lower TiO_2 concentration was needed to achieve that removal efficiency in 8h irradiation time. As seen from the Figure 4.20, increasing the initial TiO_2 concentration from 50 to 125 mg/L resulted in a decrease in color removal efficiency and increasing the initial TiO_2 concentration from 125 to 250 mg/L enhanced the oxygen utilization. However, when TiO_2 concentration was 50mg/L, decolorization efficiency was higher than that of 250mg/L.

The efficiency also increased with increasing Fe(III) concentration from 0 to 0.79mM but decreased with increasing Fe(III) concentration from 0.79 to 1.0mM. Herewith, 0.79mM Fe(III) and 50mg/L TiO_2 concentrations were found to be the optimum treatment conditions when the flowrate was at 30L/h.

(c)At maximum flowrate (Q=50L/h);

Color removal efficiencies with Fe(III)/TiO_2/Solar-UV process of synthetic wastewater at maximum flowrate are presented in Figure 4.21.

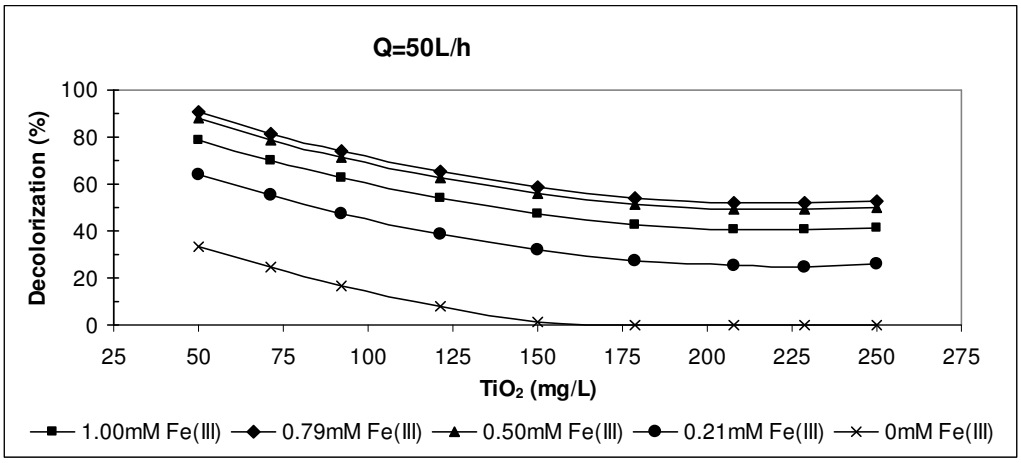

Figure 4.21 Variation of decolorization efficiency of synthetic wastewater at maximum flowrate with Fe(III)/TiO_2/Solar-UV process.

Color removal efficiencies varied between 0% and 90% at maximum flowrate. As seen from the results, when the flowrate increased from 10 to 30L/h, maximum color removal efficiency increased from 95.49 to 98.40. In addition, lower TiO_2 concentration was required to achieve that removal efficiency in 8h irradiation time. As seen from the Figure 4.20, increasing the initial TiO_2 concentration from 50 to 125 mg/L resulted in a decrease in color removal efficiency and increasing the initial TiO_2 concentration from 125 to 250 mg/L enhanced the oxygen utilization. Yet, when TiO_2 concentration was 50mg/L, decolorization efficiency was higher than that of 250mg/L.

The efficiency also increased with increasing Fe(III) concentration from 0 to 0.79mM but decreased with increasing Fe(III) concentration from 0.79 to 1.0mM. Herewith, 0.79mM Fe(III) and 50mg/L TiO_2 concentrations were found to be the optimum treatment conditions when the flowrate was at 50L/h.

4.1.2.3.2 TOC removal

(a)At minimum flowrate (Q=10L/h);

TOC removal efficiencies with Fe(III)/TiO_2/Solar-UV process of synthetic wastewater at minimum flowrate are presented in Figure 4.22.

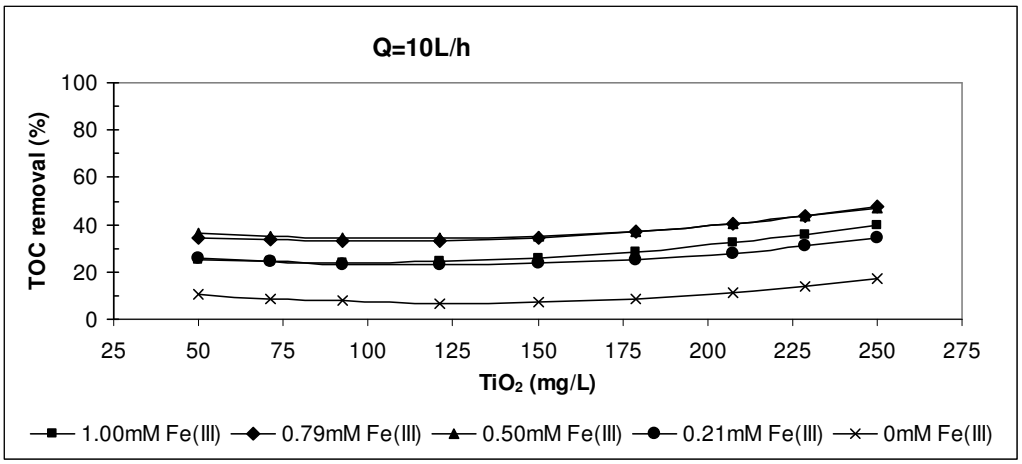

Figure 4.22 Variation of TOC removal efficiency of synthetic wastewater at minimum flowrate with Fe(III)/TiO_2/Solar-UV process.

TOC removal efficiencies ranged from 7% to 47% at minimum flowrate. The efficiency increased with increasing Fe(III) concentration from 0 to 0.79mM but decreased with increasing Fe(III) concentration from 0.79 to 1.0mM. There was no significant difference between TOC removal efficiencies when Fe(III) concentration was 0.5 and 0.79mM. Nevertheless, maximum efficiency was achieved at a Fe(III) concentration of 0.79 mM. The addition of Fe(III) more than 0.79mM did not enhance the process performance. Increasing the initial TiO_2 concentration from 50 to 125 mg/L resulted in a decrease in TOC removal efficiency. However, increasing the initial TiO_2 concentration from 125 to 250 mg/L increased the efficiency. Herewith, 0.79mM Fe(III) and 250mg/L TiO_2 concentrations were found to be the optimum treatment conditions when the flowrate was at 10L/h.

(b) At average flowrate (Q=30L/h);

TOC removal efficiencies with Fe(III)/TiO_2/Solar-UV process of synthetic wastewater at average flowrate are presented in Figure 4.23.

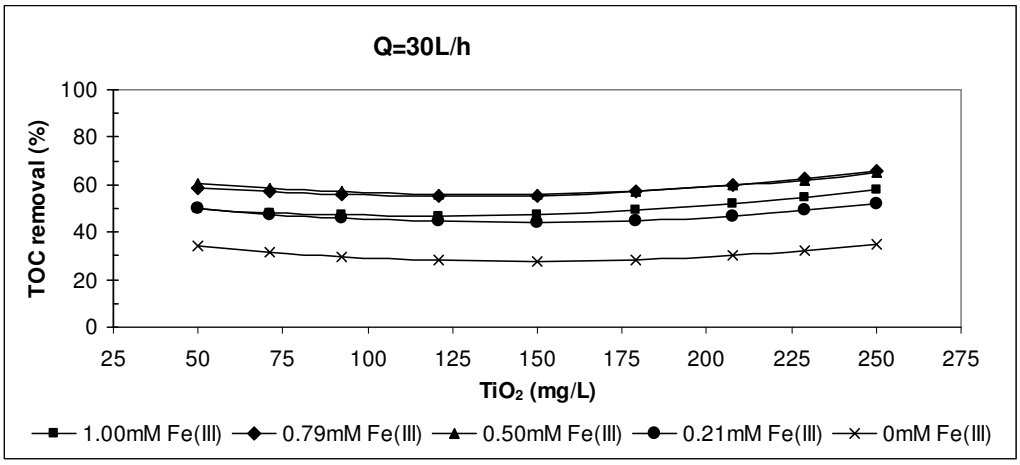

Figure 4.23 Variation of TOC removal efficiency of synthetic wastewater at average flowrate with Fe(III)/TiO_2/Solar-UV process.

TOC removal efficiencies varied between 28% and 66% at average flowrate. As seen from the results, when the flowrate increased from 10 to 30L/h, maximum TOC removal efficiency increased from 47.48 to 65.52 at the same Fe(III) and TiO_2 concentrations which were 0.79mM and 250mg/L, respectively. The efficiency also increased with increasing Fe(III) concentration from 0 to 0.79mM but decreased with increasing Fe(III) concentration from 0.79 to 1.0mM. Increasing the initial TiO_2 concentration from 50 to 125 mg/L resulted in a decrease in TOC removal efficiency and increasing the initial TiO_2 concentration from 125 to 250 mg/L enhanced the oxygen utilization. Nonetheless, there was no significant difference between TOC removal efficiencies when TiO_2 concentration was 125 and 250mg/L. Herewith, 0.79mM Fe(III) and 250mg/L TiO_2 concentrations were found to be the optimum treatment conditions when the flowrate was at 30L/h.

(c) At maximum flowrate (Q=50L/h);

TOC removal efficiencies with Fe(III)/TiO_2/Solar-UV process of synthetic wastewater at maximum flowrate are presented in Figure 4.24.

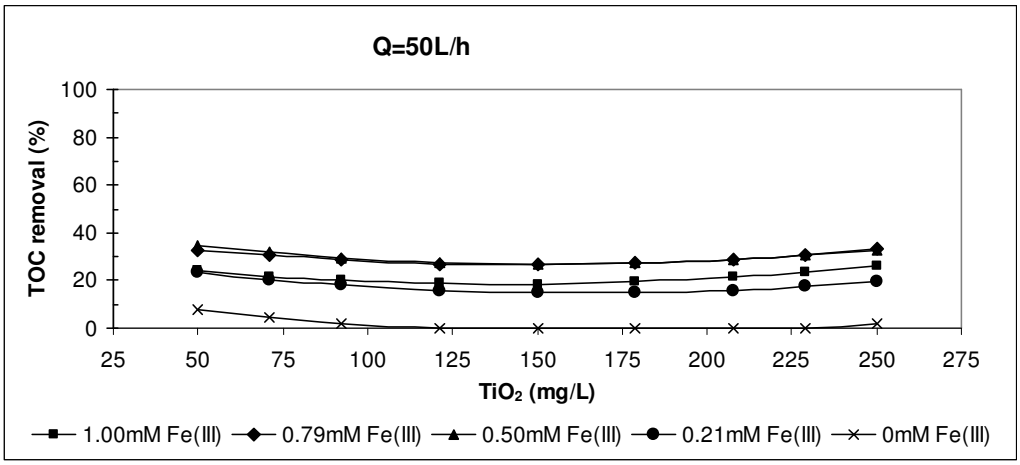

Figure 4.24 Variation of TOC removal efficiency of synthetic wastewater at maximum flowrate with Fe(III)/TiO_2/Solar-UV process.

TOC removal efficiencies varied between 0% and 34% at maximum flowrate. When the flowrate increased from 30 to 50L/h, maximum TOC removal efficiency decreased from 66% to 34%. In addition, maximum TOC removal efficiency at flowrate of 50L/h was found as the lowest efficiency. In the same way, increasing the initial TiO_2 concentration from 50 to 175 mg/L resulted in a decrease in TOC removal efficiency and increasing the initial TiO_2 concentration from 175 to 250 mg/L did not increase the efficiency significantly. The efficiency also increased with increasing Fe(III) concentration from 0 to 0.5mM but decreased by increasing Fe(III) concentration from 0.5 to 1.0mM. Herewith, 0.5mM Fe(III) and 50mg/L TiO_2 concentrations were found to be the optimum treatment conditions when the flowrate was at 50L/h.

Throughout the Fe(III)/TiO_2/Solar-UV process, optimum flowrate and Fe(III) concentration were determined as 30L/h and 0.79mM to achieve maximum color and TOC removal efficiency, respectively. Although high TOC removal efficiency

was determined at high TiO_2 concentration as 250mg/L, high TiO_2 concentration started to inhibit color removal efficiency because of turbidity. TOC removal efficiency was calculated by using response function (Eq. 4.4) at the experimental condition which gives maximum color removal efficiency (30L/h flowrate, 0.79mM Fe(III) and 50mg/L TiO_2). Predicted TOC removal efficiency was 59%. This efficiency was higher than maximum TOC removal efficiencies achieved when flowrate was 10L/h (47%) or 50L/h (34%). As a conclusion, experimental condition at which maximum color removal efficiency was achieved (30L/h flowrate, 0.79mM Fe(III) and 50mg/L TiO_2) was accepted optimum experimental condition for TOC removal (59%). Consequently, 30L/h flowrate, 0.79mM Fe(III) and 50mg/L TiO_2 were determined for optimum treatment condition of synthetic wastewater of Remazol Brilliant Blue R-A textile dyestuff at a concentration of 50mg/L for Fe(III)/ TiO_2/Solar-UV process. As seen in Table 4.7, there was no significant difference between color removal efficiencies of two processes but maximum TOC removal efficiency of Fe(III)/H_2O_2/Solar-UV process (85%) was higher then Fe(III)/TiO_2/Solar-UV process (59%) because of the fact that H_2O_2 was one of the most powerful oxidizer and is stronger than TiO_2.

Table 4.7 Optimum treatment conditions and color and TOC removal efficiencies determined by the Box–Wilson statistical design of synthetic wastewater with Fe(III)/H_2O_2/Solar-UV and Fe(III)/TiO_2/Solar-UV processes.

Fe(III)/ H_2O_2/Solar-UV				
Dosage of H_2O_2 (mg/L)	Dosage of Fe(III) (mM)	Flowrate (L/h)	Color removal efficiency (%)	TOC removal efficiency (%)
2281	0.79	10	100	85
Fe(III)/ TiO_2/Solar-UV				
Dosage of TiO_2 (mg/L)	Dosage of Fe(III) (mM)	Flowrate (L/h)	Color removal efficiency (%)	TOC removal efficiency (%)
50	0.79	30	98	59

4.2 Application of Box–Wilson Experimental Design Method for the Solar Degradation of Textile Industry Wastewater by Advanced Oxidation Processes

4.2.1 Introduction

Effluents from the textile industry commonly contain high concentrations of organic and inorganic chemicals and are characterized by high COD, BOD and TOC values as well as strong color. The major concern with color is its aesthetic character at the point of discharge with respect to visibility in rivers (Kurbus, Le Marechal and Vončina, 2003). Color in textile effluents has become particularly identified with the dyeing of cotton products and the use of reactive azo dyes since up to 30% of the used dyestuffs remain in the spent dye-bath after the dyeing process. The release of those colored wastewaters in the environment is a considerable source of non-aesthetic pollution and eutrophication and can originate dangerous byproducts through oxidation, hydrolysis, or other chemical reactions taking place in the wastewater phase (Prieto, Fermoso, Nuňez, Del Vale and Irusta, 2005).

This chapter includes the application of Box-Wilson Experimantal Design Method for the solar degradation of textile industry wastewater by advanced oxidation.

4.2.2 Wastewater characterization

Textile industry wastewater samples were obtained from a stabilization pond of a textile industry wastewater treatment plant located in Torbalı/İzmir, Turkey. Wastewaters have been analyzed before experimental studies. The pH values of textile industry effluent samples used in the experimental studies varied from 7.40 to 8.63. COD concentrations of samples varied from 664mg/L to 880mg/L. BOD concentrations of samples were between 400mg/L and 510mg/L. TOC concentrations of samples varied from 170.1mg/L to 308.3mg/L.

Wavelength scan also was conducted to find peak wavelength that gives maximum absorbance for each textile industry wastewater samples taken from a textile industry wastewater treatment plant. All wavelength scan results are given in Appendix-A. Peak wavelengths and maximum absorbance values were found 509 nm and 0.507, 393nm and 0.509, 393nm and 0.509, 393nm and 0.509, 391nm and 0.637 and 384nm and 0.549. In every wavelength scan process, color measurements were carried at the wavelength which gives maximum absorbance and the beginning absorbance value at this wavelength came up to 100 unit color concentration.

4.2.3 Photo-Fenton-like Process (Fe(III)/H_2O_2/Solar-UV)

4.2.3.1 Experimental Procedure

Experimental procedure with wastewater was explained in chapter 3.2.2.4. The significant independent and dependent variables are the same as for Fe(III)/H_2O_2/Solar-UV process with synthetic wastewater. Experimental points and conditions determined by the Box–Wilson statistical design are presented in Table 4.1 and 4.2.

4.2.3.2 Regression Model

Figure 4.25-4.30 depict variation of decolorization and TOC removal efficiency with irradiation time. Computation was carried out using multiple regression analysis that uses the least squares method. The following response functions (Eq. 4.5 and 4.6) were utilized in the correlation of the color removal efficiency (Y_C) and TOC removal efficiency (Y_{TOC}) with other independent parameters ($X1$–$X3$). The Statistica computer program was employed for the determination of the coefficients of response functions by regression analysis of the experimental data. Response functions with calculated coefficients were given in Eq. 4.5 and 4.6, and were used in calculating predicted values of color and TOC removal efficiencies.

Observed and predicted color and TOC removal efficiencies with COD and BOD removal efficiencies were given in Table 4.8.

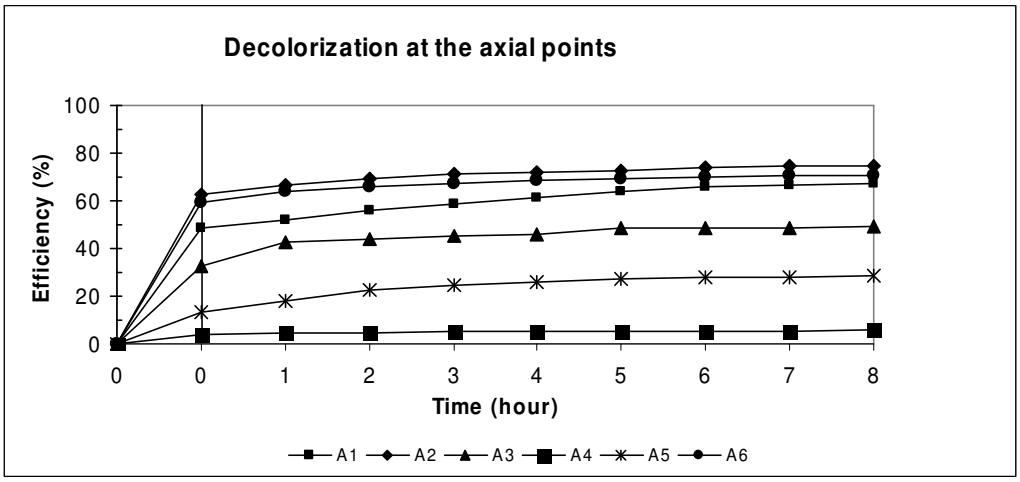

Figure 4.25 Variation of decolorization efficiency with irradiation time at axial points with Fe(III)/H_2O_2/Solar-UV process

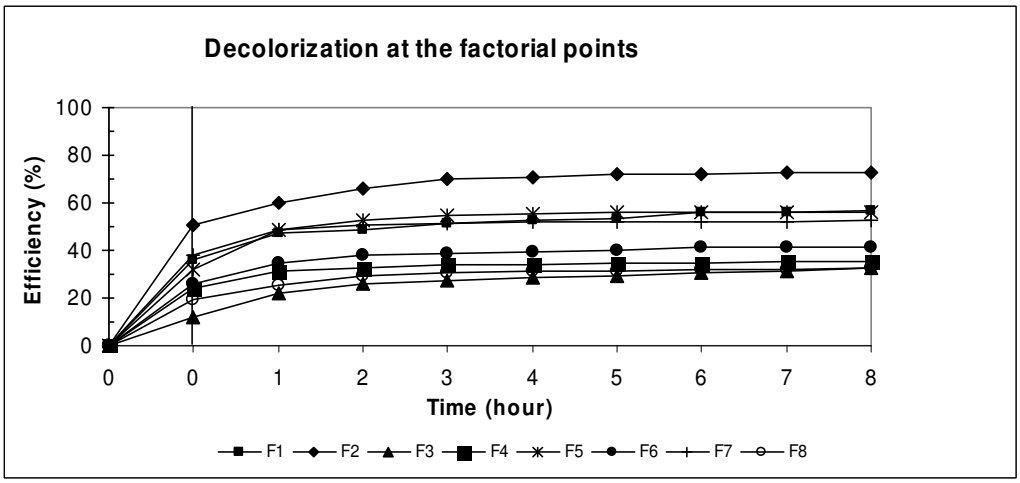

Figure 4.26 Variation of decolorization efficiency with irradiation time at factorial points with Fe(III)/H_2O_2/Solar-UV process

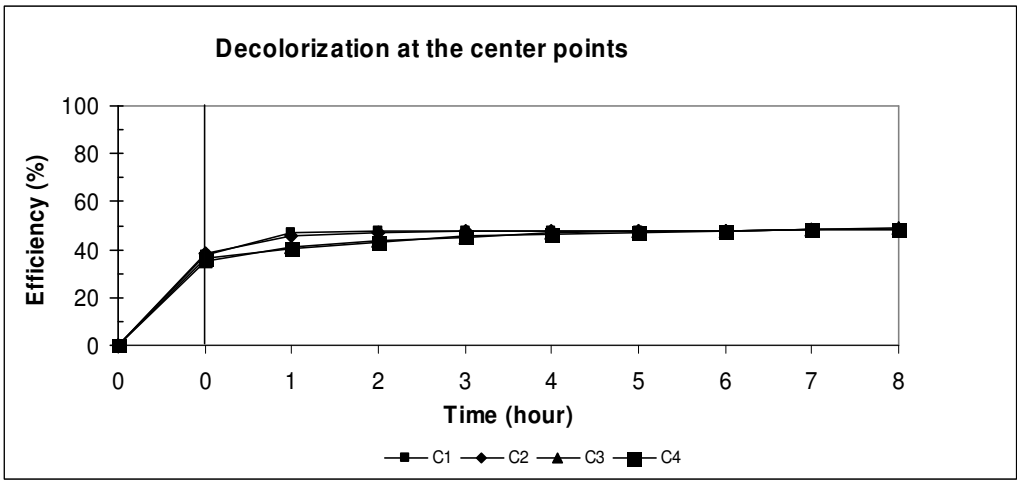

Figure 4.27 Variation of decolorization efficiency with irradiation time at center points with Fe(III)/H_2O_2/Solar-UV process.

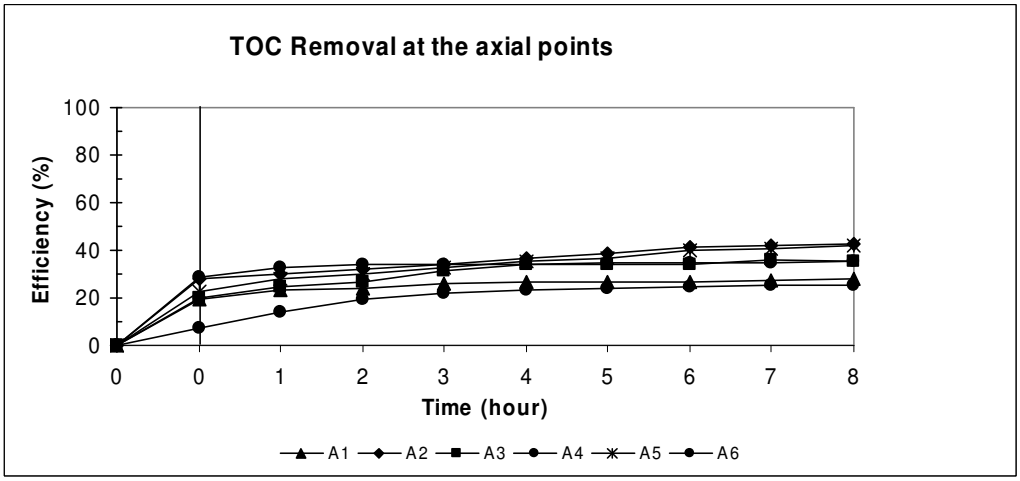

Figure 4.28 Variation of TOC removal efficiency with irradiation time at axial points with Fe(III)/H_2O_2/Solar-UV process.

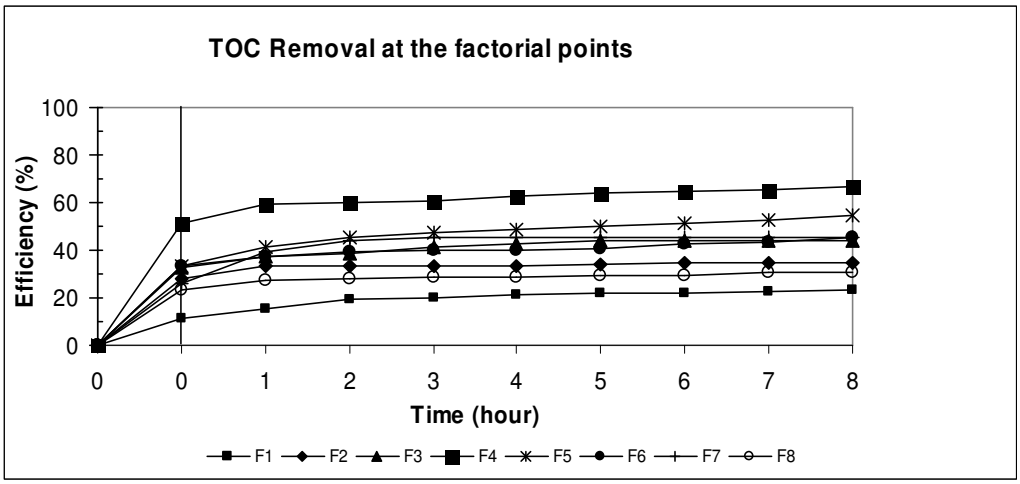

Figure 4.29 Variation of TOC removal efficiency with irradiation time at factorial points with Fe(III)/H_2O_2/Solar-UV process.

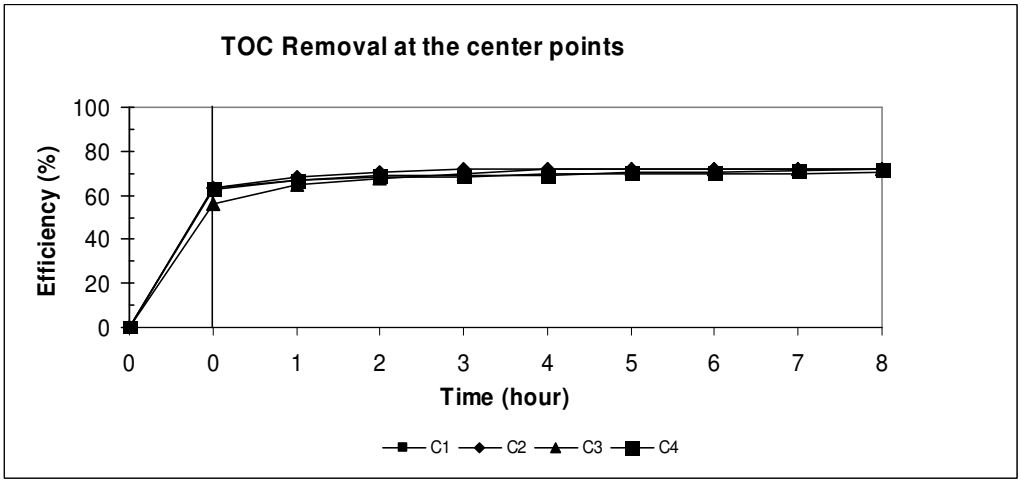

Figure 4.30 Variation of TOC removal efficiency with irradiation time at center points with Fe(III)/H_2O_2/Solar-UV process.

Response function (Y_{COL}) for color removal;

$$Y_{COL} = -68.38952 + 0.07348\ X_1 + 141.98047\ X_2 + 2.94049\ X_3 - 0.01803\ X_1X_2 + 0.00041\ X_1X_3 - 0.60109\ X_2X_3 - 0.00002\ X_1^2 - 95.00537\ X_2^2 - 0.06152\ X_3^2 \quad (R^2 = 0.8663) \qquad \text{(Eq. 4.5)}$$

Response function (Y_{TOC}) for TOC removal;

$$Y_{TOC} = -235.70719 + 0.17962\ X_1 + 242.34807\ X_2 + 0.6.25229\ X_3 - 0.05893\ X_1X_2 - 0.00116\ X_1X_3 + 0.17283\ X_2X_3 - 0.00004\ X_1^2 - 141.92556\ X_2^2 - 0.06943\ X_3^2 \quad (R^2 = 0.9345) \qquad \text{(Eq. 4.6)}$$

The correlation coefficient (R^2) was 0.8663 for Y_{COL} and indicated a not good agreement between the observed and predicted values of color removal efficiencies. The correlation coefficient was 0.9345 for Y_{TOC} and indicated a fairly well agreement between the observed and predicted values of TOC removal efficiencies.

Table 4.8 Observed and predicted color and TOC removal efficiencies determined by the Box–Wilson statistical design with COD and BOD removal efficiencies (textile industry wastewater, Fe(III)/H_2O_2/Solar-UV process).

No.	% Color removal		% TOC removal		% BOD removal	% COD removal
	observed	predicted	observed	predicted	observed	observed
A1	67	75	28	34	55	36
A2	75	65	43	48	80	47
A3	50	42	36	38	51	40
A4	6	11	26	35	50	37
A5	29	34	42	47	48	29
A6	71	64	35	41	64	46
F1	57	49	23	22	38	32
F2	73	79	35	31	50	35
F3	33	28	44	38	58	44
F4	35	44	66	63	72	37
F5	56	49	54	50	70	43
F6	41	36	45	41	60	42
F7	52	58	46	44	80	55
F8	33	42	31	24	70	47
C1	48	48	71	72	71	63
C2	48	48	72	72	72	64
C3	49	48	72	72	72	65
C4	48	48	72	72	70	65

Maximum color and TOC removal efficiencis were 75% and 72% and were achieved at A2 (803.1mg/L H_2O_2, 0.5mM Fe(III) and 30L/h flowrate) and C (1740mg/L H_2O_2, 0.5mM Fe(III) and 30L/h flowrate) experimental conditions, respectively. More experimental results were needed to comment on the regression model better. Color and TOC removal efficiencies were predicted by using Eq. 4.5 and 4.6 when flowrate kept constant at minimum (10L/h), average (30L/h) and maximum (50L/h) value in order. Results are given in Figure 4.31-4.36.

4.2.3.2.1 Decolorization

(a) At minimum flowrate (Q=10L/h);

Color removal efficiencies with Fe(III)/H_2O_2/Solar-UV process of textile industry wastewater at minimum flowrate are presented in Figure 4.31.

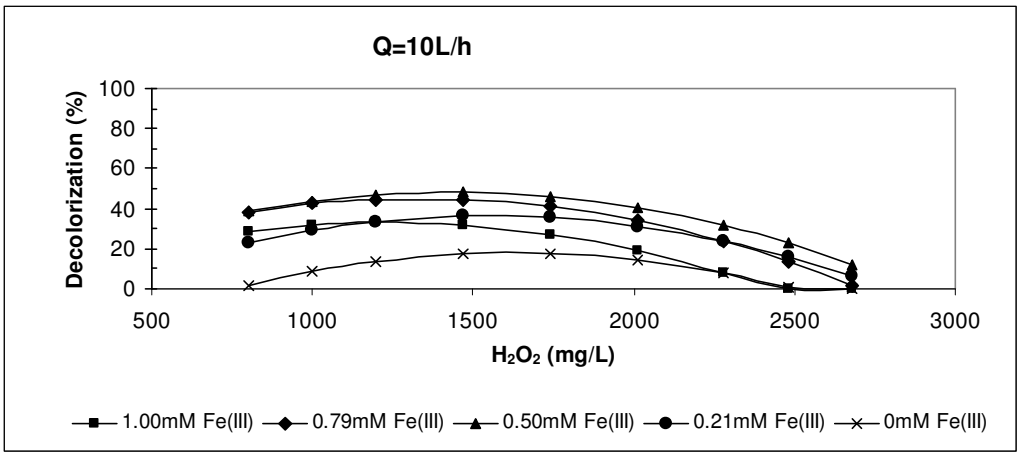

Figure 4.31 Variation of decolorization efficiency of textile industry wastewater at minimum flowrate with Fe(III)/H_2O_2/Solar-UV process.

Color removal efficiencies varied between 0% and 48% at minimum flowrate. The efficiency increased with increasing Fe(III) concentration. However, increasing the initial Fe(III)concentration enhanced the oxygen utilization to a certain point where Fe(III)started to inhibit the color removal efficiency, after reaching the maximum efficiency that can be achieved at a certain Fe(III) concentration, the efficiency decreased with the increasing of Fe(III) concentration. At Fe(III) concentrations higher than 0.5mM, treatment efficiency decreased as shown in Figure 4.31.

In addition, the efficiency increased with increasing H_2O_2 concentration from 803.1 to 1469.5mg/L but the efficiency started to decrease by increasing H_2O_2 concentration from 1469.5 to 2677 mg/L at all Fe(III) concentrations. The decreases in removal efficiency at high oxidant concentrations are thought to be

due to the side reactions taking place between the •OH radicals and the excess H_2O_2. When the flowrate was at a minumun value, optimum concentrations of H_2O_2 and Fe(III) were 1469.5mg/L and 0.5mM, respectively to achieve maximum color removal efficiency.

(b) At average flowrate (Q=30L/h);

Color removal efficiencies with Fe(III)/H_2O_2/Solar-UV process of textile industry wastewater at average flowrate are presented in Figure 4.32.

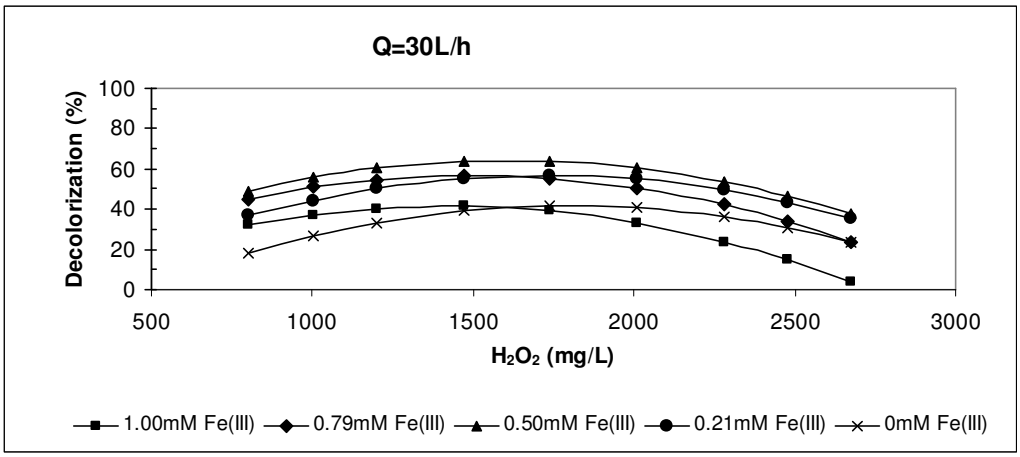

Figure 4.32 Variation of decolorization efficiency of textile industry wastewater at average flowrate with Fe(III)/H_2O_2/Solar-UV process.

Color removal efficiencies varied between 4% and 64% at average flowrate. As seen from the results, inceasing the flowrate from 10 to 30 L/h increased the maximum decolorization efficiency from 48% to 64%. The efficiency increased with increasing Fe(III) concentration from 0 to 0.5mM. Increasing the Fe(III) concentration from 0.5 to 1.0 resulted in a decrease in color removal efficiency.

The efficiency increased with increasing H_2O_2 concentration from 803.1 to 1740mg/L but the efficiency started to decrease with increasing H_2O_2 concentration from 1740 to 2677 mg/L at all Fe(III) concentrations. When the flowrate was at a average value, optimum concentrations of H_2O_2 and Fe(III) were

1740mg/L and 0.5mM, respectively to achieve maximum color removal efficiency.

(c)At maximum flowrate (Q=50L/h);

Color removal efficiencies with Fe(III)/H_2O_2/Solar-UV process of textile industry wastewater at maximum flowrate are presented in Figure 4.33.

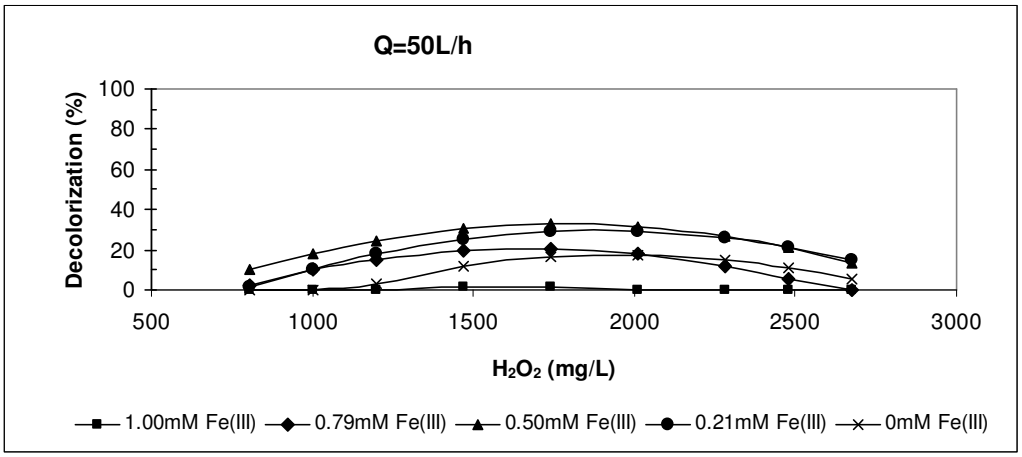

Figure 4.33 Variation of decolorization efficiency of textile industry wastewater at maximum flowrate with Fe(III)/H_2O_2/Solar-UV process.

Color removal efficiencies varied between 0% and 33% at maximum flowrate. Increasing the flowrate from 30L to 50L/h did not result in an increase in color removal efficiency. Efficiency decreased from 64% to 33% when flowrate increased from 30 to 50L/h.

The efficiency increased with increasing Fe(III) concentration from 0 to 0.50mM but decreased with increasing Fe(III) concentration from 0.50 to 1.0mM. The efficiency increased with increasing H_2O_2 concentration from 803.1 to 1740mg/L but the efficiency started to decrease with increasing H_2O_2 concentration from 1740 to 2677 mg/L at all Fe(III) concentrations. Herewith, 0.50mM Fe(III) and 1740mg/L H_2O_2 concentrations were found to be the optimum treatment condition when the flowrate was at 50L/h.

As a result of Box Wilson experimental design method, maximum color removal condition for textile industry wastewater was 0.5mM Fe(III), 1740mg/L H_2O_2 and 30L/h flowrate.

4.2.3.2.2 TOC removal

(a) At minimum flowrate (Q=10L/h);

TOC removal efficiencies with Fe(III)/H_2O_2/Solar-UV process of textile industry wastewater at minimum flowrate are presented in Figure 4.34.

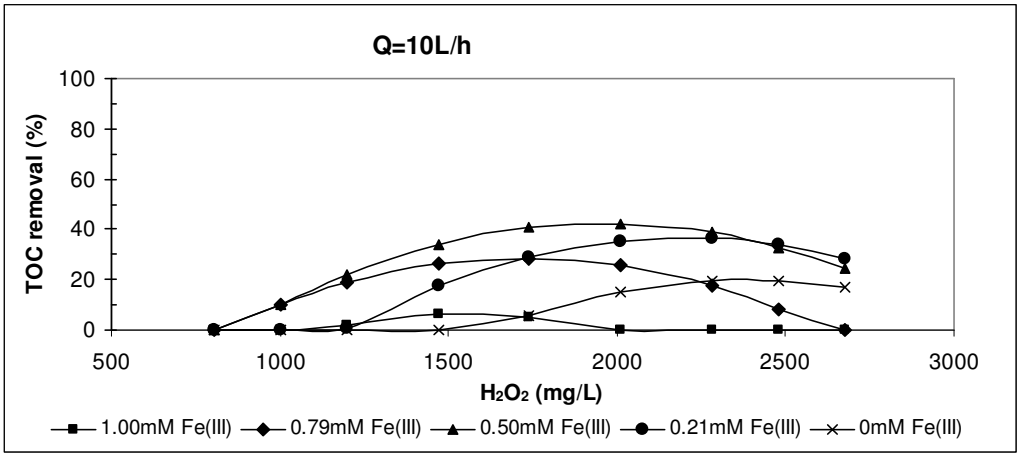

Figure 4.34 Variation of TOC removal efficiency of textile industry wastewater at minimum flowrate with Fe(III)/H_2O_2/Solar-UV process.

TOC removal efficiencies varied from 0% to 42% at flowrate of 10L/h. When the Fe(III) concentration was 1.0mM TOC removal efficiency was nearly zero. Reason of this was inhibition of Fe(III) ions of TOC removal efficieny. When Fe(III) concentration decreased from 1.0 to 0.5mM TOC removal efficiency increased. When Fe(III) concentration decreased from 0.5 to 0mM TOC removal efficiency decreased again.

Efficiency increased with increasing of H_2O_2 concentration up to a certain point. After that point efficiency started to decrease at all Fe(III) concentrations

because of generation of byproducts when the H_2O_2 concentration was higher than necessary. That point was at 2010.5mg/L H_2O_2 concentration where maximum removal efficiency was achieved at 0.5mM Fe(III) and 10L/h flowrate.

(b) At average flowrate (Q=30L/h);

TOC removal efficiencies with Fe(III)/H_2O_2/Solar-UV process of textile industry wastewater at minimum flowrate are presented in Figure 4.35.

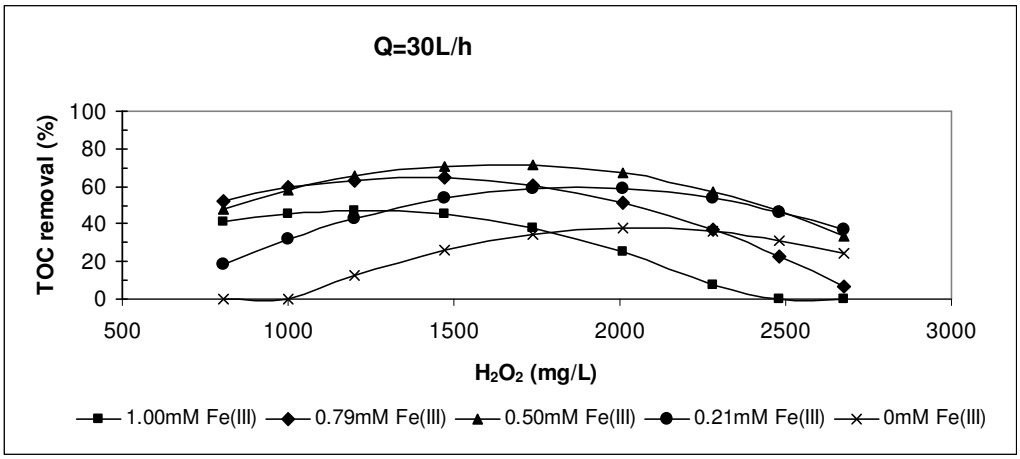

Figure 4.35 Variation of TOC removal efficiency of textile industry wastewater at average flowrate with Fe(III)/H_2O_2/Solar-UV process.

TOC removal efficiencies varied from 0% to 72% at flowrate of 30L/h. Inceasing the flowrate from 10L/h to 30 L/h increased the maximum TOC removal efficiency from 42% to 72%. The efficiency increased with increasing Fe(III) concentration from 0 to 0.5mM. Increasing the Fe(III) concentration from 0.5 to 1.0 resulted in a decrease in TOC removal efficiency.

Efficiency increased with increasing H_2O_2 concentration up to a certain point. After that point efficiency started to decrease at all Fe(III) concentrations again. The efficiency increased with increasing H_2O_2 concentration from 803.1 to 1740mg/L but the efficiency started to decrease with increasing H_2O_2 concentration from 1740 to 2677 mg/L at Fe(III) concentration of 0.5mM.

When the flowrate was 30L/h, optimum concentrations of H_2O_2 and Fe(III) were 1740mg/L and 0.5mM, respectively, to achieve maximum TOC removal efficiency.

(c) At maximum flowrate (Q=50L/h);

TOC removal efficiencies with Fe(III)/H_2O_2/Solar-UV process of textile industry wastewater at minimum flowrate are presented in Figure 4.36.

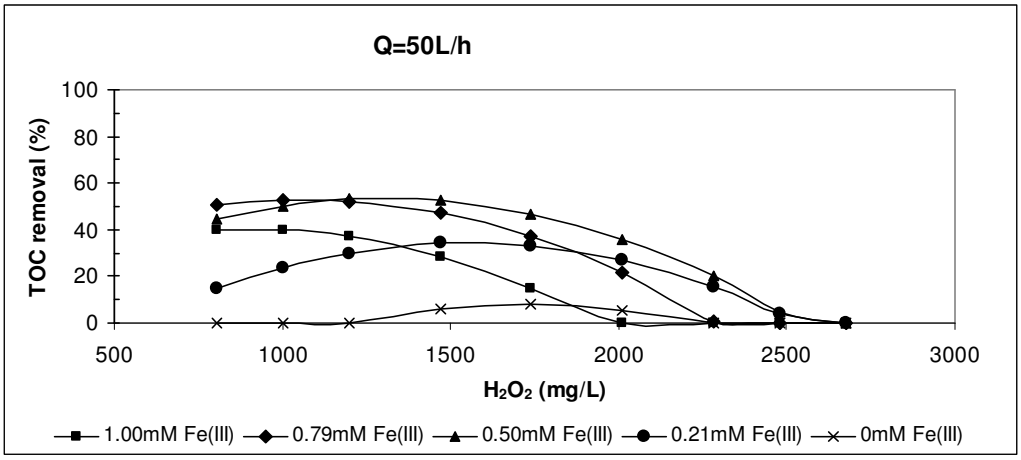

Figure 4.36 Variation of TOC removal efficiency of textile industry wastewater at maximum flowrate with Fe(III)/H_2O_2/Solar-UV process.

TOC removal efficiencies varied from 0 to 53% at flowrate of 50L/h. Inceasing the flowrate from 30L/h to 50L/h decreased maximum TOC removal efficiency from 72% to 53%. Increasing H_2O_2 concentration from 803.1mg/L to 1740mg/L did not increase efficiency significantly. But, at higher H_2O_2 concentrations than 1740mg/L efficiency decreased significantly.

Increasing Fe(III) concentration from 0 to 0.5mM increased TOC removal efficiency but increasing Fe(III) concentration from 0.5 to 1.0mM decreased TOC removal efficiency again.

As a consequence, maximum color and TOC removal efficiencies (64% and 72%, respectively) were achieved at the same experimental condition which was 1740mg/L H_2O_2 and 0.5mM Fe(III) at a flowrate of 30L/h for Fe(III)/TiO_2/Solar-UV process with textile industry wastewater.

4.2.4 Solar TiO_2 Catalysis (Fe(III)/ TiO_2/Solar-UV)

4.2.4.1 Experimental Procedure

Experimental procedure with wastewater was explained in chapter 3.2.2.4. The significant independent and dependent variables are as same as variables for Fe(III)/TiO_2/Solar-UV process with synthetic wastewater. Experimental points and conditions determined by the Box–Wilson statistical design are presented in Table 4.1 and 4.2.

4.2.4.2 Regression Model

Figure 4.37-4.42 depict variation of decolorization and TOC removal efficiency with irradiation time. Computation was carried out using multiple regression analysis that uses the least squares method. The following response functions (Eq. 4.7 and 4.8) were utilized in the correlation of the color removal efficiency (Y_C) and TOC removal efficiency (Y_{TOC}) with other independent parameters ($X1$–$X3$). The Statistica computer program was employed for the determination of the coefficients of response functions by regression analysis of the experimental data. Response functions with calculated coefficients were given in Eq. 4.7 and 4.8, and were used in calculating predicted values of color and TOC removal efficiencies. Observed and predicted color and TOC removal efficiencies with COD and BOD removal efficiencies were given in Table 4.9.

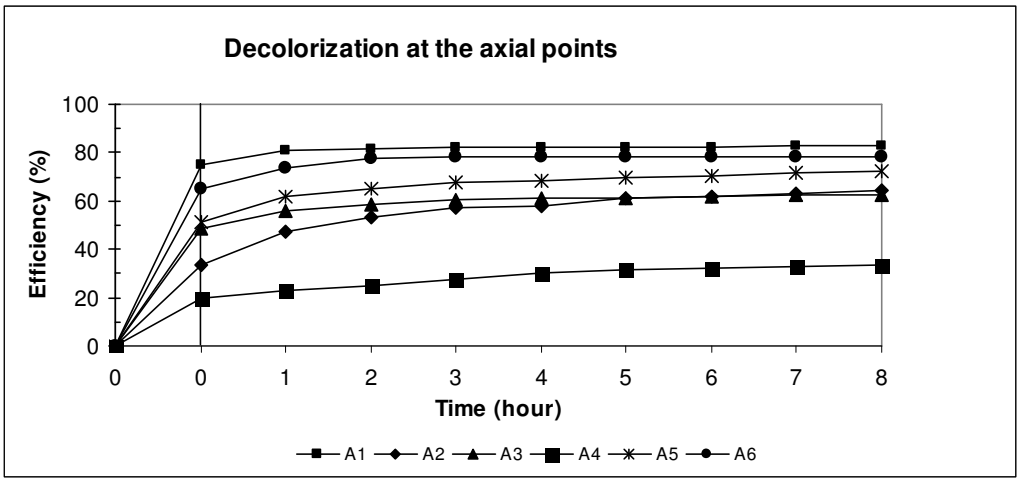

Figure 4.37 Variation of decolorization efficiency with irradiation time at axial points with Fe(III)/TiO_2/Solar-UV process

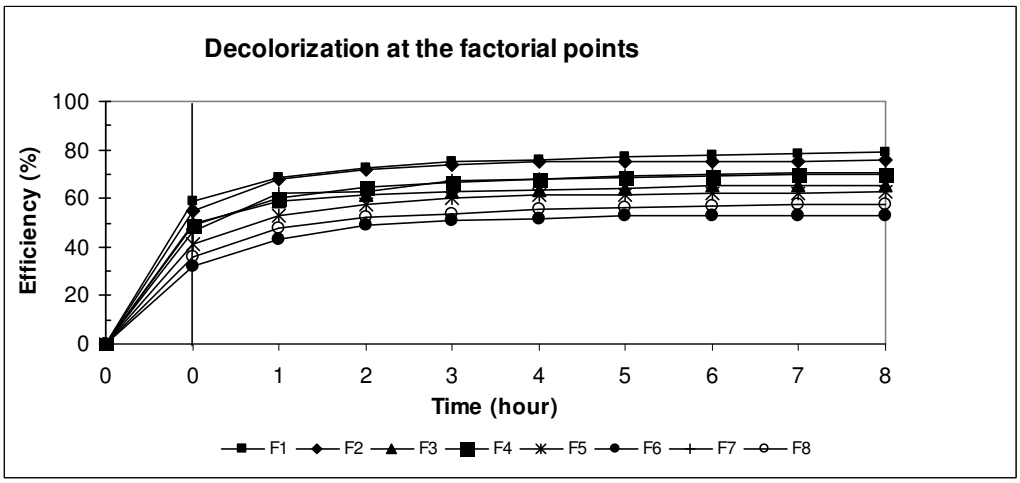

Figure 4.38 Variation of decolorization efficiency with irradiation time at factorial points with Fe(III)/TiO_2/Solar-UV process

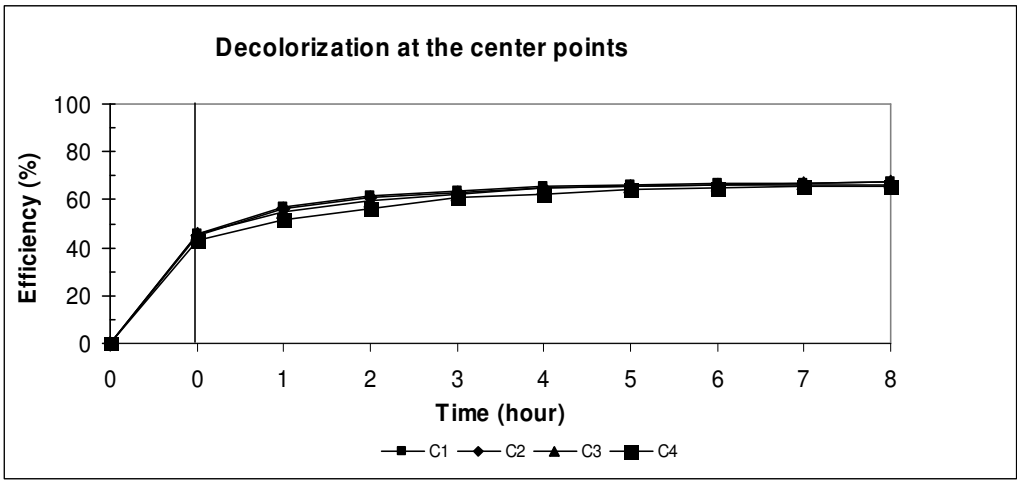

Figure 4.39 Variation of decolorization efficiency with irradiation time at center points with Fe(III)/TiO_2/Solar-UV process

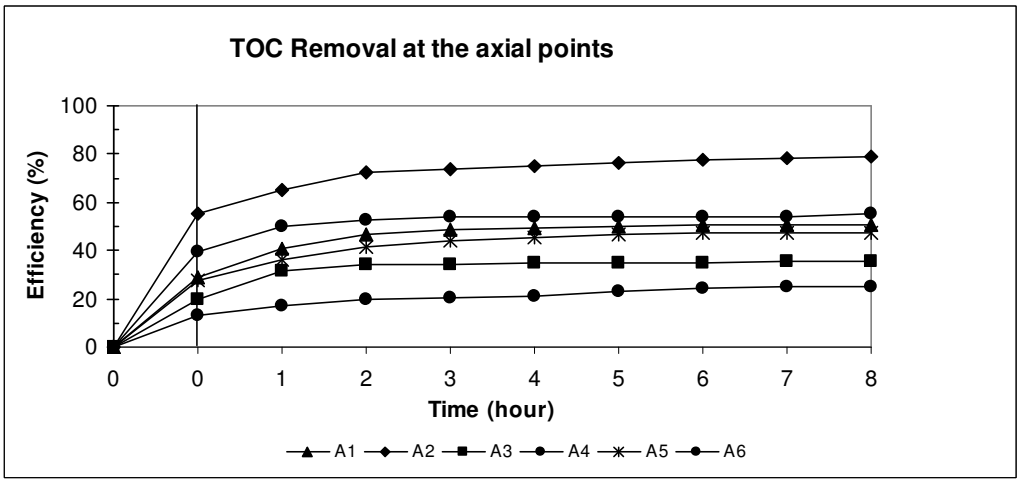

Figure 4.40 Variation of TOC removal efficiency with irradiation time at axial points with Fe(III)/TiO_2/Solar-UV process

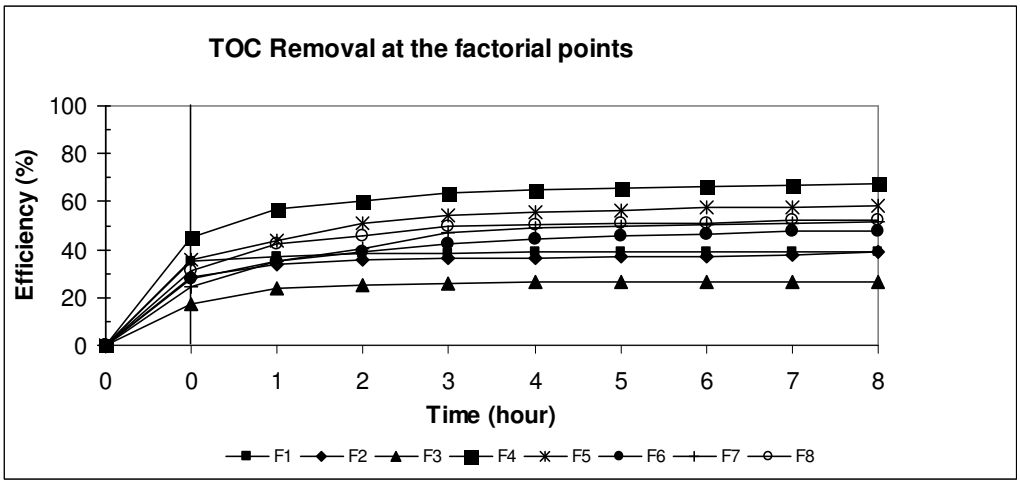

Figure 4.41 Variation of TOC removal efficiency with irradiation time at factorial points with Fe(III)/TiO_2/Solar-UV process

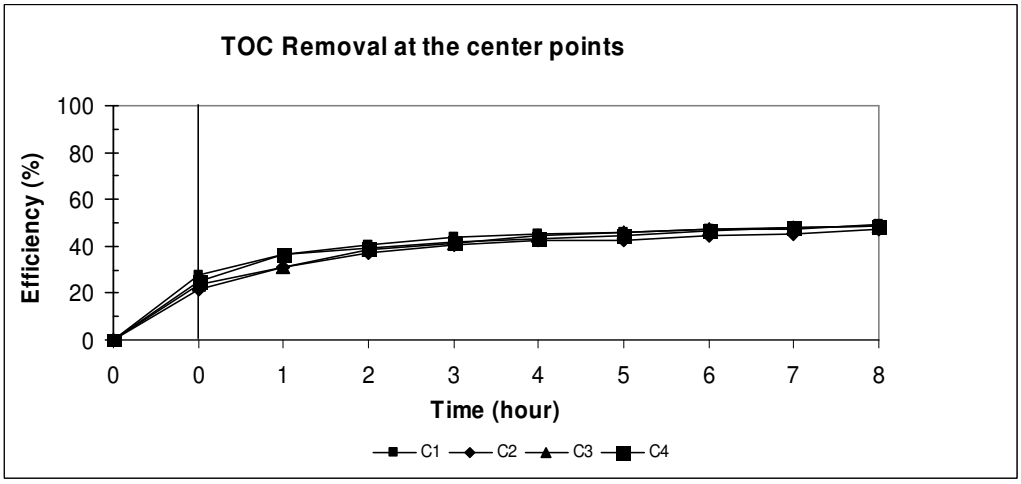

Figure 4.42 Variation of TOC removal efficiency with irradiation time at center points with Fe(III)/TiO_2/Solar-UV process

Response function (Y_{COL}) for color removal;

$$Y_{COL} = 75.45109 - 0.20627\ X_1 + 95.21014\ X_2 - 1.90194\ X_3 - 0.02533\ X_1X_2 + 0.00218\ X_1X_3 + 0.16848\ X_2X_3 - 0.00078\ X_1^2 - 70.61512\ X_2^2 + 0.02379\ X_3^2 \quad (R^2 = 0.9790) \qquad \text{(Eq. 4.7)}$$

Response function (Y_{TOC}) for TOC removal;

$$Y_{TOC} = 73.41030 - 0.28254\ X_1 + 50.55524\ X_2 - 0.36740\ X_3 - 0.18322\ X_1X_2 - 0.00803\ X_1X_3 + 1.90906\ X_2X_3 - 0.00162\ X_1^2 - 73.41846\ X_2^2 + 0.00691\ X_3^2 \quad (R^2 = 0.9884) \qquad \text{(Eq. 4.8)}$$

The correlation coefficients (R^2) between the observed and predicted values were 0.9790 and 0.9884 for Y_{COL} and Y_{TOC}, respectively indicating a good agreement between the observed and predicted values of color and TOC removal efficiencies.

Table 4.9 Observed and predicted color and TOC removal efficiencies determined by the Box–Wilson statistical design with COD and BOD removal efficiencies (textile industry wastewater, Fe(III)/TiO_2/Solar-UV process).

No.	% Color removal		% TOC removal		% BOD removal	% COD removal
	observed	predicted	observed	predicted	observed	observed
A1	83	82	51	52	65	67
A2	64	67	79	77	59	60
A3	63	62	35	33	61	64
A4	33	36	25	26	37	38
A5	72	75	48	47	47	50
A6	78	78	55	55	41	42
F1	79	79	39	38	67	68
F2	76	77	39	41	51	54
F3	66	64	27	27	60	60
F4	70	68	67	70	49	53
F5	63	63	58	56	37	42
F6	53	51	48	47	53	55
F7	71	71	51	51	50	55
F8	58	56	53	54	46	50
C1	68	67	49	48	54	55
C2	67	67	47	48	52	53
C3	67	67	49	48	53	56
C4	66	67	49	48	53	55

Maximum color and TOC removal efficiencis were 83% and 79% and were achieved at A1 (250mg/L TiO_2, 0.5mM Fe(III) and 30L/h flowrate) and A2 (50mg/L TiO_2, 0.5mM Fe(III) and 30L/h flowrate) experimental conditions, respectively. More experimental results were needed to comment on the regression model better. Color and TOC removal efficiencies were predicted by using Eq. 4.7 and 4.8 when flowrate kept constant at minimum (10L/h), average (30L/h) and maximum (50L/h) value in order. Results are given in Figure 4.43-4.48.

4.2.4.2.1 Decolorization

(a) At minimum flowrate (Q=10L/h);

Color removal efficiencies with Fe(III)/TiO_2/Solar-UV process of textile industry wastewater at minimum flowrate are presented in Figure 4.43.

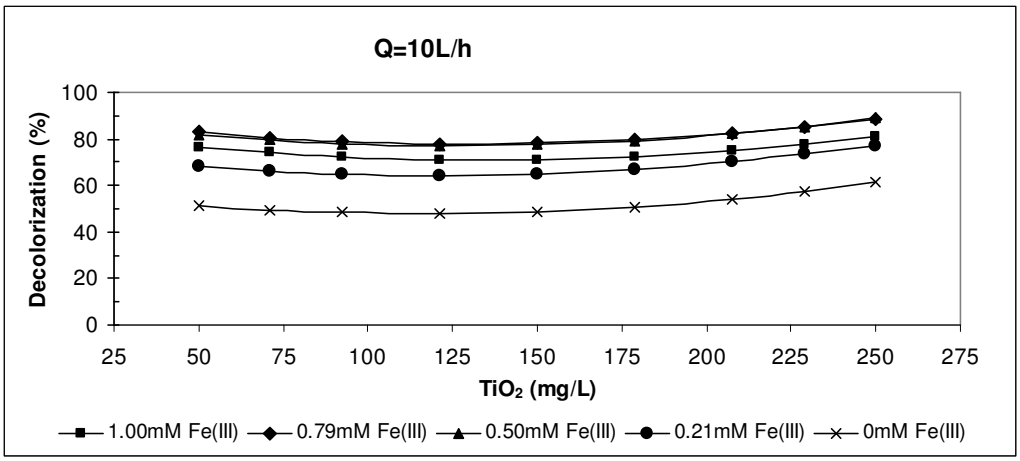

Figure 4.43 Variation of decolorization efficiency of textile industry wastewater at minimum flowrate with Fe(III)/TiO_2/Solar-UV process.

Color removal efficiencies varied between 48% and 89% at minimum flowrate. The efficiency increased with increasing Fe(III) concentration from 0 to 0.50mM at all TiO_2 concentrations. Increasing Fe(III) concentration from 0.5 to 0.79mM did not change efficiency significantly. Nevertheless, maximum efficiency was achieved at a Fe(III) concentration of 0.50mM but efficiency decreased with increasing Fe(III) concentration from 0.79 to 1.0mM.

Increasing the initial TiO_2 concentration from 50 to 150 mg/L resulted in a decrease in color removal efficiency but not significantly. Increasing TiO_2 concentration from 150 to 250 mg/L increased the efficiency at all Fe(III) concentrations. Herewith, 0.50mM Fe(III) and 250mg/L TiO_2 concentrations were found to be the optimum treatment conditions when the flowrate was at 10L/h.

(b) At average flowrate (Q=30L/h);

Color removal efficiencies with Fe(III)/TiO_2/Solar-UV process of textile industry wastewater at average flowrate are presented in Figure 4.44.

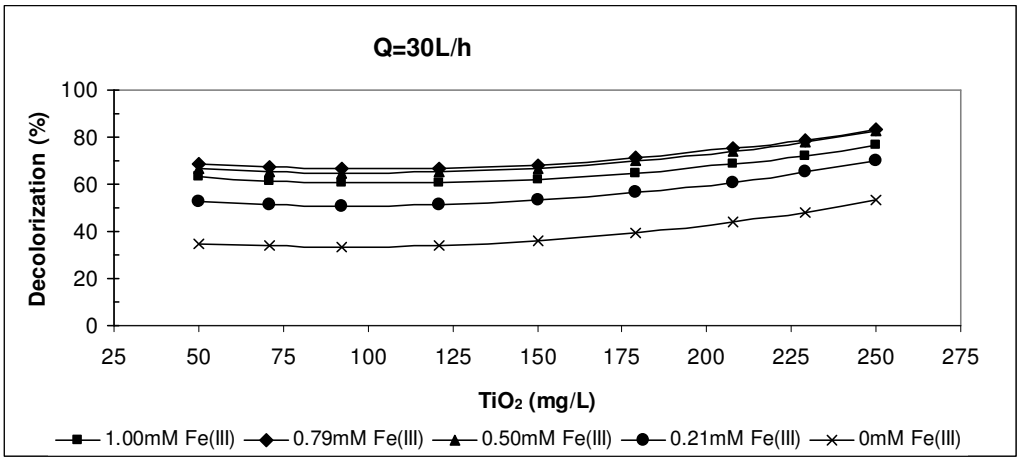

Figure 4.44 Variation of decolorization efficiency of textile industry wastewater at average flowrate with Fe(III)/TiO_2/Solar-UV process.

Color removal efficiencies varied between 33% and 83% at 30L/h flowrate. Increasing the flowrate from 10 to 30L/h decreased maximum color removal efficiency from 89% to 83%.

In experiments at 10L/h, the efficiency increased with increasing Fe(III) concentration from 0 to 0.50mM at all TiO_2 concentrations. Increasing Fe(III) concentration from 0.5 to 0.79mM did not change efficiency significantly again. Nevertheless, maximum efficiency was achieved at a Fe(III) concentration of 0.79 mM. But efficiency decreased with increasing Fe(III) concentration from 0.79 to 1.0mM. Increasing the initial TiO_2 concentration from 50 to 125 mg/L resulted in a decrease in color removal efficiency but increasing TiO_2 concentration from 125 to 250 mg/L increased the efficiency at all Fe(III) concentrations. Therewith, 0.79mM Fe(III) and 250mg/L TiO_2 concentrations were found to be the optimum treatment conditions when the flowrate was at 30L/h.

(c) At maximum flowrate (Q=50L/h);

Color removal efficiencies with Fe(III)/TiO_2/Solar-UV process of textile industry wastewater at maximum flowrate are presented in Figure 4.45.

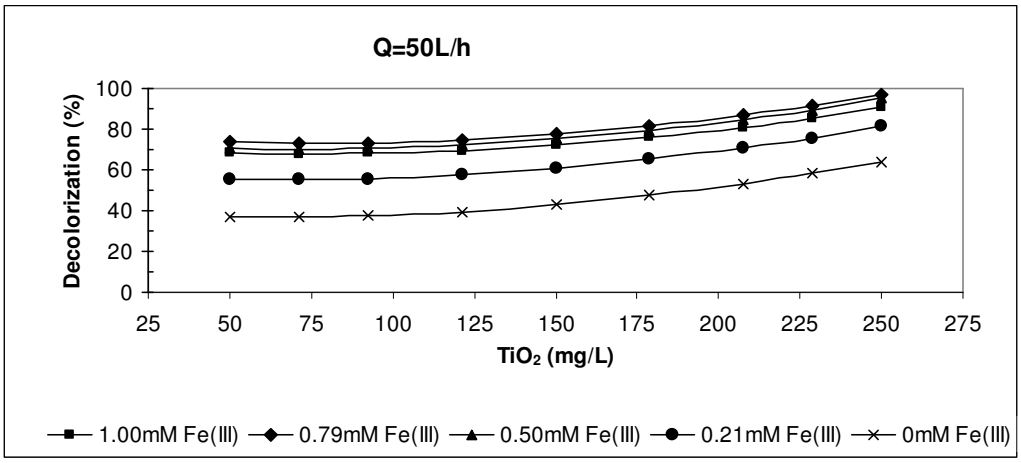

Figure 4.45 Variation of decolorization efficiency of textile industry wastewater at maximum flowrate with Fe(III)/TiO_2/Solar-UV process.

Color removal efficiencies varied between 37% and 97% at 50L/h flowrate. Increasing the flowrate from 30 to 50L/h increased maximum color removal efficiency from 83% to 97%. As a result, maximum color removal efficiency was achieved when flowrate was 50L/h.

The efficiency increased with increasing Fe(III) concentration from 0 to 0.50mM at all TiO_2 concentrations. Increasing Fe(III) concentration from 0.5 to 0.10mM decreased efficiency significantly.

Increasing the initial TiO_2 concentration from 50 to 250 mg/L resulted in an increase in color removal efficiency at all Fe(III) concentrations. 0.79mM Fe(III) and 250mg/L TiO_2 concentrations were found to be the optimum treatment conditions when the flowrate was at 50L/h for maximum color removal.

4.2.4.2.2 TOC removal

(a) At minimum flowrate (Q=10L/h);

TOC removal efficiencies with Fe(III)/TiO_2/Solar-UV process of textile industry wastewater at minimum flowrate are presented in Figure 4.46.

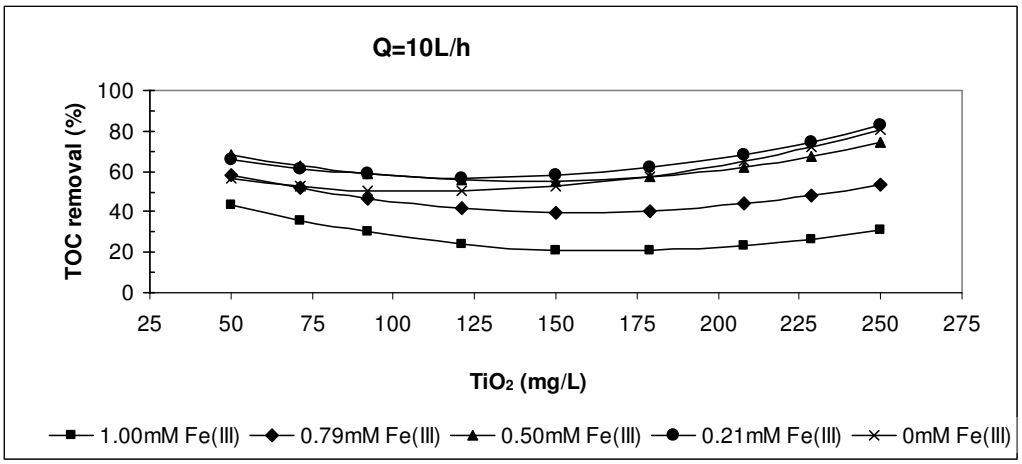

Figure 4.46 Variation of TOC removal efficiency of textile industry wastewater at minimum flowrate with Fe(III)/TiO_2/Solar-UV process.

TOC removal efficiencies varied from 21% to 83% at flowrate of 10L/h. Increasing Fe(III) concentration from 0 to 0.29mM increased TOC removal efficiency. But increasing Fe(III) concentration from 0.29 to 1.0mM TOC removal efficiency started to decrease.

Increasing TiO_2 concentration from 50 to 150 mg/L resulted in a decrease in TOC removal efficiency but increasing TiO_2 concentration from 150 to 250 mg/L increased TOC removal efficiency at all Fe(III) concentrations. Herewith, 0.21mM Fe(III) and 250mg/L TiO_2 concentrations were found to be the optimum treatment conditions when the flowrate was at 10L/h.

(b) At average flowrate (Q=30L/h);

TOC removal efficiencies with Fe(III)/TiO_2/Solar-UV process of textile industry wastewater at average flowrate are presented in Figure 4.47.

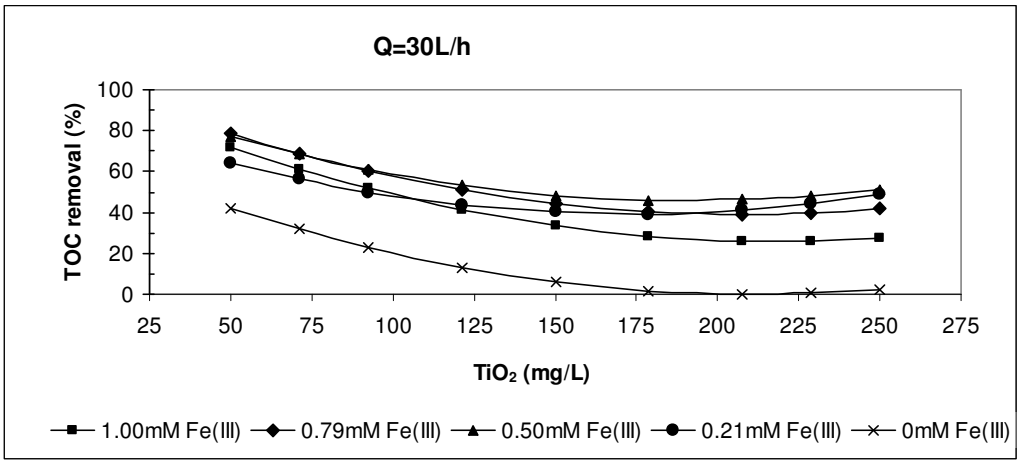

Figure 4.47 Variation of TOC removal efficiency of textile industry wastewater at average flowrate with Fe(III)/TiO_2/Solar-UV process.

TOC removal efficiencies varied from 26% to 79% at flowrate of 30L/h. When the flowrate increased from 10 to 30L/h, maximum TOC removal efficiency decreased from 83% to 79%. Increasing Fe(III) concentration from 0 to 0.79mM increased the efficiency at all TiO_2 concentrations. When Fe(III) concentration incereased from 0.79 to 1.0mM the efficiency decreased.

Maximum TOC removal efficiency was achieved when TiO_2 concentration was 50mg/L. Increasing TiO_2 concentration from 50 to 250 mg/L decreased TOC removal efficiency. Herewith, 0.79mM Fe(III) and 50mg/L TiO_2 concentrations were found to be the optimum treatment conditions when the flowrate was 30L/h.

(c) At maximum flowrate (Q=50L/h);

TOC removal efficiencies with Fe(III)/TiO_2/Solar-UV process of textile industry wastewater at maximum flowrate are presented in Figure 4.48.

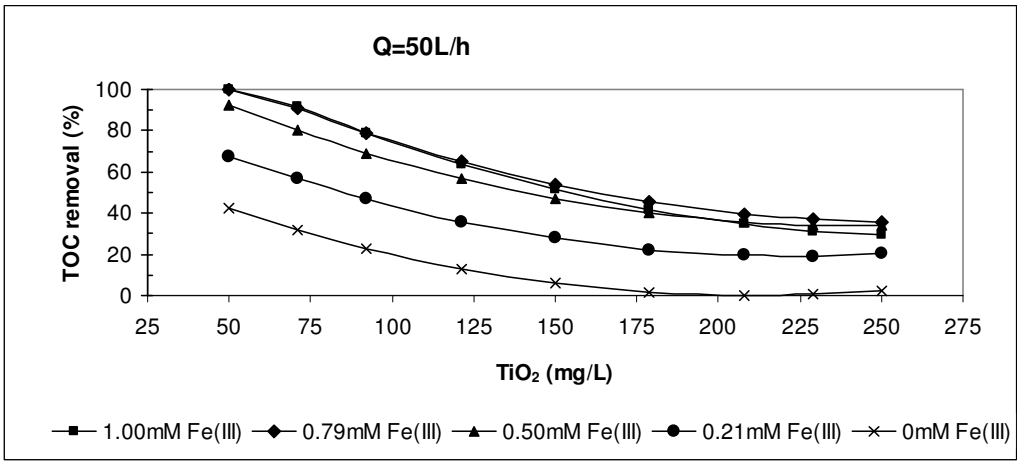

Figure 4.48 Variation of TOC removal efficiency of textile industry wastewater at maximum flowrate with Fe(III)/TiO_2/Solar-UV process.

TOC removal efficiencies varied between 0% and 100% at maximum flowrate. When the flowrate increased from 30 to 50L/h, maximum TOC removal efficiency decreased from 79% to 100%. The efficiency increased with increasing Fe(III) concentration from 0 to 0.79mM but decreased with increasing Fe(III) concentration from 0.79 to 1.0mM.

Such in average flowrate, maximum TOC removal efficiency was achieved when TiO_2 concentration was 50mg/L. Increasing TiO_2 concentration from 50 to 250 mg/L decreased TOC removal efficiency significantly. Herewith, 0.79mM Fe(III) and 50mg/L TiO_2 concentrations were found to be the optimum treatment conditions when the flowrate was at 50L/h.

Throughout the Fe(III)/TiO_2/Solar-UV process with textile industry wastewater, maximum color removal efficiency was achieved at an experimental condition where Fe(III) and TiO_2 concentrations were 0.79mM and 250mg/L, respectively,

at a flowrate of 50L/h. For maximum TOC removal Fe(III) and TiO_2 concentrations were 0.79mM and 50mg/L, respectively at a flowrate of 50L/h. It seemed that at the same Fe(III) concentration and flowrate (0.79mM and 50L/h, respectively) higher amount of TiO_2 was needed to achieve maximum decolorization than was needed to achieve maximum TOC removal.

Color removal efficiency was calculated by using response function (Eq. 4.7) at the experimental condition which gives maximum TOC removal efficiency (50L/h flowrate, 0.79mM Fe(III) and 50mg/L TiO_2). Predicted color removal efficiency was 74%, which was lower than maximum color removal efficiencies achieved when flowrate was 10L/h (89%) or 30L/h (83%). Then, TOC removal efficiency was calculated by using response function (Eq. 4.8) at the experimental condition which gives the maximum color removal efficiency (50L/h flowrate, 0.79mM Fe(III) and 250mg/L TiO_2). Predicted TOC removal efficiency was 36%. This efficiency was lower than maximum TOC removal efficiencies achieved when flowrate was 10L/h (83%) or 30L/h (79%). As a conclusion, optimum TiO_2 concentration was 250mg/L for maximum color removal and 50mg/L for maximum TOC removal at 0.79mM Fe(III) and 50L/h flowrate.

As seen in Table 4.10, maximum color and TOC removal efficiencies which were achieved with Fe(III)/TiO_2/Solar-UV process (74% and 100%, respectively) were higher than the efficiencies achieved with Fe(III)/H_2O_2/Solar-UV process (64% and 72%, respectively). Performance of the Fe(III)/TiO_2/Solar-UV process at the treatment condition which maximum color removal was obtained was unsatisfactory yielding low percent removal of TOC.

Table 4.10 Optimum treatment conditions and color and TOC removal efficiencies determined by the Box–Wilson statistical design of textile industry wastewater with Fe(III)/H_2O_2/Solar-UV and Fe(III)/TiO_2/Solar-UV processes.

Fe(III)/ H_2O_2/Solar-UV				
Dosage of H_2O_2 (mg/L)	Dosage of Fe(III) (mM)	Flowrate (L/h)	Color removal efficiency(%)	TOC removal efficiency(%)
1740	0.50	30	64	72
Fe(III)/ TiO_2/Solar-UV				
Dosage of TiO_2 (mg/L)	Dosage of Fe(III) (mM)	Flowrate (L/h)	Color removal efficiency (%)	TOC removal efficiency (%)
50	0.79	50	74	100
250	0.79	50	97	36

4.3 Application of Box–Wilson Experimental Design Method for the Solar Degradation of Paper Industry Wastewater by Advanced Oxidation Processes

4.3.1 Introduction

Effluents of the paper industry contain a number of toxic compounds and may cause deleterious environmental impacts upon direct discharge to receiving waters. Paper industry processes utilize large amounts of water. The most significant sources of pollution in paper industry are wood preparation, pulping, pulp washing, screening, bleaching and coating operations. Among the various processing steps, pulping generates a high-strength wastewater containing toxic chemicals such as phenolics (Çatalkaya and Kargı, 2006).

Three main groups of organic compounds present in paper industry are, (a) starch degradation products, such as saccharides or carboxylic acids, (b) phenolic compounds arising from lignin and (c) other pollutants that may be present in the fresh waters such as surfactants. Major pollutants present in the effluents of paper industry are suspended solids, chemical oxygen demand (COD), toxicity, color, adsorbable organic halogens (AOX) and high concentration of nutrients that cause eutrophication in receiving water. Since some of the contaminants in pulp and paper industry effluents are non-biodegradable, conventional biological treatment processes are not sufficient for treatment. The extent of toxicity and color removal by conventional biological treatment vary depending on the pulping process used. In order to meet increasingly stringent discharge limits, pulp mills are forced to adopt technologically advanced treatment systems. Organic compounds such as chlorophenols are not fully degraded by biological processes which require advanced oxidation after biological treatment to reduce refractory organics and color of the pulp mill wastewater (Çatalkaya and Kargı, 2006).

This chapter includes the application of Box-Wilson Experimantal Design Method for the solar degradation of paper industry wastewater by advanced oxidation.

4.3.2 Wastewater characterization

Paper industry wastewater samples were obtained from a stabilization pond of a paper industry wastewater treatment plant located in Aliağa/İzmir, Turkey. Composition of the wastewater used in this study was analyzed before experimental studies. The pH values of paper industry effluent samples used in the experimental studies varied from 7.12 to 8.50. COD concentrations of samples varied from 608mg/L to 1500mg/L. BOD concentrations of samples were between 260mg/L and 500mg/L. TOC concentrations of samples varied from 206.2mg/L to 303.2mg/L and AOX concentrations of samples were between 136µg/L and 2864µg/L.

Wavelength scan also was done to find peak wavelength that gives maximum absorbance for each paper industry wastewater samples which were obtained from a paper industry wastewater treatment plant. Peak wavelengths and maximum absorbance values of wavelength scan were nearly similar. So, wavelength scan result giving maximum absorbance is presented in Appendix-A. Peak wavelength and the maximum absorbance values were found 480 nm and 0.141. Color measurements were carried at the wavelength 480nm and the beginning absorbance value at this wavelength came up to 100 unit color concentration.

4.3.3 Photo-Fenton-like Process (Fe(III)/H_2O_2/Solar-UV)

4.3.3.1 Experimental Procedure

Experimental procedure with wastewater was explained in chapter 3.2.2.4. The significant independent and dependent variables are the same as for Fe(III)/H_2O_2/Solar-UV process with synthetic wastewater. Experimental points

and conditions determined by the Box–Wilson statistical design are presented in Table 4.1 and 4.2.

4.3.3.2 Regression Model

Figure 4.49-4.54 depict variation of decolorization and TOC removal efficiency with irradiation time. Computation was carried out using multiple regression analysis that uses the least squares method. The following response functions (Eq. 4.9 and 4.10) were utilized in the correlation of the color removal efficiency (Y_C) and TOC removal efficiency (Y_{TOC}) with other independent parameters ($X1$–$X3$). The Statistica computer program was employed for the determination of the coefficients of response functions by regression analysis of the experimental data. Response functions with calculated coefficients were given in Eq. 4.9 and 4.10, and were used in calculating predicted values of color and TOC removal efficiencies. Observed and predicted color and TOC removal efficiencies with COD, BOD and AOX removal efficiencies were given in Table 4.11.

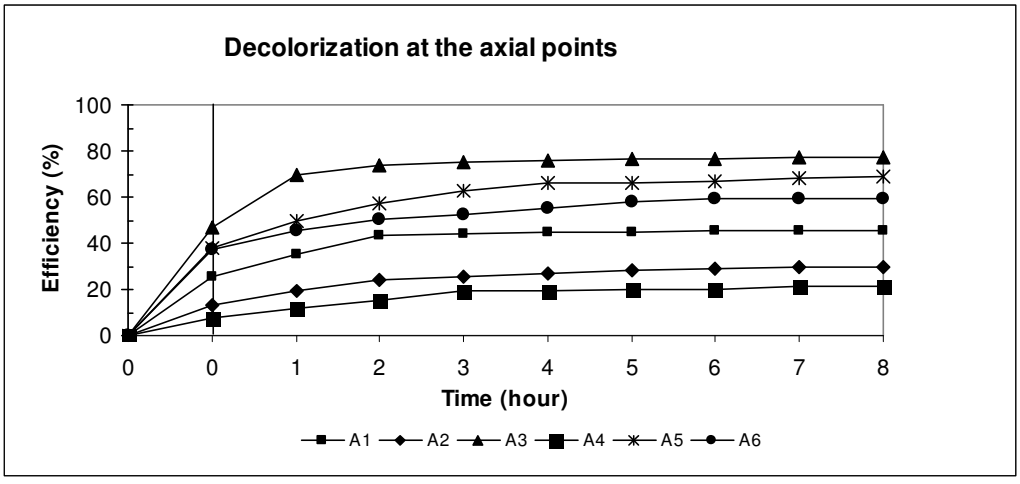

Figure 4.49 Variation of decolorization efficiency with irradiation time at axial points with Fe(III)/H_2O_2/Solar-UV process

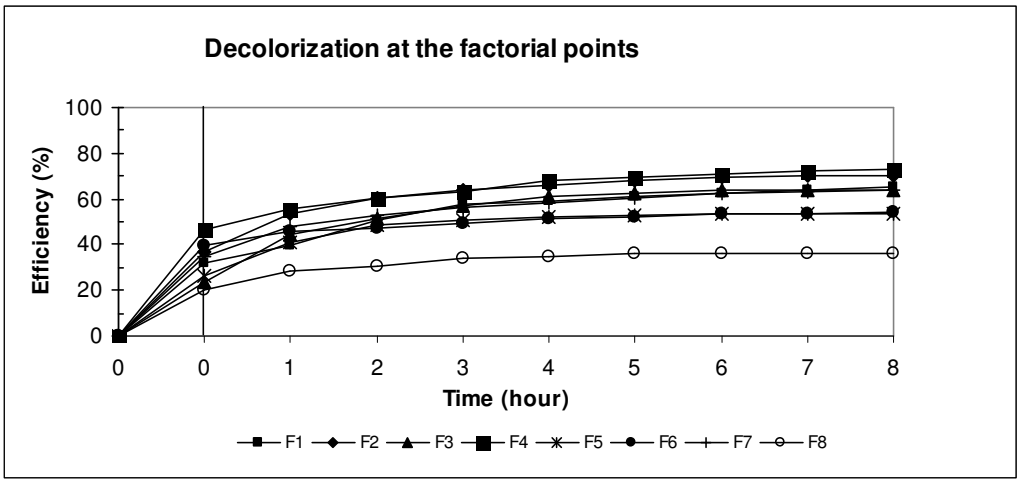

Figure 4.50 Variation of decolorization efficiency with irradiation time at factorial points with Fe(III)/H_2O_2/Solar-UV process

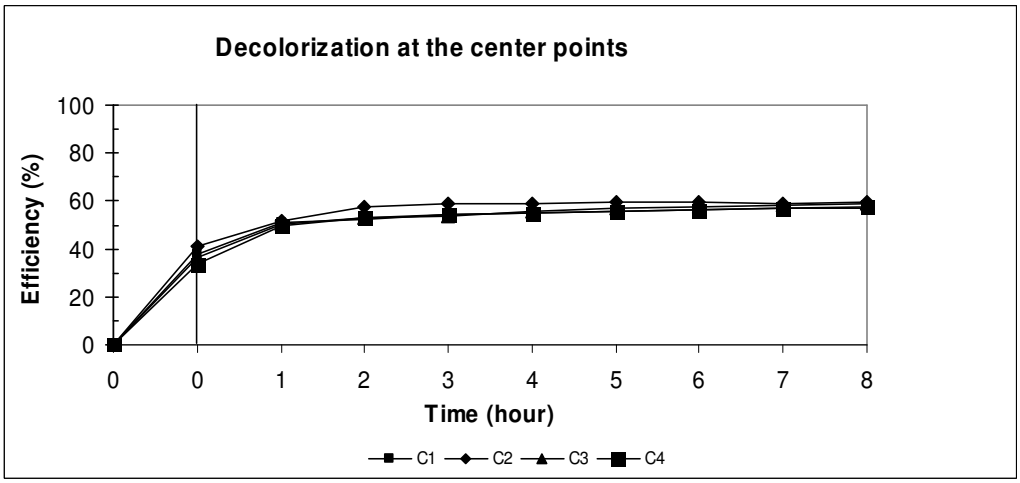

Figure 4.51 Variation of decolorization efficiency with irradiation time at center points with Fe(III)/H_2O_2/Solar-UV process

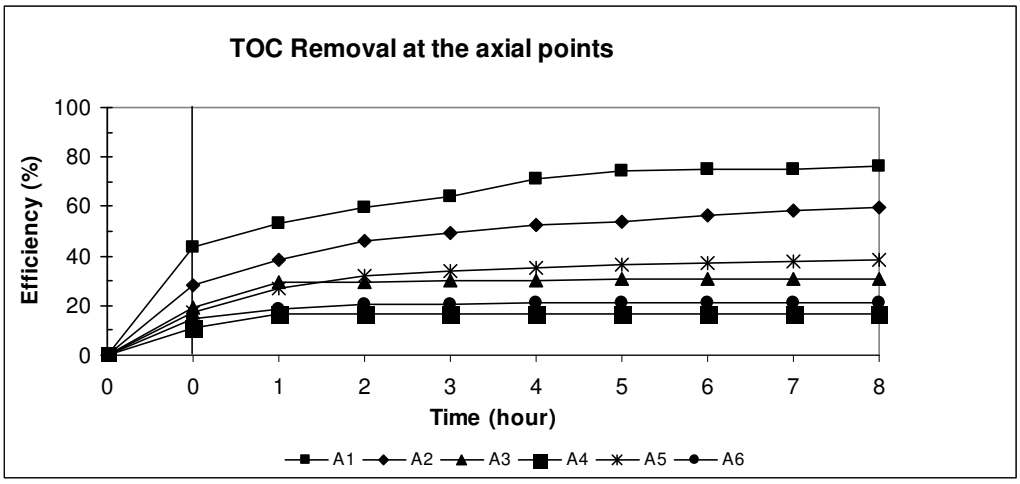

Figure 4.52 Variation of TOC removal efficiency with irradiation time at axial points with Fe(III)/H_2O_2/Solar-UV process

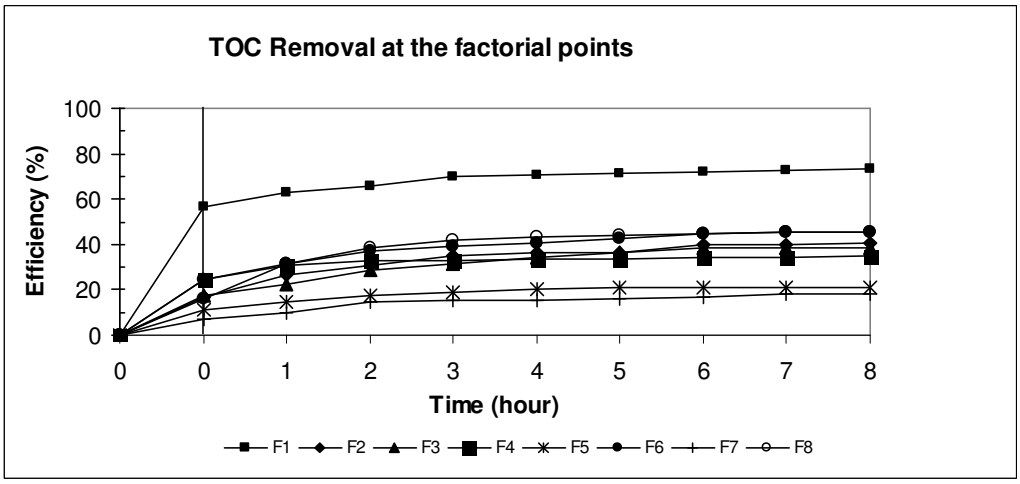

Figure 4.53 Variation of TOC removal efficiency with irradiation time at factorial points with Fe(III)/H_2O_2/Solar-UV process

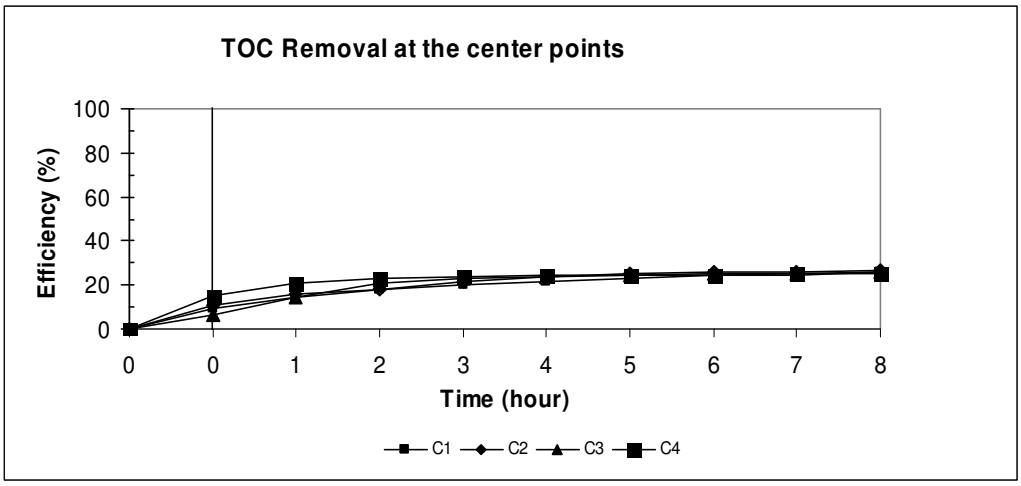

Figure 4.54 Variation of TOC removal efficiency with irradiation time at center points with Fe(III)/H_2O_2/Solar-UV process

Response function (Y_{COL}) for color removal;

$$Y_{COL} = -65.98959 + 0.09072\ X_1 + 113.46333\ X_2 - 0.24095\ X_3 - 0.02170\ X_1X_2 - 0.00044\ X_1X_3 - 0.85761\ X_2X_3 - 0.00002\ X_1^2 - 11.37103\ X_2^2 + 0.02893\ X_3^2 \quad (R^2 = 0.8390) \qquad \text{(Eq. 4.9)}$$

Response function (Y_{TOC}) for TOC removal;

$$Y_{TOC} = 253.69943 - 0.21407\ X_1 - 137.54947\ X_2 - 1.68520\ X_3 + 0.07123\ X_1X_2 + 0.00068\ X_1X_3 + 1.12971\ X_2X_3 + 0.00005\ X_1^2 - 10.41381\ X_2^2 + 0.00888\ X_3^2 \quad (R^2 = 0.9883) \qquad \text{(Eq. 4.10)}$$

The correlation coefficient (R^2) was 0.8390 for Y_{COL} and indicated a not good agreement between the observed and predicted values of color removal efficiencies. The correlation coefficient was 0.9883 for Y_{TOC} and indicated a good agreement between the observed and predicted values of TOC removal efficiencies.

Table 4.11 Observed and predicted color and TOC removal efficiencies determined by the Box–Wilson statistical design with COD, BOD and AOX removal efficiencies (paper industry wastewater, Fe(III)/H_2O_2/Solar-UV process).

No.	% Color removal		% TOC removal		% BOD removal	% COD removal	% AOX removal
	observed	predicted	observed	predicted	observed	observed	observed
A1	45	50	76	75	85	87	48
A2	30	36	60	61	85	88	33
A3	77	75	31	28	65	68	62
A4	21	36	17	18	42	47	29
A5	69	76	38	41	62	70	63
A6	59	64	21	17	58	70	66
F1	65	66	74	74	85	94	62
F2	70	70	41	44	69	74	65
F3	64	55	39	37	56	60	51
F4	73	70	35	34	63	62	45
F5	54	48	21	22	63	65	52
F6	54	46	46	43	68	71	33
F7	64	64	18	21	63	67	60
F8	36	28	45	46	81	83	50
C1	57	58	26	26	63	64	30
C2	60	58	27	26	64	66	30
C3	59	58	26	26	65	66	29
C4	57	58	25	26	65	65	31

Maximum color and TOC removal efficiencis were 77% and 76% and were achieved at A3 (1740mg/L H_2O_2, 1.0mM Fe(III) and 30L/h flowrate) and A1 (2677mg/L H_2O_2, 0.5mM Fe(III) and 30L/h flowrate) experimental conditions, respectively. More experimental results were needed to comment on the regression model better. Color and TOC removal efficiencies were predicted by using Eq. 4.9 and 4.10 when flowrate kept constant at minimum (10L/h), average (30L/h) and maximum (50L/h) value in order. Results are given in Figure 4.55-4.60.

4.3.3.2.1 Decolorization

(a)At minimum flowrate (Q=10L/h);

Color removal efficiencies with Fe(III)/H_2O_2/Solar-UV process of paper industry wastewater at minimum flowrate are presented in Figure 4.55.

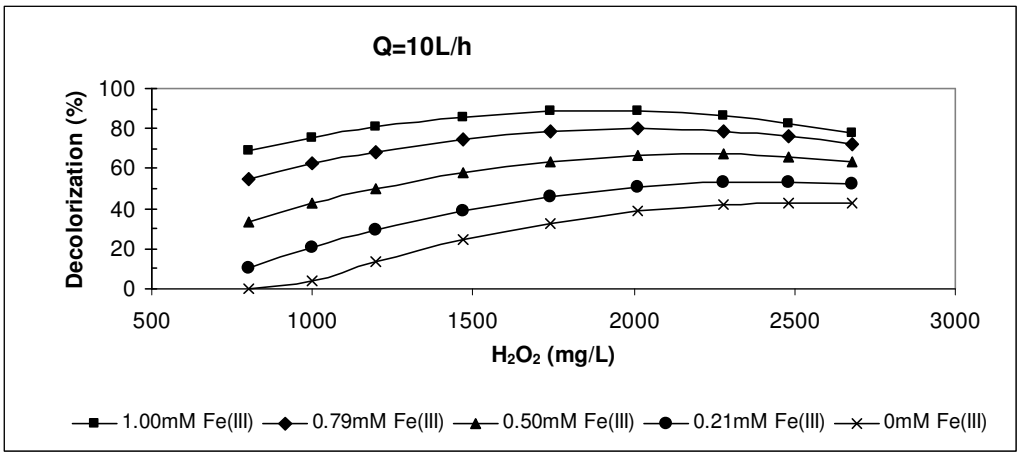

Figure 4.55 Variation of decolorization efficiency of paper industry wastewater at minimum flowrate with Fe(III)/H_2O_2/Solar-UV process.

Color removal efficiencies varied between 0% and 89% at minimum flowrate. The efficiency increased with increasing Fe(III) concentration. At the highest concentration of Fe(III) maximum color removal efficincies were achieved at various H_2O_2 concentrations. In addition, the efficiency increased with increasing H_2O_2 concentration from 803.1 to 2010.5mg/L but the efficiency started to decrease with increasing H_2O_2 concentration from 2010.5 to 2677 mg/L at all Fe(III) concentrations. The decreases in removal efficiency at high oxidant concentrations are thought to be due to the side reactions taking place between the •OH radicals and the excess H_2O_2. When the flowrate was at a minumun value, optimum concentrations of H_2O_2 and Fe(III) were 2010.5mg/L and 1.0mM, respectively to achieve maximum color removal efficiency.

(b) At average flowrate (Q=30L/h);

Color removal efficiencies with Fe(III)/H_2O_2/Solar-UV process of paper industry wastewater at average flowrate are presented in Figure 4.56.

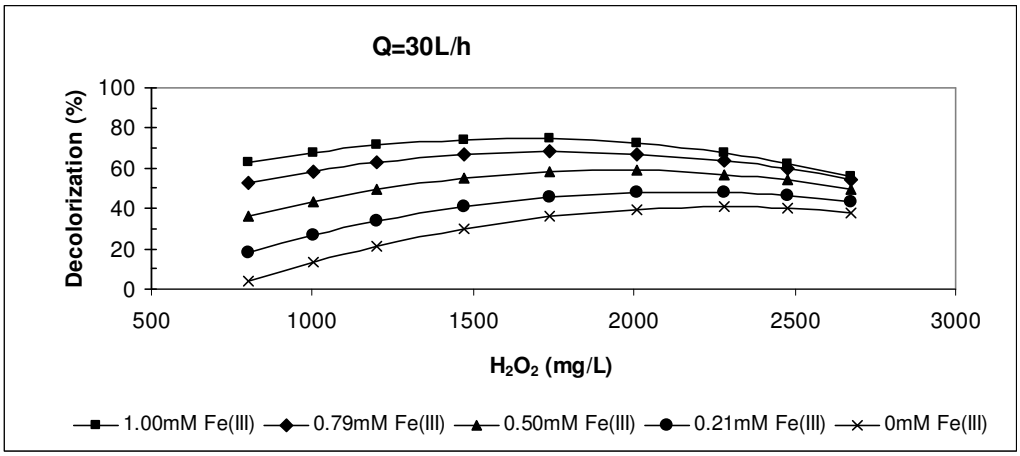

Figure 4.56 Variation of decolorization efficiency of paper industry wastewater at average flowrate with Fe(III)/H_2O_2/Solar-UV process.

Color removal efficiencies varied between 4% and 75% at average flowrate. As seen from the results, inceasing the flowrate from 10 to 30 L/h increased the maximum decolorization efficiency from 89% to 75%. The efficiency increased with increasing Fe(III) concentration from 0 to 1.0mM. At the highest concentration of Fe(III) maximum color removal efficincies were achieved at various H_2O_2 concentrations again.

The efficiency increased with increasing H_2O_2 concentration from 803.1 to 1740mg/L but the efficiency started to decrease with increasing H_2O_2 concentration from 1740 to 2677 mg/L at all Fe(III) concentrations. When the flowrate was at an average value, optimum concentrations of H_2O_2 and Fe(III) were 1740mg/L and 1.0mM, respectively, to achieve maximum color removal efficiency.

(c)At maximum flowrate (Q=50L/h);

Color removal efficiencies with Fe(III)/H_2O_2/Solar-UV process of paper industry wastewater at maximum flowrate are presented in Figure 4.57.

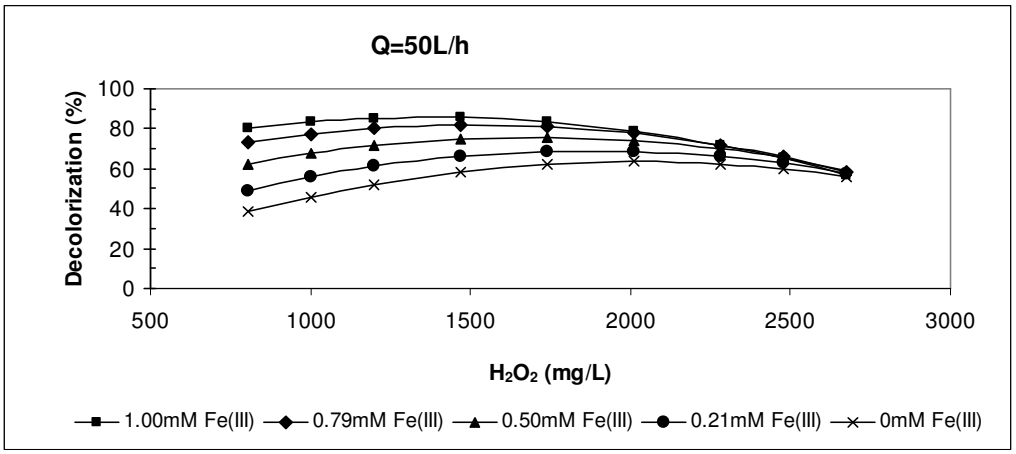

Figure 4.57 Variation of decolorization efficiency of paper industry wastewater at maximum flowrate with Fe(III)/H_2O_2/Solar-UV process.

Color removal efficiencies varied between 39% and 86% at the maximum flowrate. Inceasing the flowrate from 30 to 50L/h did not resulted in an increase in color removal efficiency. Efficiency decreased from 75% to 86% when flowrate increased from 30L/h to 50L/h but did not achieve maximum color removal efficiency.

The efficiency increased with increasing Fe(III) concentration from 0 to 1.0mM. And also, the efficiency increased with increasing H_2O_2 concentration from 803.1 to 1469.5mg/L but the efficiency started to decrease with increasing H_2O_2 concentration from 1469.5 to 2677mg/L at all Fe(III) concentrations. Herewith, 1.0mM Fe(III) and 1469.5mg/L H_2O_2 concentrations were found to be the optimum treatment condition when the flowrate was at 50L/h.

As a result of Box Wilson experimental design method, maximum color removal condition for paper industry wastewater was 1.0mM Fe(III), 1469.5mg/L H_2O_2 and 10L/h flowrate.

4.3.3.2.2 TOC removal

(a) At minimum flowrate (Q=10L/h);

TOC removal efficiencies with Fe(III)/H_2O_2/Solar-UV process of paper industry wastewater at minimum flowrate are presented in Figure 4.58.

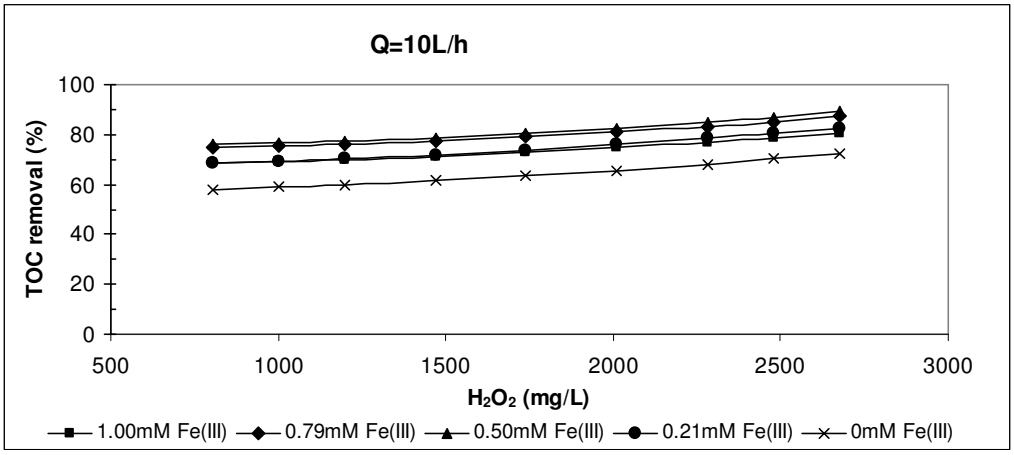

Figure 4.58 Variation of TOC removal efficiency of paper industry wastewater at minimum flowrate with Fe(III)/H_2O_2/Solar-UV process.

TOC removal efficiencies varied from 58% to 89% at flowrate of 10L/h. The efficiency increased with increasing Fe(III) concentration. However, increasing the initial Fe(III)concentration increased the efficiency, and then Fe(III)started to inhibit the TOC removal efficiency. Thus, after reaching the maximum efficiency that can be achieved at a certain Fe(III) concentration, efficiency decreased with the increasing of Fe(III) concentration. At Fe(III) concentrations higher than 0.50 mM, efficiency was decreased as shown in Figure 4.52.

In addition, the efficiency increased with increasing H_2O_2 concentration. But there was no significant difference when Fe(III) concentration was ranged from 0.50 to 0.79mM. When the flowrate was at a minumun value, optimum concentrations of H_2O_2 and Fe(III) were 2677mg/L and 0.50mM, respectively, to achieve maximum TOC removal efficiency.

(b) At average flowrate (Q=30L/h);

TOC removal efficiencies with Fe(III)/H_2O_2/Solar-UV process of paper industry wastewater at minimum flowrate are presented in Figure 4.59.

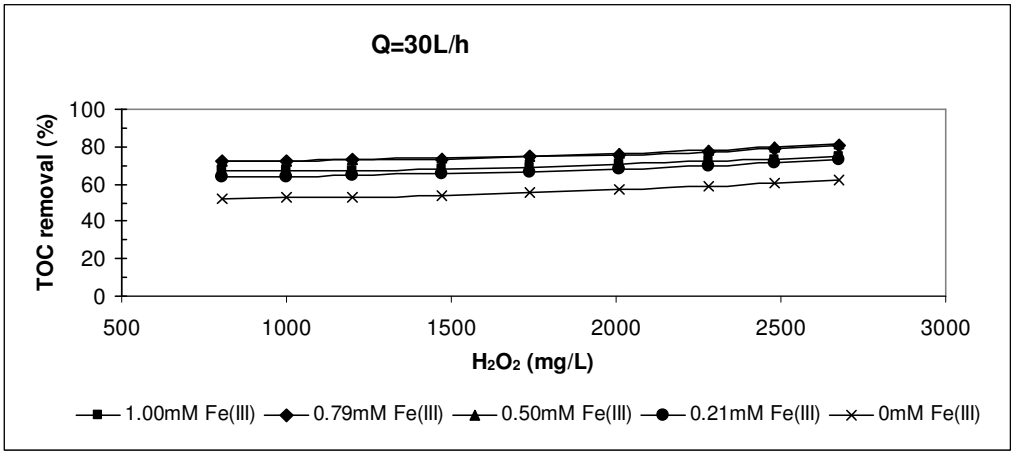

Figure 4.59 Variation of TOC removal efficiency of paper industry wastewater at average flowrate with Fe(III)/H_2O_2/Solar-UV process.

TOC removal efficiencies varied from 52% to 81% at flowrate of 30L/h. Inceasing the flowrate from 10 to 30 L/h decreased the maximum TOC removal efficiency from 89% to 81%. The efficiency increased with increasing Fe(III) concentration from 0 to 0.5mM but increasing the Fe(III) concentration from 0.5 to 1.0mM decreased TOC removal efficiency.

As in 10L/h flowrate, the efficiency increased by increasing H_2O_2 concentration. But there were no significant differences when Fe(III) concentration was ranged from 0.50 to 0.79mM. When the flowrate was at an average value,

optimum concentrations of H_2O_2 and Fe(III) were 2677mg/L and 0.50mM, respectively, to achieve maximum TOC removal efficiency.

(c) At maximum flowrate (Q=50L/h);

TOC removal efficiencies with Fe(III)/H_2O_2/Solar-UV process of paper industry wastewater at minimum flowrate were presented in Figure 4.60.

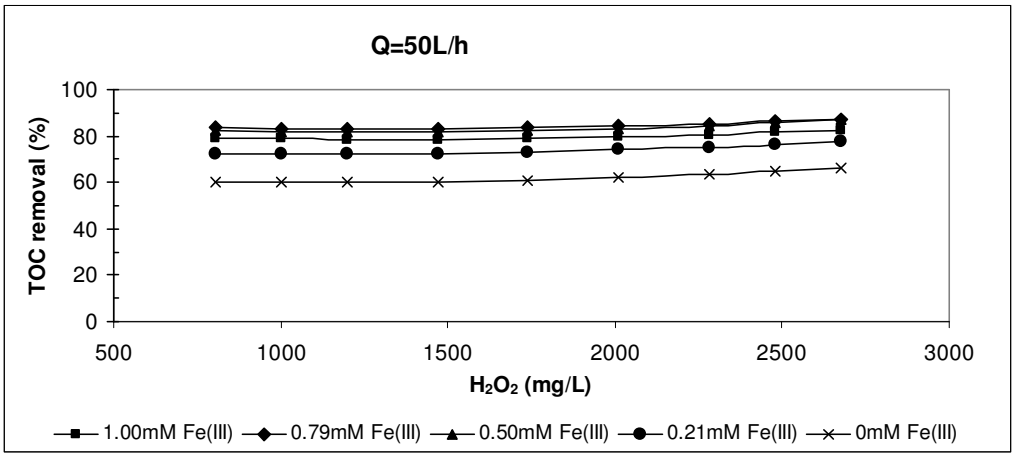

Figure 4.60 Variation of TOC removal efficiency of paper industry wastewater at maximum flowrate with Fe(III)/H_2O_2/Solar-UV process.

TOC removal efficiencies ranged from 60% to 88% at maximum flowrate. Increasing of flowrate from 30 to 50L/h increased efficiency from 81 to 87% but increasing of flowrate from 10 to 50L/h did not rise the efficiency. The efficiency increased with increasing Fe(III) concentration from 0 to 0.79mM but increasing the Fe(III) concentration from 0.79 to 1.0mM decreased TOC removal efficiency.

The efficiency increased with increasing H_2O_2 concentration. When the flowrate was at a maximum value, optimum concentrations of H_2O_2 and Fe(III) were 2677mg/L and 0.79mM, respectively, to achieve maximum TOC removal efficiency.

Throughout the Fe(III)/H_2O_2/Solar-UV process, optimum flowrate was determined as 10L/h. Although high TOC removal efficiency was determined at high H_2O_2 concentration which started to inhibit color removal efficiency. Maximum color removal efficiency was achieved at a condition of 2010.5mg/L H_2O_2, 1.0mM Fe(III) and 10L/h. TOC removal efficiency was calculated at this experimental condition by using response function (Eq. 4.10). Predicted TOC removal efficiency was 75%. This efficiency was lower than the obtained maximum TOC removal efficiency. As a conclusion, two different experimental conditions were determined, one was for maximum color removal and the other was for maximum TOC removal. The maximum color removal efficiency was achieved at a condition of 2010.5mg/L H_2O_2 and 1.0mM Fe(III) at a flowrate of 10L/h. Moreover, the maximum TOC removal efficiency was achieved at a condition of 2677mg/L H_2O_2 and 0.5mM Fe(III) at a flowrate of 10L/h with Fe(III)/H_2O_2/Solar-UV process for paper industry wastewater.

4.3.4 Solar TiO_2 Catalysis (Fe(III)/ TiO_2/Solar-UV)

4.3.4.1 Experimental Procedure

Experimental procedure with wastewater was explained in chapter 3.2.2.4. The significant independent and dependent variables are the same as for Fe(III)/TiO_2/Solar-UV process with synthetic wastewater. Experimental points and conditions determined by the Box–Wilson statistical design are presented in Table 4.1 and 4.2.

4.3.4.2 Regression Model

Figure 4.61-4.66 depict variation of decolorization and TOC removal efficiency with irradiation time. Computation was carried out using multiple regression analysis that uses the least squares method. The following response functions (Eq. 4.11 and 4.12) were utilized in the correlation of the color removal efficiency (Y_C) and TOC removal efficiency (Y_{TOC}) with other independent parameters ($X1$–$X3$).

The Statistica computer program was employed for the determination of the coefficients of response functions by regression analysis of the experimental data. Response functions with calculated coefficients were given in Eq. 4.11 and 4.12, and were used in calculating predicted values of color and TOC removal efficiencies. Observed and predicted color and TOC removal efficiencies with COD, BOD and AOX removal efficiencies were given in Table 4.12.

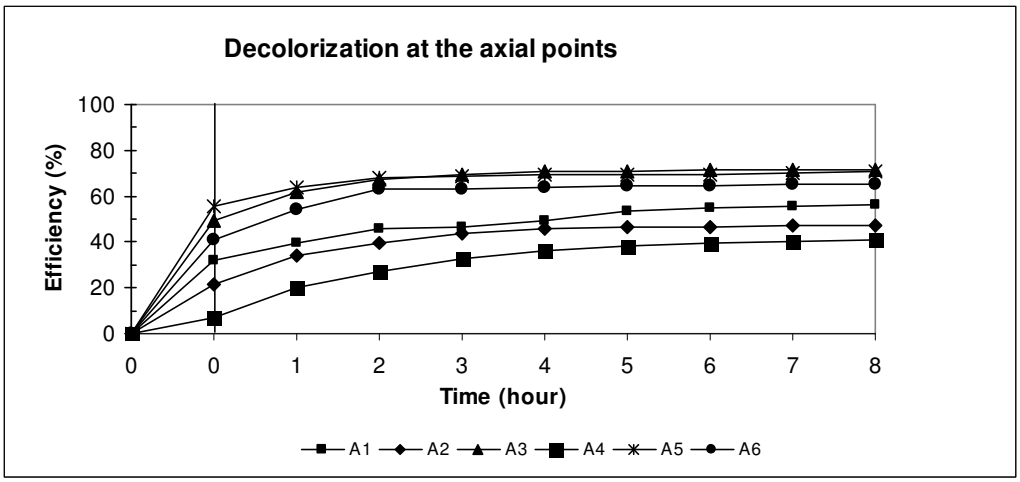

Figure 4.61 Variation of decolorization efficiency with irradiation time at axial points with Fe(III)/TiO_2/Solar-UV process

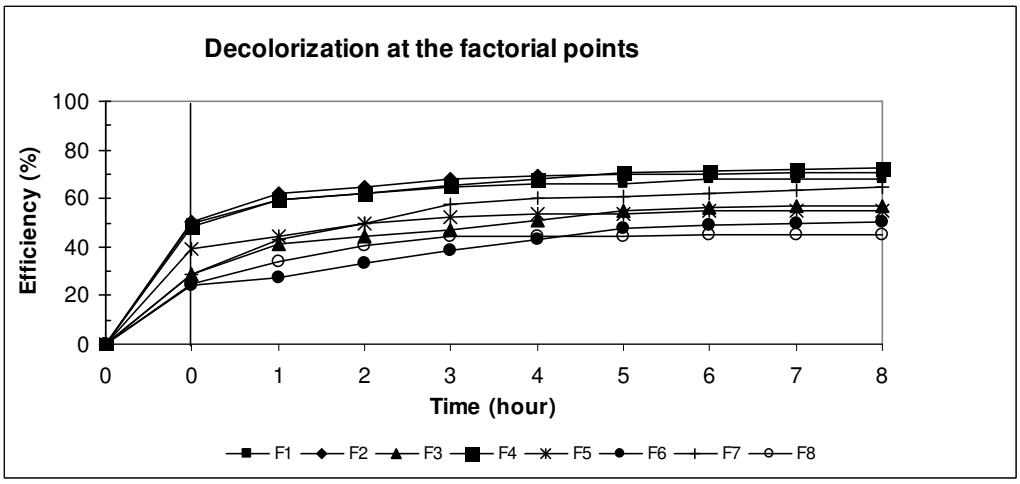

Figure 4.62 Variation of decolorization efficiency with irradiation time at factorial points with Fe(III)/TiO_2/Solar-UV process

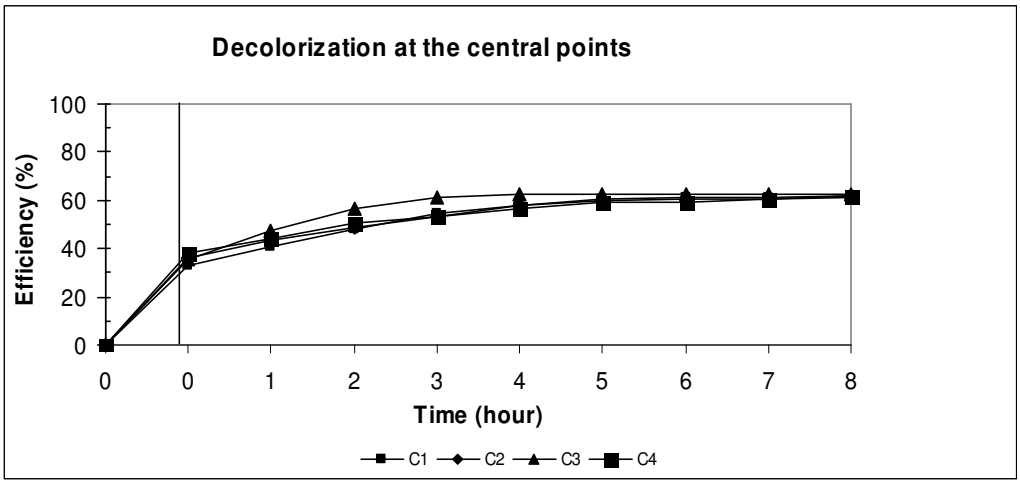

Figure 4.63 Variation of decolorization efficiency with irradiation time at center points with Fe(III)/TiO_2/Solar-UV process

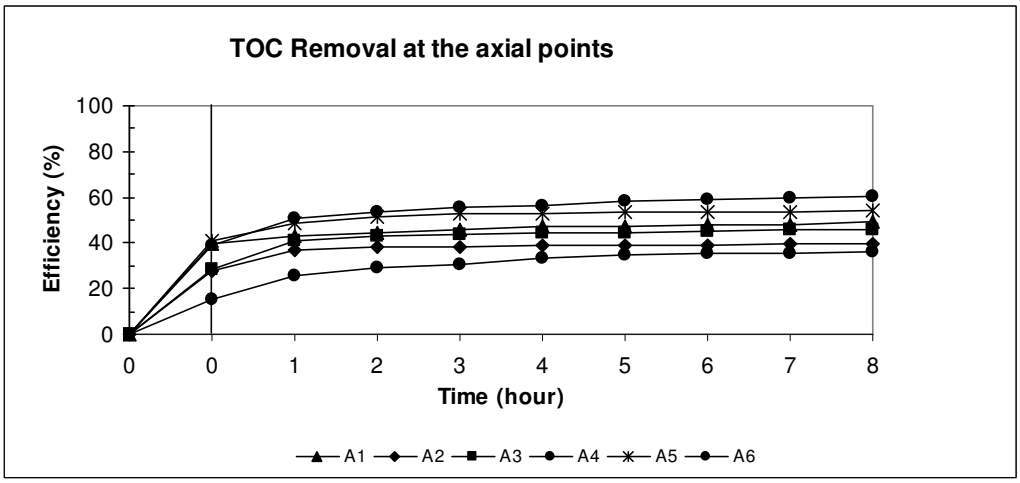

Figure 4.64 Variation of TOC removal efficiency with irradiation time at axial points with Fe(III)/TiO_2/Solar-UV process

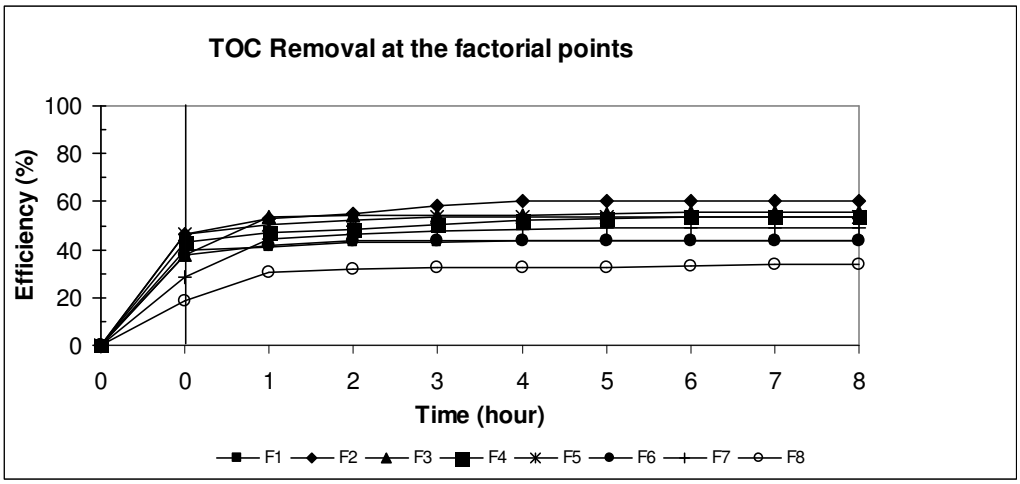

Figure 4.65 Variation of TOC removal efficiency with irradiation time at factorial points with Fe(III)/TiO_2/Solar-UV process

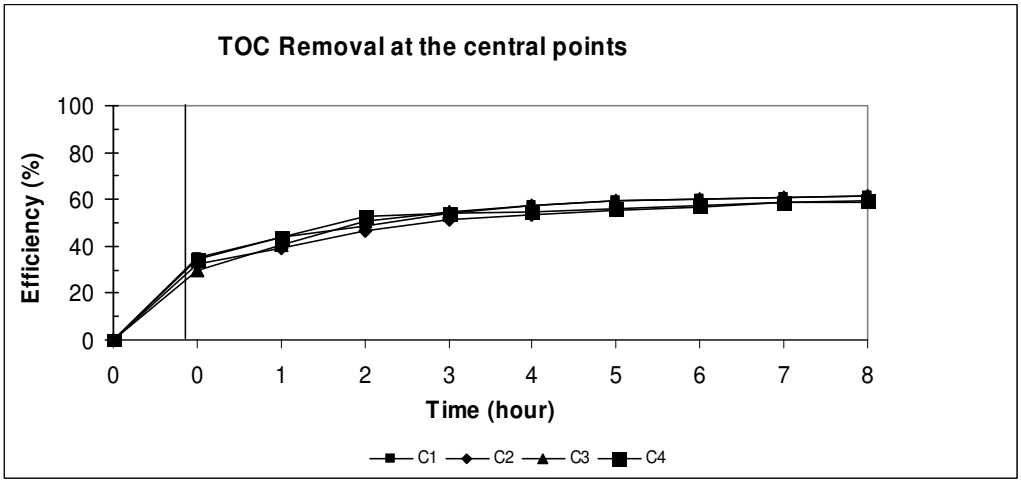

Figure 4.66 Variation of TOC removal efficiency with irradiation time at center points with Fe(III)/TiO_2/Solar-UV process

Response function (Y_{COL}) for color removal;

$$Y_{COL} = 8.75283 + 0.44483\ X_1 - 63.09758\ X_2 - 0.57972\ X_3 - 0.10529\ X_1X_2 - 0.00256\ X_1X_3 - 0.05978\ X_2X_3 - 0.00091\ X_1^2 - 16.35559\ X_2^2 + 0.01888\ X_3^2 \quad (R^2 = 0.9869) \qquad \text{(Eq. 4.11)}$$

Response function (Y_{TOC}) for TOC removal;

$$Y_{TOC} = -63.04574 + 0.79617\ X_1 + 135.65916\ X_2 + 1.56572\ X_3 - 0.22103\ X_1X_2 - 0.00551\ X_1X_3 - 0.86413\ X_2X_3 - 0.00152\ X_1^2 - 65.88671\ X_2^2 - 0.00629\ X_3^2 \quad (R^2 = 0.9573) \qquad \text{(Eq. 4.12)}$$

The correlation coefficients (R^2) between the observed and predicted values were 0.9869 and 0.9573 for Y_{COL} and Y_{TOC}, respectively indicating a good agreement between the observed and predicted values of color and TOC removal efficiencies.

Table 4.12 Observed and predicted color and TOC removal efficiencies determined by the Box–Wilson statistical design with COD, BOD and AOX removal efficiencies (paper industry wastewater, Fe(III)/TiO_2/Solar-UV process).

No.	% Color removal		% TOC removal		% BOD removal	% COD removal	% AOX removal
	observed	predicted	observed	predicted	observed	observed	observed
A1	56	57	49	51	60	62	36
A2	47	48	39	39	49	51	38
A3	72	72	50	49	57	59	50
A4	41	43	36	39	37	39	35
A5	71	72	54	56	60	62	59
A6	66	66	60	59	62	58	65
F1	68	69	44	44	61	62	53
F2	70	69	60	59	71	71	35
F3	57	55	55	51	58	58	50
F4	73	71	54	52	49	48	52
F5	55	55	54	54	42	45	46
F6	51	50	44	44	49	50	42
F7	64	65	49	52	66	68	51
F8	45	43	34	32	49	50	53
C1	62	62	62	60	56	57	69
C2	61	62	59	60	58	56	67
C3	62	62	61	60	56	54	68
C4	62	62	60	60	57	57	69

Maximum color and TOC removal efficiencies were 73% and 62% and were achieved at F4 (92.26mg/L TiO_2, 0.79mM Fe(III) and 41.5L/h flowrate) and C (150mg/L TiO_2, 0.5mM Fe(III) and 30L/h flowrate) experimental conditions, respectively. More experimental results were needed to comment on the regression model better. Color and TOC removal efficiencies were predicted by using Eq. 4.11 and 4.12 when flowrate kept constant at minimum (10L/h), average (30L/h) and maximum (50L/h) value in order. Results are given in Figure 4.67-4.72.

4.3.4.2.1 Decolorization

(a) At minimum flowrate (Q=10L/h);

Color removal efficiencies with Fe(III)/TiO_2/Solar-UV process of paper industry wastewater at minimum flowrate were presented in Figure 4.67.

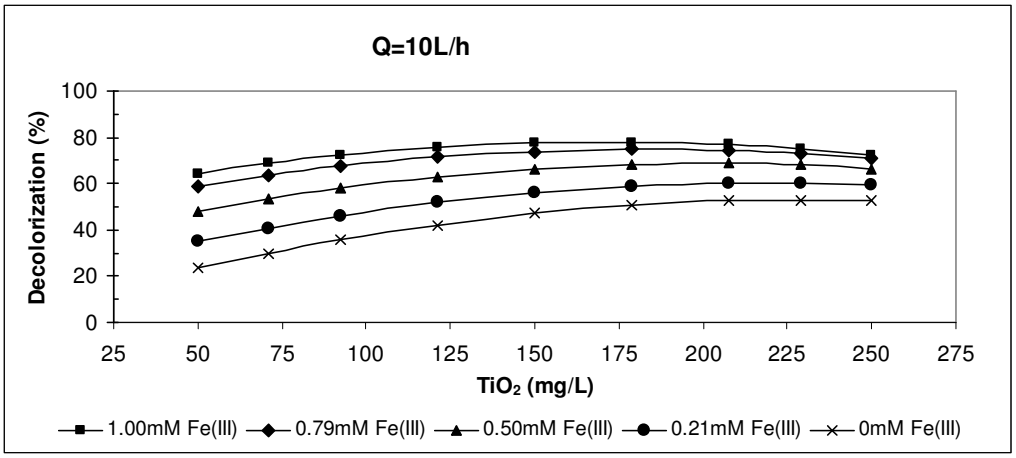

Figure 4.67 Variation of decolorization efficiency of paper industry wastewater at minimum flowrate with Fe(III)/TiO_2/Solar-UV process.

Color removal efficiencies varied between 24% and 78% at minimum flowrate. The efficiency increased with increasing Fe(III) concentration from 0 to 1.0mM at all TiO_2 concentrations.

Increasing the initial TiO_2 concentration from 50 to 178.9mg/L increased color removal efficiency but increasing TiO_2 concentration from 178.9 to 250mg/L decreased the efficiency at all Fe(III) concentrations. Herewith, 1.0mM Fe(III) and 178.9mg/L TiO_2 concentrations were found to be the optimum treatment conditions when the flowrate was at 10L/h to achieve maximum color removal efficiency.

(b) At average flowrate (Q=30L/h);

Color removal efficiencies with Fe(III)/TiO_2/Solar-UV process of paper industry wastewater at average flowrate were presented in Figure 4.68.

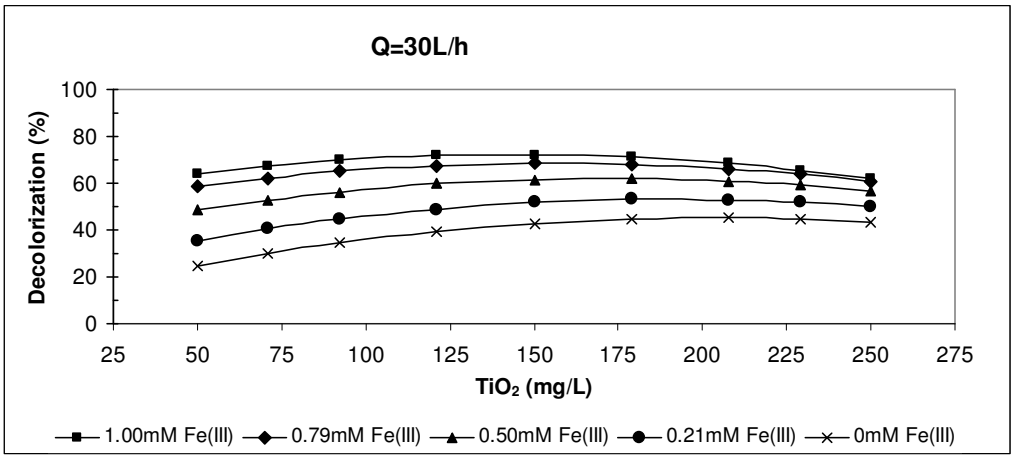

Figure 4.68 Variation of decolorization efficiency of paper industry wastewater at average flowrate with Fe(III)/TiO_2/Solar-UV process.

Color removal efficiencies varied between 24% and 72% at 30L/h flowrate. Increasing the flowrate from 10 to 30L/h decreased maximum color removal efficiency from 78% to 72%.

In experiments at 10L/h, the efficiency increased with increasing Fe(III) concentration from 0 to 0.1mM at all TiO_2 concentrations. Maximum color removal efficiency was achieved when Fe(III) concentration was 1.0mM. Increasing the initial TiO_2 concentration from 50 to 150 mg/L increased color removal efficiency but increasing TiO_2 concentration from 150 to 250mg/L decreased the efficiency at all Fe(III) concentrations. Therewith, 0.1mM Fe(III) and 150mg/L TiO_2 concentrations were found to be the optimum treatment conditions when the flowrate was at 30L/h.

(c) At maximum flowrate (Q=50L/h);

Color removal efficiencies with Fe(III)/TiO_2/Solar-UV process of paper industry wastewater at maximum flowrate are presented in Figure 4.69.

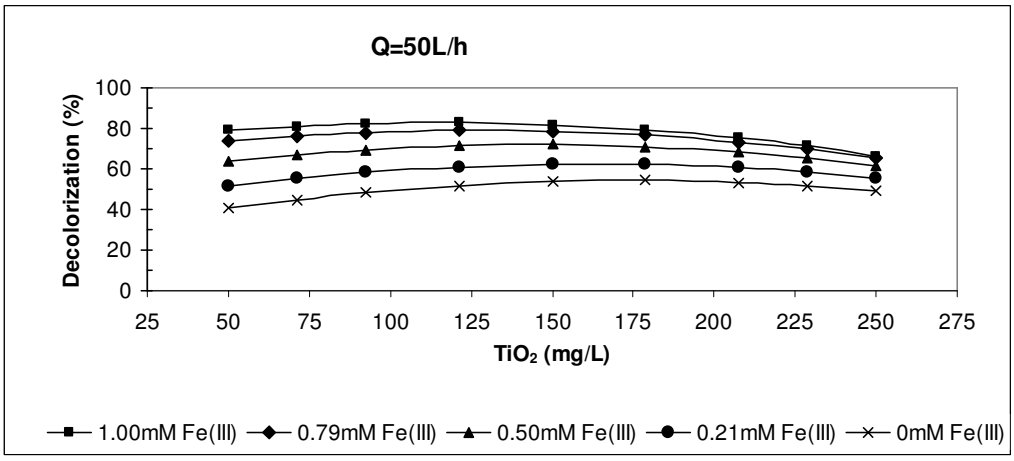

Figure 4.69 Variation of decolorization efficiency of paper industry wastewater at maximum flowrate with Fe(III)/TiO_2/Solar-UV process.

Color removal efficiencies varied between 41% and 83% at 50L/h flowrate. Increasing the flowrate from 30 to 50L/h increased maximum color removal efficiency from 72% to 83%. As a result, maximum color removal efficiency was achieved when flowrate was 50L/h.

In experiments at 10 and 30L/h, the efficiency increased with increasing Fe(III) concentration from 0 to 0.1mM at all TiO_2 concentrations. Maximum color removal efficiency was achieved when Fe(III) concentration was 1.0mM. Increasing the initial TiO_2 concentration from 50 to 121.1 mg/L increased color removal efficiency but increasing TiO_2 concentration from 121.1 to 250mg/L decreased the efficiency at all Fe(III) concentrations. Therewith, 1.0mM Fe(III) and 121.1mg/L TiO_2 concentrations were found to be the optimum treatment conditions when the flowrate was at 50L/h.

As a result of Box Wilson experimental design method, maximum color removal condition for paper industry wastewater was 1.0mM Fe(III), 121.1mg/L TiO_2 and 50L/h flowrate.

4.3.4.2.2 TOC removal

(a) At minimum flowrate (Q=10L/h);

TOC removal efficiencies with Fe(III)/TiO_2/Solar-UV process of paper industry wastewater at minimum flowrate are presented in Figure 4.70.

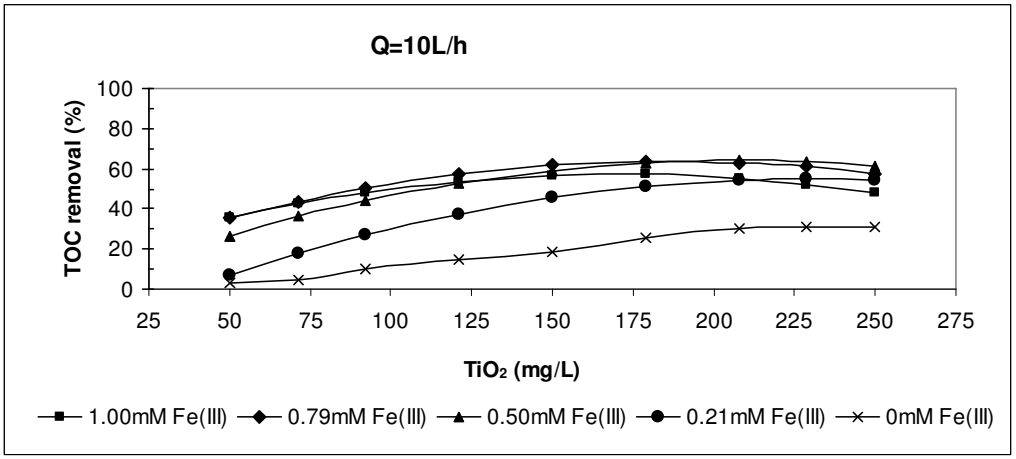

Figure 4.70 Variation of TOC removal efficiency of paper industry wastewater at minimum flowrate with Fe(III)/TiO_2/Solar-UV process.

TOC removal efficiencies varied from 3% to 64% at flowrate of 10L/h. Increasing Fe(III) concentration from 0 to 0.50mM increased TOC removal efficiency. However, increasing Fe(III) concentration from 0.50 to 1.0mM TOC removal efficiency started to decrease. Maximum TOC removal efficiency was achieved when Fe(III) concentration was 0.50mM.

Increasing TiO_2 concentration from 50 to 207.7mg/L increased TOC removal efficiency but increasing TiO_2 concentration from 207.7 to 250 mg/L decreased TOC removal efficiency at all Fe(III) concentrations. Herewith, 0.50mM Fe(III)

and 207.7mg/L TiO_2 concentrations were found to be the optimum treatment conditions when the flowrate was at 10L/h.

(b) At average flowrate (Q=30L/h);

TOC removal efficiencies with Fe(III)/TiO_2/Solar-UV process of paper industry wastewater at average flowrate are presented in Figure 4.71.

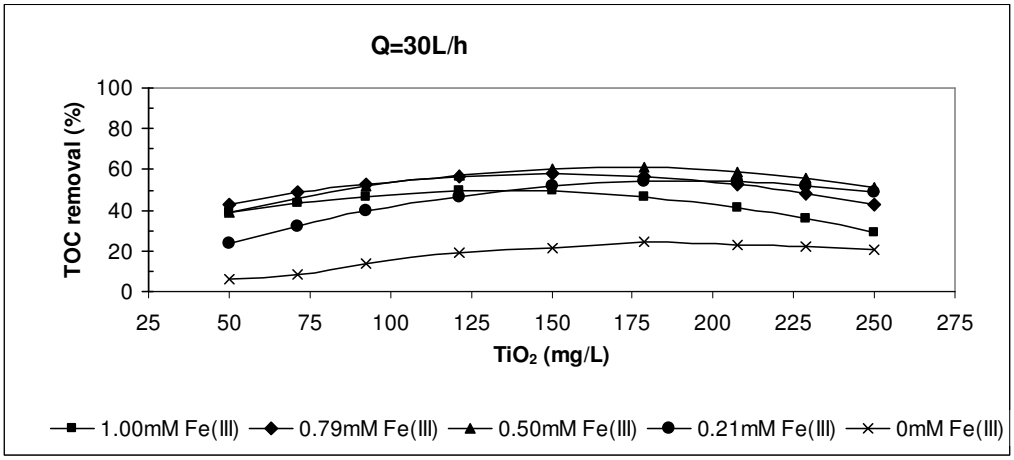

Figure 4.71 Variation of TOC removal efficiency of paper industry wastewater at average flowrate with Fe(III)/TiO_2/Solar-UV process.

TOC removal efficiencies varied from 6% to 61% at flowrate of 30L/h. When the flowrate increased from 10 to 30L/h, maximum TOC removal efficiency decreased from 64% to 61%. Increasing Fe(III) concentration from 0 to 0.50mM, increased the efficiency at all TiO_2 concentrations. When Fe(III) concentration incereased from 0.50 to 1.0mM, the efficiency decreased.

Increasing TiO_2 concentration from 50 to 178.9mg/L increased TOC removal efficiency but increasing TiO_2 concentration from 178.9 to 250 mg/L decreased TOC removal efficiency at all Fe(III) concentrations. Herewith, 0.50mM Fe(III) and 178.9mg/L TiO_2 concentrations were found to be the optimum treatment conditions when the flowrate was at 30L/h.

(c) At maximum flowrate (Q=50L/h);

TOC removal efficiencies with Fe(III)/TiO_2/Solar-UV process of paper industry wastewater at maximum flowrate are presented in Figure 4.72.

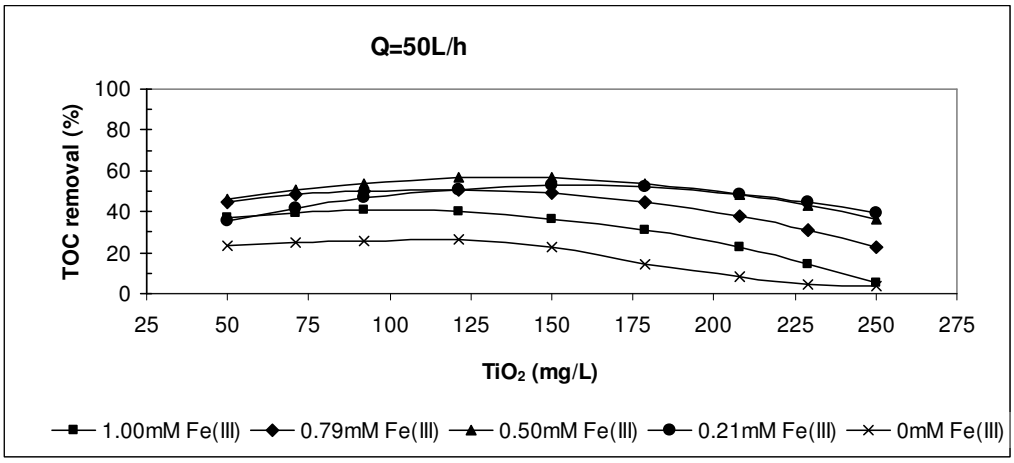

Figure 4.72 Variation of TOC removal efficiency of paper industry wastewater at maximum flowrate with Fe(III)/TiO_2/Solar-UV process.

TOC removal efficiencies varied between 4% and 57% at the maximum flowrate. When the flowrate increased from 30 to 50L/h, maximum TOC removal efficiency decreased from 61% to 57%. The efficiency increased with increasing increase in Fe(III) concentration from 0 to 0.50mM but decreased with increasing increase in Fe(III) concentration from 0.50 to 1.0mM.

Increasing TiO_2 concentration from 50 to 121.1mg/L increased TOC removal efficiency but increasing TiO_2 concentration from 121.1 to 250 mg/L decreased TOC removal efficiency at all Fe(III) concentrations. Herewith, 0.50mM Fe(III) and 121.1mg/L TiO_2 concentrations were found to be the optimum treatment conditions when the flowrate was at 50L/h.

As a result of Box Wilson experimental design method, maximum TOC removal condition for paper industry wastewater was 0.5mM Fe(III), 207.7mg/L TiO_2 and 50L/h flowrate.

Although high TOC removal efficiency was determined at high TiO_2 concentration, high TiO_2 concentration started to inhibit color removal efficiency. Maximum color removal efficiency was achieved at a condition of 121.1mg/L TiO_2, 1.0mM Fe(III) and 50L/h. TOC removal efficiency was calculated at this experimental condition by using response function (Eq. 4.12). Predicted TOC removal efficiency was 40%, which was very lower than the obtained maximum TOC removal efficiency. And also it seemed that higher amount of Fe(III) and higher flowrate was needed to achieve maximum color removal efficiency than required to achieve maximum TOC removal efficiency. As a conclusion, two different experimental conditions were determined, one was for the maximum color removal and the other was for the maximum TOC removal. The maximum color removal efficiency was achieved at a condition of 121.1mg/L TiO_2 and 1.0mM Fe(III) at a flowrate of 50L/h and the maximum TOC removal efficiency was achieved at a condition of 207.7mg/L TiO_2 and 0.5mM Fe(III) at a flowrate of 10L/h with Fe(III)/TiO_2/Solar-UV process for paper industry wastewater. Optimum treatment conditions and color and TOC removal efficiencies determined by the Box–Wilson statistical design of paper industry wastewater with Fe(III)/H_2O_2/Solar-UV and Fe(III)/TiO_2/Solar-UV processes are given in Table 4.13.

Table 4.13 Optimum treatment conditions and color and TOC removal efficiencies determined by the Box–Wilson statistical design of paper industry wastewater with Fe(III)/H_2O_2/Solar-UV and Fe(III)/TiO_2/Solar-UV processes.

Fe(III)/ H_2O_2/Solar-UV				
Dosage of H_2O_2 (mg/L)	Dosage of Fe(III) (mM)	Flowrate (L/h)	Color removal efficiency(%)	TOC removal efficiency(%)
2010.5	1.0	10	89	75
2677	0.5	10	63	89
Fe(III)/ TiO_2/Solar-UV				
Dosage of TiO_2 (mg/L)	Dosage of Fe(III) (mM)	Flowrate (L/h)	Color removal efficiency (%)	TOC removal efficiency (%)
121.1	1.0	50	83	40
207.7	0.5	10	69	64

CHAPTER FIVE
CONCLUSIONS AND RECOMMENDATIONS

5.1 Conclusions

This study was performed to investigate the performance of the solar reactor for the treatment of synthetic wastewater prepared with the azo dye Remazol Brilliant Blue R-A and textile and paper industry wastewaters by application Box-Wilson Experimantal Design Method. The effects of hydrogen peroxide (H_2O_2), titanium dioxide (TiO_2) and Fe(III)(Fe(III)) concentrations and flowrate were evaluated. Performance of Fe(III)/H_2O_2/Solar-UV and Fe(III)/TiO_2/Solar-UV processes were compared.

Table 4.14 Optimum treatment conditions and maximum color and TOC removal efficiencies

Type of process	**Type of wastewater**	**Dosage of H_2O_2/TiO_2 (mg/L)**	**Dosage of Fe(III) (mM)**	**Flowrate (L/h)**	**Color removal efficiency (%)**	**TOC removal efficiency (%)**
Fe(III)/H_2O_2/ Solar-UV	Synthetic	2281	0.79	10	100	85
	Textile ind.	1740	0.50	30	64	72
	Paper ind.	2010.5	1.0	10	89	75
		2677	0.5	10	63	89
Fe(III)/TiO_2 /Solar-UV	Synthetic	50	0.79	30	98	59
	Textile ind.	50	0.79	50	74	100
		250	0.79	50	97	36
	Paper ind.	121.1	1.0	50	83	40
		207.7	0.5	10	69	64

Depending on the experimental results, which were given in Table 4.14, the following conclusions could be drawn:

1. Fe(III)/H_2O_2/Solar-UV process was found to be very effective in the decolorization of synthetic wastewater. The decolorization was very fast and was usually completed within a few minutes after the mixing of the reaction components. The maximum efficiency achieved with 0.79mM Fe(III) as the catalyst was 100%. Efficiency decreased at higher amount of Fe(III) concentration because of recolorization of water with excess of Fe(III). Fe(III)/H_2O_2/Solar-UV process was also found to be very effective in the TOC removal of synthetic wastewater. The maximum efficiency achieved with Fe(III) as the catalyst was 85%.

2. With the experiments of textile industry wastewater maximum color and TOC removal efficiencies were 64% and 72%, respectively, with Fe(III)/H_2O_2/Solar-UV process. Necessary H_2O_2 concentration was lower for textile industry than synthetic wastewater to achieve maximum color and TOC removal efficiencies because of COD concentration of textile industry was lower than the COD concentration of synthetic wastewater.

3. With the experiments of paper industry wastewater maximum color and TOC removal efficiencies were achieved with two different experimental conditions with Fe(III)/H_2O_2/Solar-UV process. At the condition which maximum color removal efficiency was achieved (89%) did not result in maximum TOC removal. Higher amount of H_2O_2 was needed for maximum TOC removal (89%).

4. Fe(III)/TiO_2/Solar-UV process was also found to be very effective in the decolorization of synthetic wastewater. There were no significant difference between the maximum color removal efficincy which was achieved with Fe(III)/TiO_2/Solar-UV process and Fe(III)/H_2O_2/Solar-UV process. Decolorization efficiencies of both processes were almost same at reaction

period (after 8 hours). The decolorization was very fast again. The maximum efficiency achieved with 0.79mM Fe(III) as the catalyst was 98%. Fe(III)/TiO_2/Solar-UV process was not found to be as effective in the TOC removal of synthetic wastewater as Fe(III)/H_2O_2/Solar-UV process. Maximum TOC removal efficiency was 59%.

5. With the experiments of textile industry wastewater with Fe(III)/TiO_2/Solar-UV process, there were two optimum experimental conditions. Higher amount of TiO_2 (250mg/L) was needed to achieve maxiumum TOC removal efficiency than the amount of TiO_2 (50mg/L) was needed to achieve maxiumum color removal efficiency. Maximum color removal efficieny was 97% and was almost same as the efficiency achieved with synthetic wastewater (98%).

6. With the experiments of paper industry wastewater maximum color and TOC removal efficiencies were achieved with two different experimental conditions Fe(III)/TiO_2/Solar-UV process. At the condition which maximum color removal efficiency was achieved (83%) did not result in maximum TOC removal. For maximum TOC removal (64%) higher amount of TiO_2 and lower amount of Fe(III) were needed.

7. Both processes were found to be feasible for treatment of synthetic wastewater and textile and paper industry wastewaters. Various characterization of industrial wastewaters in time made difficult to design an empirical modeling of Box-Wilson statistical desing. For this reason, correlation coefficients of response fonctions of some experiments were low such as 0.8663 and 0.8390 for decolorization study of textile and paper industry, respectively, with Fe(III)/H_2O_2/Solar-UV process. But contrarily, correlation coefficients of response fonctions of Fe(III)/TiO_2/Solar-UV process were higher than 0.95.

8. Sudies have shown that the effectiveness of Fe(III)/H_2O_2/Solar-UV process in waste treatment depends on the initial concentrations of H_2O_2 and Fe(III) and their ratios. Firstly, the higher initial concentration of H_2O_2 increased the TOC

removal efficiency, but an increased use of H_2O_2 for obtaining higher TOC removal has to be justified on a decresea. Secondly, the optimal initial Fe(III) concentration depends on the initial H_2O_2 concentration as well as waste composition was important. Therefore, determination of their optimal ratio is necessary for better treatment performance.

9. Weather condition was found to be an effective parameter on removal efficiencies. High temperature increased the TOC and color removal efficiencies in all experiments. Textile industry wastewater solar treatment studies were done when the season was winter. Because of this, weather temperature was low and TOC and color removal efficiencies obtained with Fe(III)/H_2O_2/Solar-UV and Fe(III)/TiO_2/Solar-UV processes of textile industry wastewater were lower than the efficiencies obtained with paper industry wastewater and synthetic wastewater despite textile industry wastewater had higher TOC value than the other used wastewaters.

10. In order to determine effect of Solar-UV on color and TOC removal efficiencies a blank experiment was executed. The experimental conditions were the experimental points that maximum color and TOC removal efficiencies achieved with Fe(III)/H_2O_2/Solar-UV process of synthetic wastewater (2281mg/L H_2O_2, 0.79mM Fe(III) and 10L/h flowrate). Color removal efficiency was decreased from 100% to 24% and TOC removal efficiency decreased from 85% to 60% without Solar-UV (Figure B.11 depicts variation of color and TOC removal efficiencies with time with Fe(III)/H_2O_2 process).

5.2 Recommendations

1. It might be beneficial to carry out a cost analysis in addition to investigation of removal efficiencies while determining the most suitable treatment method, since economy is an important parameter.

2. It might be more effective with using $KMnO_4$, Pt or Co as catalyst in the experiments to obtain higher color and TOC removal efficiencies. Process efficiencies of these catalysts should be investigated and cost analysis should also be done.

3. Performance of Fe(III)/H_2O_2/Solar-UV and Fe(III)/TiO_2/Solar-UV processes could be applied to different industrial wastewaters contain high TOC values and color.

REFERENCES

Ajona, J. I., & Vidal, A. (2000). The use of CPC collectors for detoxification of contaminated water: design, construction and preliminary results, *Solar Energy,* 68, 109-120.

Al-Bastaki, N. M. (2004). Performance of advanced methods for treatment of wastewater: UV/TiO_2, RO and UF, *Chemical Engineering and Processing,* 43, 935–940.

Amat, A.M., Arques, A., López, F., & Miranda, M. A. (2005). Solar photo-catalysis to remove paper mill wastewater pollutants, *Solar Energy*, 79, 393-401.

Augugliaro, V., Baiocchi, C., Bianco, P. A., Brussino, M. C., Vázquez, C. J., López, G. E., et al.. (1996). Photocatalytic degradation of organic dyes under solar irradiation: oxidation of methyl-orange and orange II in aqueous suspension of titanium dioxide powder, *Bioresource Technology*, 58, 217-227.

Bahnemann D. (2004). Photocatalytic water treatment: solar energy applications. *Solar Energy,* 77, 445–459.

Bali, U. (2002). Evaluation of different processes for the treatment of high strength toxic synthetic wastewaters. *Dokuz Eylül University, Graduate School of Natural and Applied Sciences*, PhD. Thesis, Izmir.

Bali U. (2004). Application of Box–Wilson experimental design method for the photodegradation of textile dyestuff with UV/H_2O_2 process. *Dyes and Pigments*, 60, 187–195.

Bali U., & Karagözoğlu B. (2007). Decolorization of Remazol- Turquoise Blue G-133 and other dyes by Cu(II)/pyridine/H_2O_2 system. *Dyes and Pigments,* 73, 133-140.

Bali, U., Çatalkaya, E., & Şengül, F. (2004). Photodegradation of Reactive Black 5, Direct Red 28 and Direct Yellow 12 using UV, UV/H_2O_2 and UV/H_2O_2/Fe^{2+}: a comparative study, *Journal of Hazardous Materials*, 114, 159-166.

Baycan, N. (2005). Advanced oxidative treatment of chlorinated hydrocarbons. Dokuz Eylül University, *Graduate School of Natural and Applied Sciences*, PhD. Thesis, Izmir.

Braun, A.M. & Oliveros, E. (1997). How to evaluate photochemical methods for water treatment. *Water Science and Technology*, 35 (4), 17-23.

Chacón J. M, Leal M. T, Sánchez M, & Bandala E. R. (2006). Solar photocatalytic degradation of azo-dyes by photo-Fenton process, *Dyes and Pigments*, 69, 144-150

Cisneros R. L, Espinoza A. G., & Litter M. I. (2002). Photodegradation of an azo dye of the textile industry, *Chemosphere*, 48, 393–399.

Ç. Çatalkaya E., & Şengül F. (2006). Application of Box–Wilson experimental design method for the photodegradation of bakery's yeast industry with UV/H_2O_2 and UV/H_2O_2/Fe(II) process, *Journal of Hazardous Materials*, 128, 201-207.

Çatalkaya E., & Kargı F. (2007). Color, TOC and AOX removals from pulp mill effluent by advanced oxidation processes: A comparative study, *Journal of Hazardous Materials*, 139, 244-253.

Gumy, D., Rincon, A. G., & Pulgarin, C. (2006). Solar photocatalysis for detoxification and disinfection of water: different types of suspended and fixed TiO_2 catalysts study, *Solar Energy* . 80, 1376-1381.

Kurbus, T., Le Marechal, A. M., & Vončina, D. B. (2003). Comparison of H_2O_2/UV, H_2O_2/O_3 and H_2O_2/Fe^{2+} processes for the decolorisation of vinylsulphone reactive dyes. *Dyes and Pigments,* 58, 245–252.

Legrini, O., Oliveros, E., & Braun, A.M. (1993). Photochemical processes for water treatment, *Chemical Reviews*, 93, 671-698.

Lizama, M. C., Yeber, M. C., Baeza, J., & Mansilla, H. D. (2001). Reactive dyes decolourization by TiO_2 ptoto- assisted catalysis, *Water Science and Technology* 44, 197-203.

Mahmoodi, N. M., Arami, M., & Limaee, N. Y. (2006). Photocatalytic degradation of triazinic ring-containing azo dye (reactive red 198) by using immobilized TiO_2 ohotoreactor: bench scale study, *Journal of Hazardous Materials*, 133, 113-118.

Martin, C. A., Alfano, O. M., & Cassano, A. E. (2001). Water decolorization using UV radiation and hydrogen peroxide: a kinetic study, *Water Science and Technology* , 44, 53-60.

McLoughlin, O.A., Ibáñez, P. F., Gernjak, W., Rodríguez, S. M., & Gill, L.W. (2004). Photocatalytic disinfection of water using low cost compound parabolic collectors, *Solar Energy*, 77, 625–633.

M. Rodriguez, S., B. Galvez, J., I. M. Rubio, M., F. Ibanez, P., Gernjak, W., & O. Alberole, I. (2005). Treatment of chlorinated solvents by TiO2 photocatalysis and photo-Fenton: influence of operating conditions in a solar pilot plant, *Chemosphere*, 58, 391-398.

Nigam, P., McMullan, G., Banat, I., & Marchant, R. (1996). Decolorization of effluent from the textile industry by a microbial consortium, *Biotechnology Letters*, 18, 117-120.

Neyens, E., & Baeyens, J. (2003). A review of classic fenton's peroxidation as an advanced oxidation technique, *Journal of Hazardous Materials*, B98, 33-50.

Oppelt, E. T. (1998). *Handbook of advanced photochemical oxidation processes*, U.S. EPA, Retrieved September 16, 2007, from http://www.epa.gov/nrmrl/pubs/ 625r98004/ 625r98004.pdf.

Prieto, O., Fermoso, J., Nuňez, Y., Del Vale, J.L., & Irusta, R. (2005). Decolouration of textile dyes in wastewaters by photocatalysis with TiO_2, *Solar Energy*, 79, 376–383.

Sano, T., Negishi, N. Takeuchi, K., & Matsuzawa, S. (2004). Degradation of toluene and acetaldehyde with Pt-loaded TiO_2 catalyst and parabolic trough concentrator, *Solar Energy,* 77, 543–552.

Standard Methods for the Examination of Water and Wastewater. 21st Ed. (2005) American Public Health Association, American Water Works Association, Water Environment Federation.

Taghipour, F., & Sozzi, A. (2005). Modeling and design of ultraviolet reactors for disinfection by-product precursor removal, *Desalination*, 176, 71-80.

Tiburtius, E. R. L., Zamora, P. P., & Emmel, A. (2005). Treatment of gasoline-contaminated waters by advanced oxidation processes, *Journal of Hazardous Materials*, 126, 86-90.

Torrades, F., & Garcıa-Montano, J. (2004). Decolorization and mineralization of commercial reactive dyes under solar light assisted photo-Fenton conditions, *Solar Energy,* 77, 573–581.

Xu M., Wang Q., & Hao Y. (2007). Removal of organic carbon from wastepaper pulp effluent by lab-scale solar photo-Fenton process. *Journal of Hazardous Materials*, 148, 103–109.

APPENDICES

APPENDIX-A

Table A.1 Results of wavelength scan of Remazol Brilliant Blue R-A solution at a concentration of 1 g/L.

nm	abs	nm	abs
340	1.963	540	2.718
350	2.033	550	2.739
360	2.110	560	2.759
370	2.291	570	2.805
380	1.910	580	2.814
390	1.957	590	2.816
400	1.873	600	2.831
410	1.562	610	2.862
420	1.165	620	2.888
430	0.827	625	2.889
440	0.675	626	2.889
450	0.726	627	2.891
460	0.889	628	2.892
470	1.127	629 (peak)	2.893 (max abs)
480	1.413	630	2.890
490	1.744	631	2.874
500	2.093	633	2.873
510	2.446	635	2.862
520	2.660	638	2.863
530	2.667	640	2.860

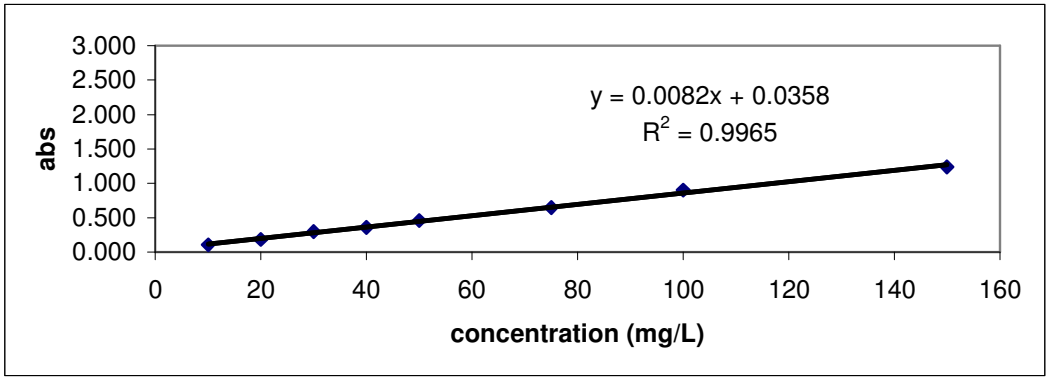

Figure A.1 Calibration curve of Remazol Brilliant Blue R-A solution at 629nm

Table A.2 Results of wavelength scan of textile industry wastewater (sample 1)

nm	**abs**	**nm**	**abs**
350	0.789	534	0.477
355	0.767	535	0.476
360	0.746	536	0.475
365	0.728	537	0.473
370	0.706	538	0.472
375	0.691	539	0.471
380	0.676	540	0.469
385	0.666	541	0.467
390	0.653	542	0.466
395	0.642	543	0.464
400	0.632	544	0.463
405	0.623	545	0.461
410	0.614	546	0.459
415	0.604	547	0.458
420	0.591	548	0.456
425	0.579	549	0.454
430	0.567	550	0.451
435	0.557	535	0.476
440	0.546	536	0.475
445	0.537	537	0.473
450	0.535	538	0.472
451	0.533	539	0.471
452	0.532	540	0.469
453	0.530	541	0.467
454	0.529	542	0.466
455	0.528	543	0.464
456	0.527	544	0.463
457	0.526	545	0.461
458	0.524	546	0.459

459	0.523	547	0.458
460	0.522	548	0.456
461	0.521	549	0.454
462	0.520	550	0.451
463	0.520	555	0.439
464	0.518	560	0.421
465	0.517	565	0.399
466	0.517	570	0.376
467	0.518	575	0.357
468	0.517	580	0.341
469	0.516	585	0.326
470	0.516	590	0.313
471	0.515	595	0.303
472	0.515	600	0.296
473	0.513	605	0.298
474	0.513	610	0.281
475	0.512	615	0.274
476	0.512	620	0.267
477	0.512	625	0.260
478	0.512	630	0.252
479	0.511	635	0.242
480	0.511	640	0.233
481	0.510	645	0.224
482	0.510	650	0.215
483	0.510	655	0.207
484	0.510	660	0.198
485	0.509	665	0.191
486	0.509	670	0.184
487	0.508	675	0.178
488	0.508	680	0.171
489	0.508	685	0.165

490	0.508	690	0.159
491	0.507	695	0.154
492	0.507	700	0.150
493	0.506	705	0.145
494	0.506	710	0.141
495	0.506	715	0.138
496	0.506	720	0.136
497	0.506	725	0.133
498	0.506	730	0.131
499	0.506	735	0.129
500	0.506	740	0.127
501	0.506	745	0.125
502	0.506	750	0.123
503	0.506	755	0.121
504	0.506	760	0.120
505	0.506	765	0.118
506	0.507	770	0.116
507	0.506	775	0.115
508	0.506	780	0.113
509 (peak)	0.507 (max)	785	0.112
510	0.507	790	0.110
511	0.506	795	0.109
512	0.506	800	0.107
513	0.505	805	0.106
514	0.505	810	0.105
515	0.504	815	0.103
516	0.503	820	0.102
517	0.502	825	0.101
518	0.501	830	0.100
519	0.499	835	0.098
520	0.497	840	0.097

521	0.496	845	0.096
522	0.494	850	0.095
523	0.493	855	0.094
524	0.491	860	0.093
525	0.490	865	0.092
526	0.488	870	0.091
527	0.487	875	0.090
528	0.485	880	0.089
529	0.484	885	0.088
530	0.483	890	0.087
531	0.481	895	0.086
532	0.480	900	0.085
533	0.479		

Table A.3 Results of wavelength scan of textile industry wastewater (sample 2)

nm	abs	nm	abs
350	0.522	446	0.472
351	0.517	447	0.472
352	0.516	448	0.471
353	0.512	449	0.471
354	0.509	450	0.471
355	0.507	455	0.468
356	0.503	460	0.465
357	0.502	465	0.463
358	0.500	470	0.463
359	0.498	475	0.464
360	0.496	480	0.462
361	0.496	485	0.460
362	0.496	490	0.454
363	0.493	495	0.447
364	0.493	500	0.441
365	0.494	505	0.436
366	0.491	510	0.433
367	0.494	515	0.430
368	0.493	520	0.428
369	0.492	525	0.424
370	0.494	530	0.420
371	0.493	535	0.416
372	0.495	540	0.413
373	0.495	545	0.410
374	0.496	550	0.408
375	0.496	555	0.406
376	0.498	560	0.405
377	0.497	565	0.404
378	0.499	570	0.402

379	0.499	575	0.400
380	0.502	580	0.397
381	0.502	585	0.394
382	0.502	590	0.389
383	0.503	595	0.384
384	0.503	600	0.379
385	0.505	605	0.373
386	0.505	610	0.365
387	0.509	615	0.355
388	0.507	620	0.344
389	0.507	625	0.330
390	0.509	630	0.313
391	0.508	635	0.290
392	0.509	640	0.267
393 (peak)	0.509 (max)	645	0.243
394	0.509	650	0.219
395	0.508	655	0.196
396	0.508	660	0.173
397	0.506	665	0.154
398	0.506	670	0.137
399	0.504	675	0.122
400	0.503	680	0.107
401	0.502	685	0.093
402	0.501	690	0.082
403	0.500	695	0.073
404	0.499	700	0.065
405	0.499	705	0.059
406	0.498	710	0.054
407	0.497	715	0.050
408	0.496	720	0.048
409	0.494	725	0.045

410	0.495	730	0.043
411	0.494	735	0.042
412	0.495	740	0.041
413	0.493	745	0.040
414	0.493	750	0.039
415	0.492	755	0.038
416	0.491	760	0.037
417	0.491	765	0.037
418	0.491	770	0.036
419	0.490	775	0.035
420	0.489	780	0.035
421	0.489	785	0.034
422	0.487	790	0.034
423	0.487	795	0.034
424	0.486	800	0.033
425	0.485	805	0.033
426	0.485	810	0.032
427	0.484	815	0.032
428	0.483	820	0.032
429	0.482	825	0.031
430	0.482	830	0.031
431	0.481	835	0.031
432	0.480	840	0.030
433	0.480	845	0.030
434	0.479	850	0.030
435	0.478	855	0.029
436	0.478	860	0.029
437	0.477	865	0.029
438	0.477	870	0.028
439	0.476	875	0.028
440	0.475	880	0.028

441	0.475	885	0.026
442	0.474	890	0.025
443	0.474	895	0.023
444	0.473	900	0.022
445	0.473		

Table A.4 Results of wavelength scan of textile industry wastewater (sample 3)

nm	abs	nm	abs
350	0.521	446	0.472
351	0.519	447	0.472
352	0.516	448	0.471
353	0.512	449	0.470
354	0.509	450	0.471
355	0.507	455	0.468
356	0.503	460	0.465
357	0.502	465	0.463
358	0.500	470	0.463
359	0.497	475	0.464
360	0.496	480	0.462
361	0.496	485	0.460
362	0.496	490	0.454
363	0.493	495	0.447
364	0.493	500	0.441
365	0.493	505	0.435
366	0.491	510	0.433
367	0.494	515	0.430
368	0.493	520	0.428
369	0.492	525	0.423
370	0.494	530	0.420
371	0.493	535	0.416
372	0.495	540	0.413
373	0.495	545	0.410
374	0.496	550	0.408
375	0.496	555	0.406
376	0.498	560	0.405
377	0.497	565	0.404
378	0.499	570	0.402
379	0.499	575	0.400

380	0.502	580	0.397
381	0.502	585	0.394
382	0.502	590	0.389
383	0.502	595	0.384
384	0.503	600	0.379
385	0.505	605	0.373
386	0.505	610	0.365
387	0.509	615	0.355
388	0.507	620	0.344
389	0.507	625	0.332
390	0.509	630	0.313
391	0.508	635	0.291
392	0.508	640	0.267
393 (peak)	0.509 (max)	645	0.243
394	0.509	650	0.219
395	0.508	655	0.196
396	0.508	660	0.173
397	0.506	665	0.154
398	0.506	670	0.137
399	0.504	675	0.122
400	0.503	680	0.107
401	0.500	685	0.092
402	0.500	690	0.082
403	0.500	692	0.073
404	0.499	700	0.065
405	0.499	705	0.059
406	0.498	710	0.054
407	0.497	715	0.050
408	0.496	720	0.048
409	0.493	725	0.044
410	0.495	730	0.041

411	0.494	735	0.042
412	0.495	740	0.041
413	0.493	745	0.040
414	0.490	750	0.039
415	0.492	755	0.038
416	0.491	760	0.037
417	0.491	765	0.037
418	0.491	774	0.036
419	0.490	775	0.035
420	0.489	780	0.035
421	0.488	785	0.034
422	0.487	790	0.034
423	0.487	795	0.034
424	0.486	800	0.033
425	0.485	805	0.033
426	0.485	810	0.032
427	0.484	815	0.032
428	0.483	820	0.032
429	0.482	825	0.031
430	0.482	830	0.031
431	0.481	835	0.031
432	0.480	840	0.030
433	0.480	845	0.032
434	0.479	858	0.031
435	0.478	855	0.029
436	0.478	860	0.029
437	0.477	865	0.029
438	0.477	870	0.027
439	0.476	875	0.028
440	0.475	880	0.028
441	0.475	885	0.026

442	0.473	890	0.027
443	0.473	895	0.025
444	0.473	900	0.024
445	0.473		

Table A.5 Results of wavelength scan of textile industry wastewater (sample 4)

nm	abs	nm	abs
350	0.522	446	0.472
351	0.517	447	0.472
352	0.516	448	0.471
353	0.512	449	0.471
354	0.509	450	0.471
355	0.507	455	0.468
356	0.503	460	0.465
357	0.502	465	0.463
358	0.500	470	0.463
359	0.498	475	0.464
360	0.496	480	0.462
361	0.496	485	0.460
362	0.496	490	0.454
363	0.493	495	0.447
364	0.493	500	0.441
365	0.494	505	0.436
366	0.491	510	0.433
367	0.494	515	0.430
368	0.493	520	0.428
369	0.492	525	0.424
370	0.494	530	0.420
371	0.493	535	0.416
372	0.495	540	0.413
373	0.495	545	0.410
374	0.496	550	0.408
375	0.496	555	0.406
376	0.498	560	0.405
377	0.497	565	0.404
378	0.499	570	0.402

379	0.499	575	0.400
380	0.502	580	0.397
381	0.502	585	0.394
382	0.502	590	0.389
383	0.503	595	0.384
384	0.503	600	0.379
385	0.505	605	0.373
386	0.505	610	0.365
387	0.509	615	0.355
388	0.507	620	0.344
389	0.507	625	0.330
390	0.509	630	0.313
391	0.508	635	0.290
392	0.509	640	0.267
393 (peak)	0.509 (max)	645	0.243
394	0.509	650	0.219
395	0.508	655	0.196
396	0.508	660	0.173
397	0.506	665	0.154
398	0.506	670	0.137
399	0.504	675	0.122
400	0.503	680	0.107
401	0.502	685	0.093
402	0.501	690	0.082
403	0.500	695	0.073
404	0.499	700	0.065
405	0.499	705	0.059
406	0.498	710	0.054
407	0.497	715	0.050
408	0.496	720	0.048
409	0.494	725	0.045

410	0.495	730	0.043
411	0.494	735	0.042
412	0.495	740	0.041
413	0.492	745	0.040
414	0.493	750	0.039
415	0.492	755	0.038
416	0.491	760	0.037
417	0.491	765	0.037
418	0.491	770	0.036
419	0.490	775	0.035
420	0.489	780	0.035
421	0.488	785	0.034
422	0.487	790	0.034
423	0.487	795	0.034
424	0.486	800	0.033
425	0.484	805	0.033
426	0.485	810	0.032
427	0.484	815	0.032
428	0.483	820	0.032
429	0.481	825	0.030
430	0.482	830	0.030
431	0.481	835	0.030
432	0.480	840	0.030
433	0.480	845	0.030
434	0.479	850	0.030
435	0.478	855	0.029
436	0.478	860	0.029
437	0.477	865	0.029
438	0.477	870	0.028
439	0.476	875	0.028
440	0.475	880	0.028

441	0.475	885	0.027
442	0.474	890	0.026
443	0.473	895	0.027
444	0.473	900	0.026
445	0.477		

Table A.6 Results of wavelength scan of textile industry wastewater (sample 5)

nm	abs	nm	abs
350	0.647	446	0.569
351	0.643	447	0.568
352	0.641	448	0.567
353	0.641	449	0.567
354	0.637	450	0.564
355	0.635	455	0.557
356	0.637	460	0.553
357	0.633	465	0.547
358	0.633	470	0.542
359	0.629	475	0.539
360	0.631	480	0.533
361	0.630	485	0.527
362	0.629	490	0.519
363	0.629	495	0.509
364	0.627	500	0.501
365	0.628	505	0.494
366	0.631	510	0.489
367	0.629	515	0.484
368	0.628	520	0.479
369	0.627	525	0.473
370	0.629	530	0.466
371	0.629	535	0.459
372	0.630	540	0.451
373	0.630	545	0.443
374	0.630	550	0.438
375	0.631	555	0.433
376	0.630	560	0.429
377	0.633	565	0.425
378	0.632	570	0.422

379	0.631	575	0.419
380	0.633	580	0.415
381	0.632	585	0.412
382	0.634	590	0.408
383	0.632	595	0.404
384	0.632	600	0.401
385	0.634	605	0.396
386	0.637	610	0.390
387	0.634	615	0.383
388	0.636	620	0.374
389	0.634	625	0.363
390	0.635	630	0.349
391 (peak)	0.637 (max)	635	0.331
392	0.634	640	0.312
393	0.634	645	0.295
394	0.634	650	0.277
395	0.634	655	0.261
396	0.632	660	0.245
397	0.632	665	0.231
398	0.631	670	0.219
399	0.629	675	0.207
400	0.629	680	0.194
401	0.629	685	0.180
402	0.627	690	0.170
403	0.626	695	0.159
404	0.625	700	0.151
405	0.625	705	0.143
406	0.623	710	0.137
407	0.622	715	0.133
408	0.621	720	0.129
409	0.619	725	0.126

410	0.619	730	0.123
411	0.620	735	0.121
412	0.617	740	0.118
413	0.616	745	0.116
414	0.615	750	0.114
415	0.614	755	0.120
416	0.613	760	0.111
417	0.611	765	0.109
418	0.609	770	0.108
419	0.608	775	0.106
420	0.606	780	0.105
421	0.604	785	0.103
422	0.602	790	0.102
423	0.601	795	0.101
424	0.599	800	0.099
425	0.598	805	0.098
426	0.596	810	0.097
427	0.595	815	0.096
428	0.593	820	0.095
429	0.592	825	0.094
430	0.590	830	0.093
431	0.589	835	0.092
432	0.587	840	0.091
433	0.586	845	0.090
434	0.585	850	0.089
435	0.583	855	0.088
436	0.581	860	0.087
437	0.581	865	0.086
438	0.580	870	0.086
439	0.578	875	0.085
440	0.576	880	0.084

441	0.575	885	0.083
442	0.574	890	0.082
443	0.573	895	0.081
444	0.572	900	0.080
445	0.570		

Table A.7 Results of wavelength scan of textile industry wastewater (sample 6)

nm	abs	nm	abs
350	0.611	446	0.471
351	0.607	447	0.469
352	0.603	448	0.466
353	0.601	449	0.464
354	0.596	450	0.462
355	0.593	455	0.421
356	0.591	460	0.413
357	0.588	465	0.407
358	0.585	470	0.401
359	0.584	475	0.397
360	0.581	480	0.393
361	0.579	485	0.389
362	0.577	490	0.387
363	0.574	495	0.384
364	0.572	500	0.381
365	0.570	505	0.378
366	0.569	510	0.376
367	0.568	515	0.372
368	0.566	520	0.368
369	0.564	525	0.362
370	0.563	530	0.356
371	0.559	535	0.350
372	0.562	540	0.344
373	0.560	545	0.337
374	0.557	550	0.330
375	0.557	555	0.321
376	0.555	560	0.312
377	0.555	565	0.302
378	0.554	570	0.291

379	0.553	575	0.279
380	0.551	580	0.269
381	0.552	585	0.260
382	0.550	590	0.252
383	0.549	595	0.245
384 (peak)	0.549 (max)	600	0.239
385	0.550	605	0.235
386	0.546	610	0.231
387	0.548	615	0.227
388	0.547	620	0.223
389	0.546	625	0.218
390	0.546	630	0.213
391	0.546	635	0.206
392	0.547	640	0.197
393	0.544	645	0.188
394	0.546	650	0.179
395	0.544	655	0.172
396	0.546	660	0.164
397	0.545	665	0.155
398	0.544	670	0.148
399	0.544	675	0.139
400	0.544	680	0.131
401	0.542	685	0.123
402	0.544	690	0.113
403	0.542	695	0.105
404	0.541	700	0.099
405	0.541	705	0.094
406	0.540	710	0.090
407	0.539	715	0.086
408	0.539	720	0.083
409	0.539	725	0.080

410	0.537	730	0.078
411	0.536	735	0.076
412	0.524	740	0.075
413	0.533	745	0.073
414	0.532	750	0.072
415	0.530	755	0.070
416	0.529	760	0.069
417	0.528	765	0.068
418	0.524	770	0.067
419	0.523	775	0.066
420	0.523	780	0.065
421	0.522	785	0.064
422	0.521	790	0.063
423	0.518	795	0.062
424	0.515	800	0.061
425	0.513	805	0.060
426	0.510	810	0.059
427	0.508	815	0.059
428	0.506	820	0.058
429	0.504	825	0.057
430	0.502	830	0.056
431	0.500	835	0.056
432	0.498	840	0.055
433	0.496	845	0.054
434	0.494	850	0.054
435	0.492	855	0.053
436	0.490	860	0.052
437	0.488	865	0.052
438	0.486	870	0.051
439	0.484	875	0.050
440	0.482	880	0.050

441	0.480	885	0.049
442	0.479	890	0.049
443	0.476	895	0.048
444	0.474	900	0.048
445	0.473		

Table A.8 Results of wavelength scan of paper industry wastewater

nm	abs	nm	abs
350	0,175	526	0,133
355	0,172	527	0,133
360	0,169	528	0,133
365	0,167	529	0,133
370	0,165	530	0,133
375	0,164	531	0,133
380	0,158	532	0,133
385	0,159	533	0,133
390	0,155	534	0,133
395	0,157	535	0,133
400	0,155	536	0,132
405	0,154	537	0,132
410	0,152	538	0,132
415	0,152	539	0,132
420	0,150	540	0,132
425	0,150	541	0,132
430	0,149	542	0,132
435	0,147	543	0,132
440	0,147	544	0,132
445	0,146	545	0,131
450	0,146	546	0,131
451	0,145	547	0,131
452	0,145	548	0,131
453	0,145	549	0,130
454	0,144	550	0,130
455	0,144	555	0,129
456	0,145	560	0,129
457	0,144	565	0,128
458	0,145	570	0,127

459	0,144	575	0,127
460	0,143	580	0,127
461	0,142	585	0,126
462	0,142	590	0,125
463	0,143	595	0,126
464	0,143	600	0,124
465	0,143	605	0,125
466	0,143	610	0,123
467	0,142	615	0,123
468	0,142	620	0,122
469	0,141	625	0,122
470	0,141	630	0,121
471	0,141	635	0,121
472	0,140	640	0,121
473	0,140	645	0,120
474	0,140	650	0,120
475	0,140	655	0,119
476	0,139	660	0,119
477	0,139	665	0,119
478	0,140	670	0,119
479	0,141	675	0,117
480 (peak)	0,141 (max)	680	0,118
481	0,140	685	0,116
482	0,140	690	0,116
483	0,139	695	0,115
484	0,138	700	0,115
485	0,138	705	0,115
486	0,137	710	0,114
487	0,138	715	0,114
488	0,138	720	0,114
489	0,139	725	0,113

490	0,139	730	0,113
491	0,139	735	0,112
492	0,138	740	0,112
493	0,139	745	0,111
494	0,138	750	0,111
495	0,138	755	0,111
496	0,138	760	0,110
497	0,137	765	0,110
498	0,137	770	0,109
499	0,136	775	0,109
500	0,137	780	0,109
501	0,136	785	0,109
502	0,136	790	0,109
503	0,135	795	0,109
504	0,136	800	0,109
505	0,136	805	0,109
506	0,136	810	0,109
507	0,136	815	0,109
508	0,136	820	0,108
509	0,136	825	0,108
510	0,135	830	0,108
511	0,135	835	0,107
512	0,135	840	0,107
513	0,135	845	0,107
514	0,135	850	0,106
515	0,136	855	0,106
516	0,136	860	0,106
517	0,136	865	0,105
518	0,135	870	0,105
519	0,135	875	0,105
520	0,134	880	0,104

521	0,134	885	0,104
522	0,133	890	0,104
523	0,133	895	0,103
524	0,133	900	0,103
525	0,133		

APPENDIX-B

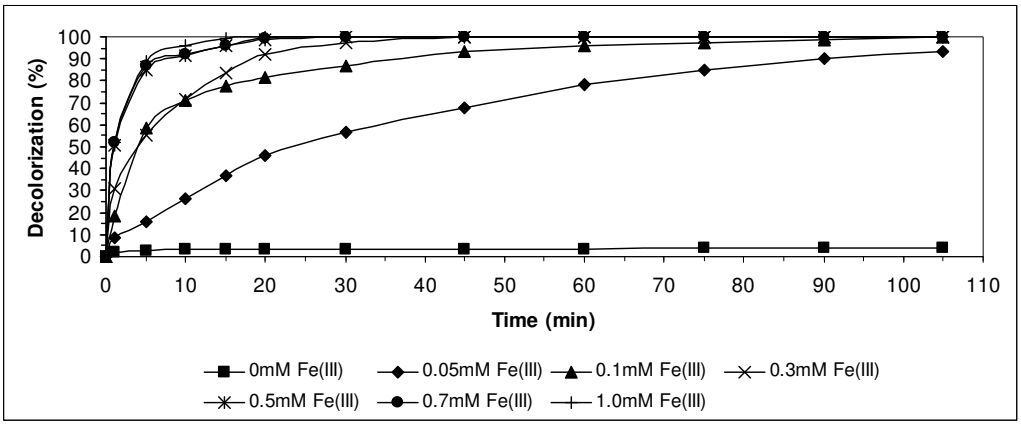

Figure B.1 Variation of decolorization efficiency with irradiation time with Fe(III)/H_2O_2 process when $[H_2O_2]/[COD] = 1.0$

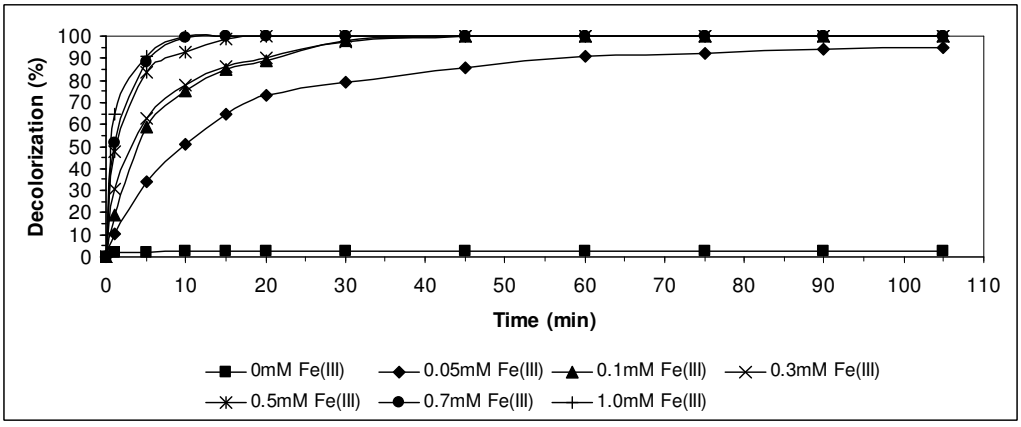

Figure B.2 Variation of decolorization efficiency with irradiation time with Fe(III)/H_2O_2 process when $[H_2O_2]/[COD] = 0.7$

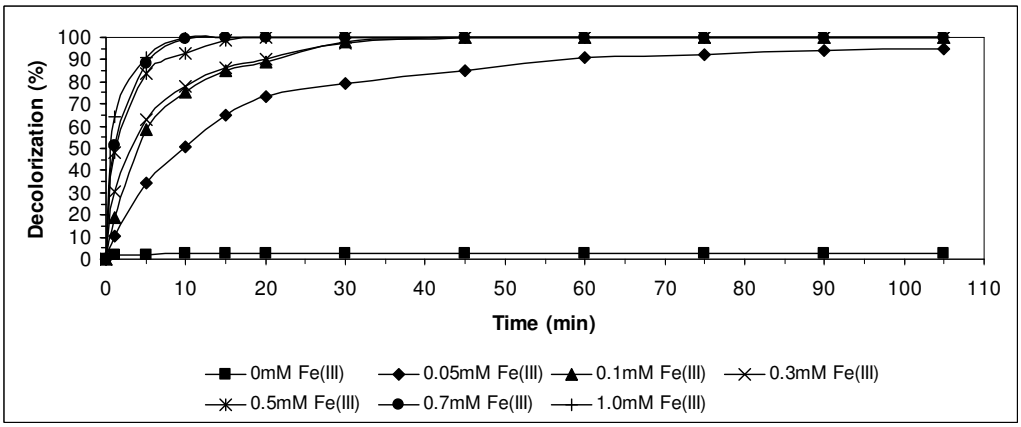

Figure B.3 Variation of decolorization efficiency with irradiation time with Fe(III)/H_2O_2 process when $[H_2O_2]/[COD] = 0.5$

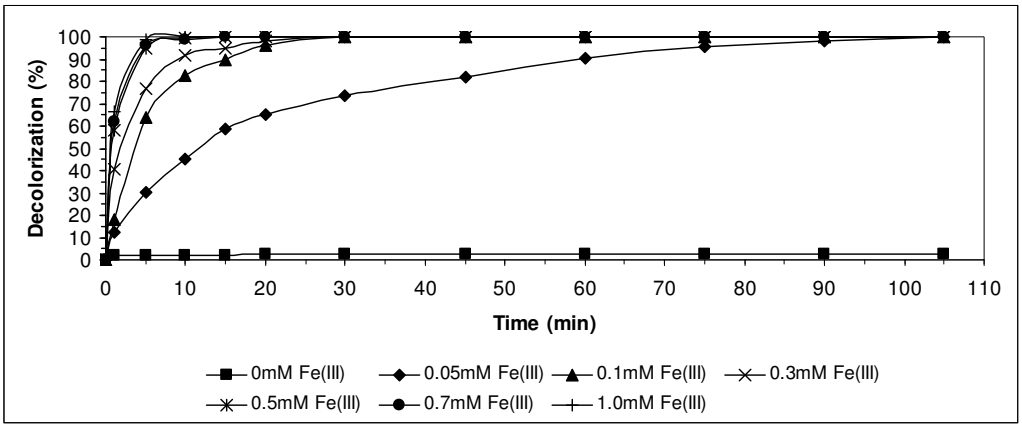

Figure B.4 Variation of decolorization efficiency with irradiation time with Fe(III)/H_2O_2 process when $[H_2O_2]/[COD] = 0.3$

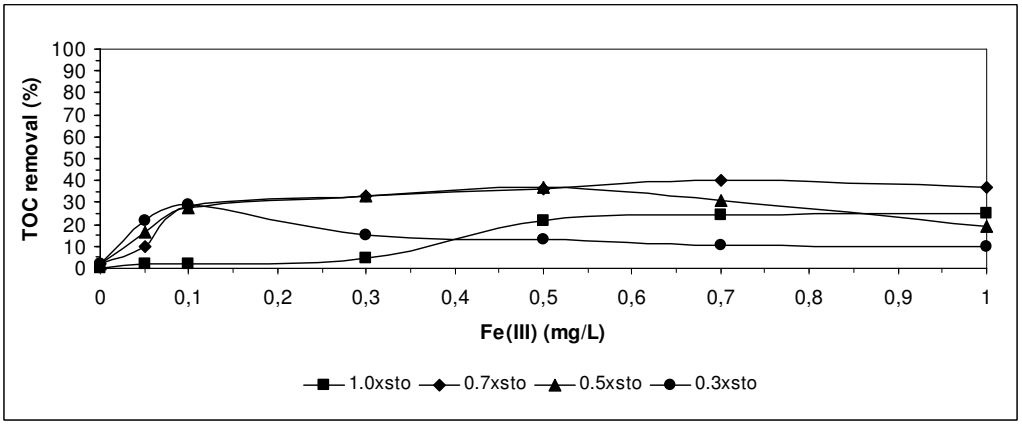

Figure B.5 Variation of TOC removal efficiency with Fe(III) concentration with Fe(III)/H_2O_2 process at different $[H_2O_2]/[COD]$ ratios

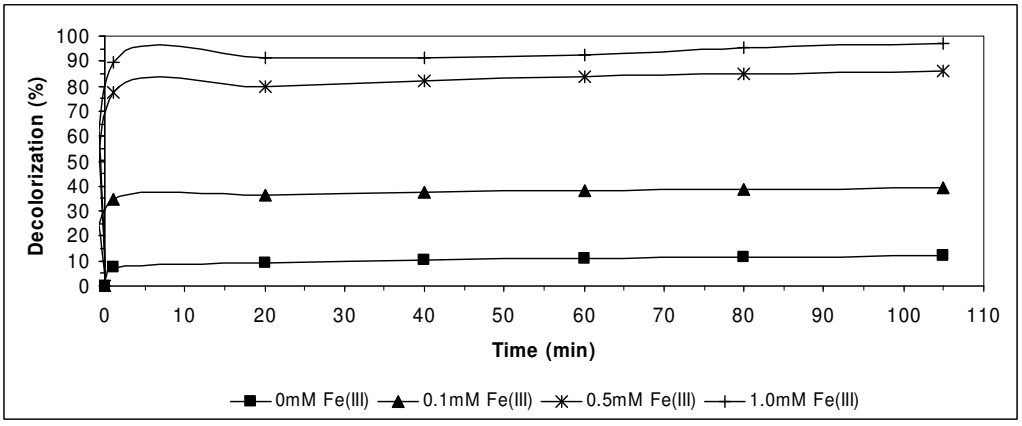

Figure B.6 Variation of decolorization efficiency with irradiation time with Fe(III)/TiO_2 process when $TiO_2 = 50mg/L$

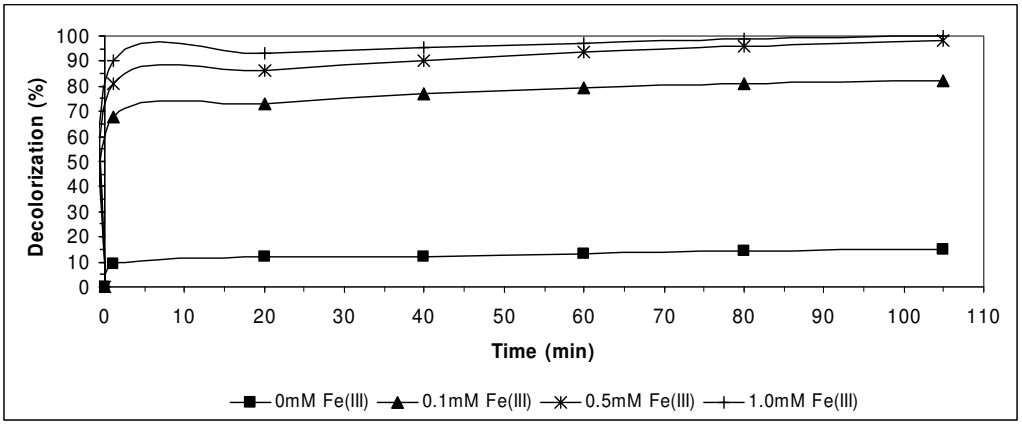

Figure B.7 Variation of decolorization efficiency with irradiation time with Fe(III)/TiO_2 process when TiO_2 = 100mg/L

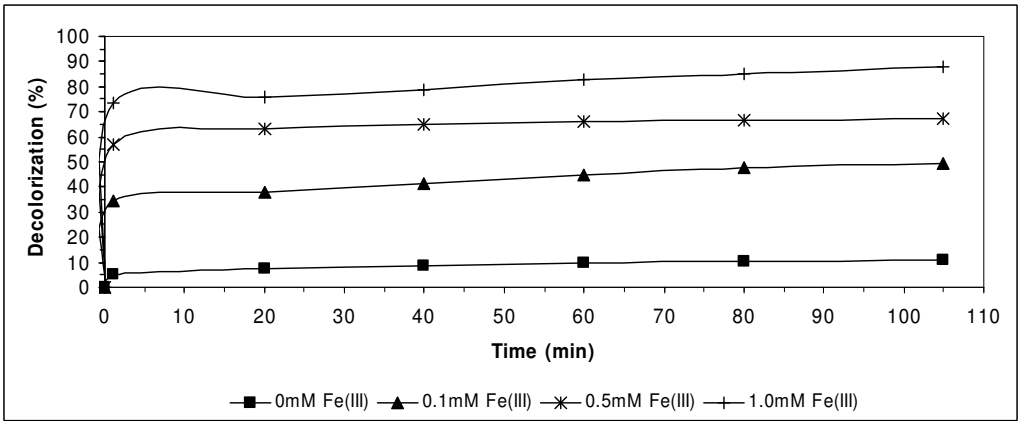

Figure B.8 Variation of decolorization efficiency with irradiation time with Fe(III)/TiO_2 process when TiO_2 = 200mg/L

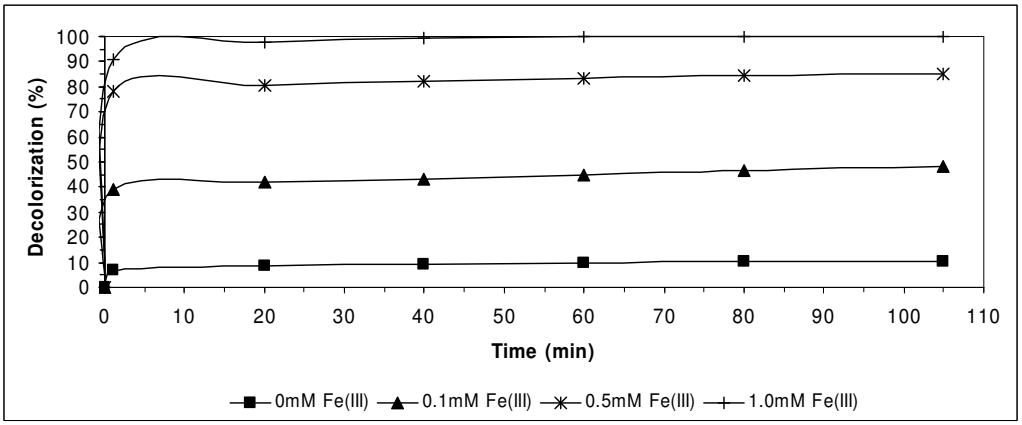

Figure B.9 Variation of decolorization efficiency with irradiation time with Fe(III)/TiO_2 process when TiO_2 = 250mg/L

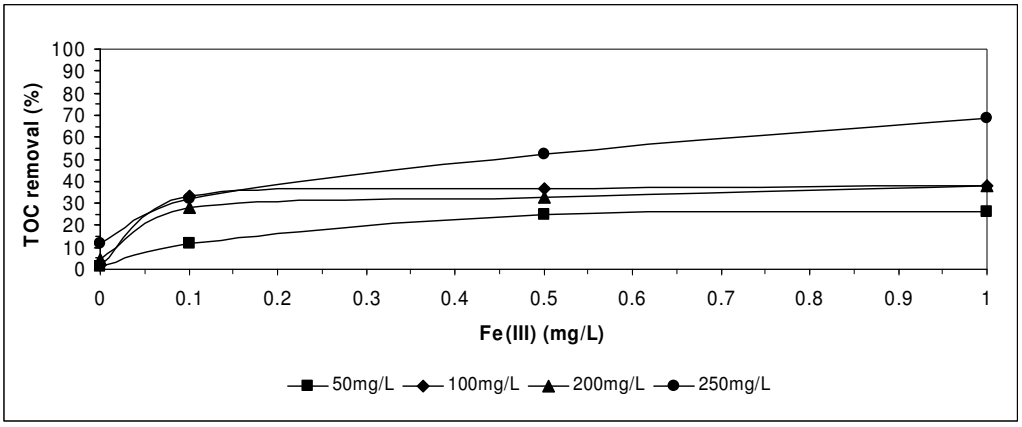

Figure B.10 Variation of TOC removal efficiency with Fe(III) concentration with Fe(III)/TiO_2 process at different TiO_2 concentrations

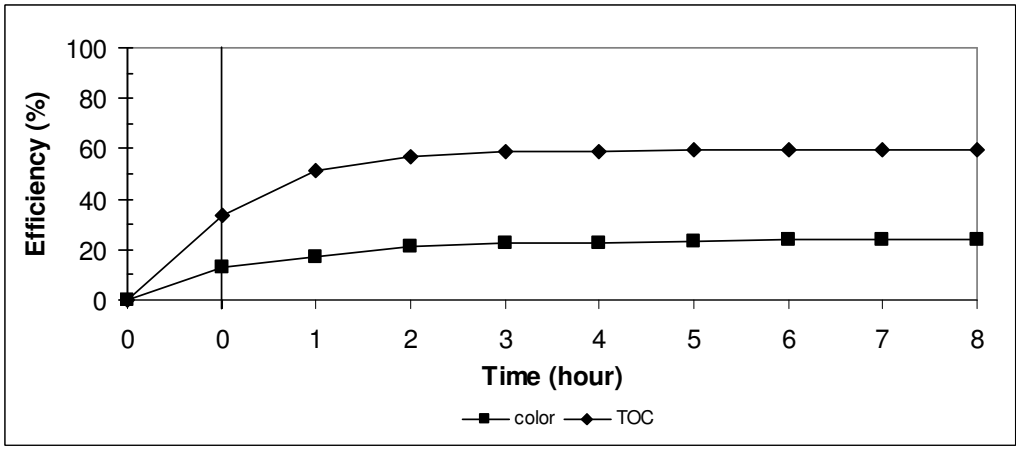

Figure B.11 Variation of color and TOC removal efficiencies with time with Fe(III)/H_2O_2 process of synthetic wastewater (a blank experiment).